

PORE DEVELOPMENT IN MEAT PRODUCTS DURING DEEP-FAT FRYING

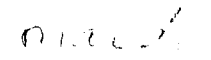
by

LAMIN SAMBOUJANG KASSAMA

Department of Bioresource Engineering
Macdonald Campus, McGill University
Ste Anne-de-Bellevue Quebec H9X 3V9
Canada

June 2003

A Thesis Submitted to the Faculty of Graduate Studies and
Research in Partial Fulfillment of the Requirements for
the Degree of Doctor of Philosophy



ABSTRACT

The relationships between moisture loss and oil uptake and their effects on porosity, pore size distribution and pore structure during deep-fat frying of chicken breast meat were investigated. Chicken meat samples were deep-fat fried in an industrial fryer. The frying oil temperatures were 170, 180 and 190°C and samples were fried for times ranging from 5 to 900 s.

Frying oil temperature and frying time significantly (P < 0.01) influenced moisture loss and fat uptake. Moisture loss was positively correlated with oil uptake only at frying times of 45 to 360 s. During the initial phase of frying (<45 s) oil uptake was independent of frying oil temperature. Oil uptake tended to reach a plateau or quasi-equilibrium after about 360 s. The effective moisture diffusivity (based on 900 s) was found to increase from 3.65E-09 m²/s at 170°C frying oil temperature to 7.42E-09 m²/s at 190°C. The effective oil diffusivity increased from 9.12E-09 to 3.32E-08 m²/s as temperature was increased from 170 to 190°C.

The physical properties of fried chicken meat were investigated. Both frying oil temperature and frying time significantly influenced changes in bulk and apparent densities of the samples. Bulk density decreased from 1.15 to 0.98, 0.95 and 0.93 g/cm³ after 900 s of deep-fat frying at 170, 180, and 190°C, respectively. In contrast, the apparent density increased from 1.13 to 1.25, 1.24 and 1.22 g/cm³ when samples were fried for 900 s at the 170, 180, and 190°C, respectively. Both bulk and apparent densities were linearly correlated with moisture loss, thus a linear model was developed. Volumetric shrinkage was

also significantly (P < 0.05) influenced by the frying levels. Linear equations represented volumetric shrinkage and moisture loss quite well over the full range of frying times. Pore development was modeled as a function of moisture loss. Porosities were 0.28, 0.24 and 0.22, respectively after 900 s of deep-fat frying at the three temperatures studied. Pore development and oil uptake data were more closely represented by exponential models than by linear models.

Restructured meat samples (beef) mixed with soy protein were fried on a griddle. Instrumental textural profiles of the pan-fried samples were obtained using a Universal Testing Machine Instron. Porosity and pore size distributions were determined by a mercury intrusion porosimeter. The results indicated that increasing soy protein concentration increased water holding capacity (WHC) and reduced Total cooking loss (TCL). Beef patties extended with textured soy-protein (TSP) were harder and more cohesive than those extended with soy-protein flour (SPF). Total mean porosities were 0.42 and 0.40 for the SPF and TSP extended samples, respectively, at a 5% concentration of extender. Samples extended with SPF had up to 84% capillary pores.

Oven fried beef patties extended with SPF developed larger pore volumes with porosity ranging from 21 to 34% whereas for the TSP extended patties, porosity ranged from 4 to 20%. The cumulative intrusion volume for patties extended with SPF and TSP was 0.33 and 0.20 mL/g, respectively. The contribution of pores with sizes larger than 10 μ m in diameter in the beef patty extended either with SPF or TSP was 80%.

Pore structures of deep-fat fried samples were influenced by oil uptake. Cumulative pore volume decreased from 2.13 to 0.51 mL/g as frying time increases (180°C oil temperature). The cumulative surface area was found to increase from 6.92 to 8.24 m²/g after 360 s of deep-fat frying. The inter-fiber (planar) pore diameter was about 10.2 μ m and the intra-fiber (internal) pore diameters ranged from 0.006 to 10 μ m. Over 84% of the pores were capillary pores. Fried samples were more porous than the restructured and extended meat samples.

RÉSUMÉ

Les rapports entre la perte d'humidité et l'absorption d'huile et leurs effets sur la porosité, la distribution de la taille des pores et la structure des pores pendant la friture en immersion de poitrine de poulet ont été examinés. Les échantillons de viande de poulet ont été cuits en grande friture dans une friteuse industrielle. Les températures de friture de l'huile étaient de 170, 180 et 190°C et les échantillons ont été frits pour une période variant de 5 à 900 s.

La température de l'huile et le temps de friture ont influencé significativement (P <0.01) la perte d'humidité et l'absorption d'huile. La perte d'humidité correspondait à l'absorption d'huile pour les temps de friture entre 45 et 360 s. Pendant la phase d'initiation de friture (<45 s) le taux d'absorption d'huile était indépendant de la température. L'absorption d'huile a eu tendance à atteindre un plateau ou un quasi équilibre après 360 s. La diffusivité effective de l'humidité (basé sur 900 s) a augmenté de 3.65E-09 m²/s à 170°C, jusqu'à 7.42E-09 m²/s à 190°C. La diffusivité de l'huile a augmenté de 9.12E-09 à 3.32E-08 m²/s, à ces températures.

Les propriétés physiques du poulet frit ont été examinées. La température de l'huile et le temps de friture ont influencé significativement les changements de densité de masse et la densité solide. La densité de masse a diminué de 1.15 à 0.98, 0.95 et 0.93 g/cm³ après 900 s de friture à 170, 180, et 190°C, respectivement. Par opposition, la densité solide a augmenté de 1.13 à 1.25, 1.24 et 1.22 g/cm³, respectivement. Les deux densités étaient en relation linéaire

avec la perte d'humidité, ainsi un modèle de prédiction linéaire a été développé. Le rétrécissement volumétrique était aussi significativement (P <0.05) influencé par les paramètres du procédé. Les équations linéaires ont représenté le recul volumétrique et la perte d'humidité de façon adéquate pendant les 900 s de friture, et ceci, à chacune des températures examinées. Le développement des pores a été modélisé en fonction de la perte d'humidité. La porosité était de 0.28, 0.24 et 0.22 respectivement après les 900 s de friture pour les trois températures étudiées. Les modèles exponentiels améliorent la représentation du développement de pores et l'absorption d'huile par rapport aux modèles linéaires.

Des échantillons restructurés de viande (boeuf) mélangé avec de la protéine de soja ont été frits sur une plaque. Les profils texturaux instrumentaux des échantillons ont été obtenus en utilisant une Machine Universelle Instron. La porosité et les distributions de taille de pore ont été déterminées par un porosimètre d'intrusion de mercure. Les résultats ont indiqué qu'une augmentation de la concentration de protéine de soja a augmenté la capacité de rétention d'eau et causé une réduction de la perte totale lors de la cuisson. Les boulettes de boeuf contenant de la protéine de soja texturé (PST) étaient plus dures et cohésives que celles contenant de la farine de soja protéique (FSP). Les porosités moyennes totales étaient de 0.42 et 0.40 pour les échantillons avec FPS et PST respectivement à une concentration de 5%. Les échantillons avec FPS avaient jusqu'à 84% de pores capillaires.

Les boulettes avec FPS frites au four ont développé un plus grand volume de pores, la porosité étant entre 21 et 34%, tandis que pour les boulettes avec de la PST, la porosité se situait entre 4 et 20%. Le volume cumulatif d'intrusion pour les boulettes contenant de la FSP et de la PST était de 0.33 et 0.20 mL/g, respectivement. Une contribution de 80% provenait de pores ayant un diamètre supérieur à 10 µm.

La structure des pores a été influencée par l'absorption d'huile. Le volume cumulatif des pores a diminué de 2.13 à 0.51 mL/g en fonction du temps de friture (à 180°C). La superficie totale a augmenté de 6.92 à 8.24 m²/g après 360 s de grande friture. Le diamètre des pores entre les fibres (planaires) était de 10.2 µm. Le diamètre des pores internes des fibres s'étendait de 0.006 à 10 µm. Plus de 84% des pores étaient des pores capillaires. Les échantillons frits étaient plus poreux que les échantillons restructurés ou mélangés.

ACKNOWLEDGEMENTS

First and foremest, the author acknowledges the grace and providence of God through the entire period of his study at McGill University. Also the parental love and support from my parents Samboujang and Nyimanding Dibba and two beloved sons Mutarr and Yankuba.

The author wishes to express his heartfelt gratitude to his thesis supervisor Dr. Michael O. Ngadi of the Department of Bioresource Engineering, Macdonald campus, McGill University, for his valuable guidance, critique, encouragement and motivation in completing this manuscript. Special thanks goes to Dr. G.V.S. Raghavan for his help and encouragement. I acknowledge the fruitful contributions of Dr Hosahalli Ramaswami, Dr. Benjamin Simpson of the Department of Food Science and Agricultural Chemistry and Dr. Shiv O. Prasher for their valuable comments and advises during my comprehensive exam. I acknowledge Mr. Peter Alvo for his assistance in editing this thesis and Dr. Valerie Orsat for her valuable time spent on the French translations.

The Food Engineering Group and all the student in the Food and Bioprocess Engineering Lab for their cooperation and staging a friendly social environment during the period of this work, and also the administrative staff of the Department of Bioresource Engineering.

I sincerely acknowledge the fraternity of The Gambian students (Baboucarr Jobe and Kebba Sabally) and the Gambian community at Montreal.

PART OF THIS THESIS HAS BEEN PUBLISHED AS FOLLOWS:

- 1. Ngadi, M.O., **L.S. Kassama** and G.S.V. Raghavan. 2001. Porosity and pore size distribution in cooked meat patties containing soy protein. *Canadian Biosystems Engineering* 43 (3): 17-24.
- Kassama, L.S., Ngadi, M.O., and G.S.V. Raghavan. 2003. Structural and instrumental textural properties of meat patties containing soy protein. International Journal of Food Properties 6 (2): 1-11.

PART OF THE THESIS HAS BEEN SUBMITTED FOR PUBLICATION:

- 1. **Kassama, L.S.**, Ngadi, M.O. 2003. Pore structure characterization of deep-fat fried chicken meat. *Journal of Food Engineering* (in Press)
- 2. **K**assama. L.S., Ngadi, M.O. 2003. Pore development in chicken meat during deep-fat frying. *Lebensmittel-Wissenschaft und-Technologie* (In Press)
- 3. **Kassama, L.S.**, Ngadi, M.O. 2003. Shrinkage, density, and porosity changes in chicken breast meat during deep-fat frying. *Journal of Food Science* (In Press)
- 4. **Kassama, L.S.**, Ngadi, M.O. 2003. The effect of bulk shrinkage on pore development in chicken meat during deep-fat frying. *Journal of the Science of Food and Agriculture*. (*In Preparation*).

5. **Kassama, L.S.**, Ngadi, M.O. 2003. Relationship between moisture loss and oil uptake in chicken meat during deep-fat frying. *Journal of Food Processing and Preservation*. (in Preparation)

PART OF THIS THESIS HAS BEEN PRESENTED AT SCIENTIFIC AND TECHNICAL CONFERENCES:

- Kassama, L. S. and M. O. Ngadi 2003. Pore Development and Moisture Transfer in Chicken Meat during Deep-fat Frying. Paper accepted for presentation at the Conference on Food Engineering of the American Institute of Chemical Engineers, San Francisco, California November 16-21.
- Kassama, L. S. and M. O. Ngadi. 2003. Modeling pore development in chicken meat during deep-fat frying. Oral presentation at the 2003 annual meeting of the IFT, Chicago, IL, July 12-16.
- Kassama, L. S. and M. O. Ngadi. 2003. Density, shrinkage and porosity of deep-fat fried chicken meat. Paper presented at the 2003 annual meeting of the ASAE. Paper no. 036107. Las Vegas, July 27-30.
- Kassama, L. S. and M. O. Ngadi. 2003. Pore structure characterization of deep-fat fried chicken meat. Paper presented at the 2003 annual meeting of the CSAE, Paper no: 03-304. Montreal, Quebec. July 6-9
- Kassama, L. S. and M. O. Ngadi. 2002. Rheology of deep-fat frying oils. Paper presented at the Annual meeting of the 17th Canadian section of the American Oil Chemists' Society, Holiday Inn Select Toronto airport, Toronto. September 28-30.

- Kassama, L. S. and M. O. Ngadi. 2001. Development of Pores and Pore Size Distribution in Chicken Meat During Deep-fat Frying. Paper presented at the 2001 CSAE/SCGR-NABEC Annual meeting sponsored by the CSAE/SCGR-NABEC. Paper no.: 01-322. University of Guelph, Ontario. July 8-11.
- Kassama, L. S. and M. O. Ngadi. 2001. Porosity and Pore Size Distribution in Fried Meat Products. Presented at the Agriculture and Agri-Food Canada conference, at the Center for Food Development and Research (CRDA), Saint-Hyacinthe. March 21.
- 8. **Kassama**, L. S., M. O. Ngadi and G. V. S. Raghavan. 2000. Porosity and Pore Size Distribution in Cooked Patties Containing Soy-protein. Presented at the Agri-Food 2000 Conference, Winnipeg, Manitoba. July 15–19.
- Kassama, L. S., M. O. Ngadi and G. V. S. Raghavan. 2000. Textural and Physical Characteristics of Cooked Beef Patties Containing Soy-protein. Presented at the 2000 ASAE Annual International Meeting. Paper no.: 00-6079. Midwest Express Center, Milwaukee, Wisconsin. July 9-12.

CONTRIBUTION OF AUTHORS

The role and contribution made by different authors are as follows: The principal author is Mr. Lamin S. Kassama, is the Ph. D. candidate who planned and executed all the experiments, data analysis and wrote the manuscript for scientific publications. Dr. Michael O. Ngadi is the thesis supervisor, who guided the candidate in the planning and execution of experiments during the course of the entire program. He corrected, edited and reviewed all the manuscripts sent for publication. Dr. G. V. J. Raghavan was a collaborator and also contributed in edited manuscripts for scientific publication.

TABLE OF CONTENTS

| ABSTRACT | I |
|--------------------------------------------------------------------------------------------------------------------------------------------------------------------------------------------------------------------------------------------------------------------------------------------------------------------------------------------------------------------------------------------------------------------------------------------------------------------------------------------------------------------------------------------------------------------------------------------------------------------------------------------------------------------|-------------|
| RÉSUMÉ | IV |
| ACKNOWLEDGEMENTS | VII |
| PART OF THIS THESIS HAS BEEN PUBLISHED AS F | OLLOWS:VIII |
| CONTRIBUTION OF AUTHORS | |
| LIST OF FIGURES | |
| LIST OF TABLES | |
| | |
| NOMENCLATURE | |
| I. GENERAL INTRODUCTION | |
| 1.1 BACKGROUND | |
| II GENERAL LITERATURE REVIEW | 7 |
| 2.1 CHEMISTRY OF FRYING OIL 2.2 THEORY OF FAT ABSORPTION 2.2.1 Factors that influence fat absorption 2.2.1.1 Frying time 2.2.1.2 Frying temperature 2.2.1.3 Moisture content 2.2.1.4 Oil quality 2.2.1.5 Interfacial tension 2.2.1.6 Product geometry 2.2.1.7 Pre-frying treatment 2.2.1.8 Post-frying oil penetration 2.3 PORE STRUCTURE 2.3.1 Macroscopic pore structure 2.3.2 Porosity and density 2.3.3 Specific surface area 2.3.4 Breakthrough pressure 2.3.5 Microscopic pore structure 2.3.6 Topology of pore structure 2.3.6.1 Connectivity 2.3.7 Pore size 2.3.8 Pore size distribution 2.3.9 Factors that influence pore structure | |
| 2.3.9 Factors that inhiderice pore structure 2.4 HIERARCHICAL STRUCTURE IN MEATS | |
| | |

| 2.5 MERCURY INTRUSION POROSIMETRY 2.5.1 Principles of mercury porosimetry 3 2.6 Mass Transfer During Deep-fat frying 3 | 30 |
|------------------------------------------------------------------------------------------------------------------------------------------------------------------------------------------------------------------------------------------------------------------------------------------------------------------------------------------------------------------------------------------------------------------------------------------------------------------------------------------------|----------------------------------------------------------------------------------|
| CONNECTING TEXT3 | 36 |
| III. RELATIONSHIP BETWEEN OIL UPTAKE AND MOISTURE LOSS DURING DEEP FAT FRYING OF CHICKEN BREAST MEAT | 37 |
| | 37 38 39 39 39 40 41 41 42 43 43 47 49 52 |
| CONNECTING TEXT | 6 |
| IV. MOISTURE DIFFUSIVITY DURING DEEP-FAT FRYING OF CHICKEN MEAT | 57 |
| 4.2 INTRODUCTION 5 4.2.1 Moisture diffusion model 6 4.3 MATERIALS AND METHODS 6 4.3.1 Frying 6 4.3.2 Analytical methods 6 4.3.2.1 Moisture content 6 4.3.2.2 Fat content 6 4.3.3 Experimental design and statistical analysis 6 4.4 RESULTS AND DISCUSSION 6 4.4.1 Moisture diffusivity 6 4.4.2 Fat uptake 6 4.5 CONCLUSIONS 7 | 50 51 52 52 53 53 53 59 74 |
| 4.6 REFERENCES | _ |

| V . | | | | | CHANGE | | CHICKEN | 80 |
|------------|------------------------|--------------------------|-------------------------|-----------------------------------------|--------------------------|---------------------------|-----------------------------------------|------------|
| 5 | .1 AB | STRACT | | ********** | | | | 80 |
| 5 | | | | | | | | |
| 5 | | | | | | | | |
| | 5.3.1 | Materia | ls | | | | | 84 |
| | 5.3.2 | | | | | | | |
| | 5.3.3 | | | | | | | |
| | 5.3.4 | | | | | | | |
| | 5.3.5 | | | | | | | |
| | | | | | | | | |
| | 5.3.6 | | | | | | | |
| | 5.3.7 | | | | | | | |
| F | | • | | _ | | | | |
| | 5.4.1 | | | | | | | |
| | 5.4.2 | | | | | | | |
| 5 | 5.5 Co | | | | | | | |
| 5 | 5.6 R | EFERENCES | 3 | • • • • • • • • • • • • • • • • • • • • | | | | 101 |
| CC | NNECT | ING TEXT | Г | | | | | 106 |
| VI. | | | | | CHICKEN | | DURING | 107 |
| 6 | 5.1 A | STRACT | | | | | | 107 |
| _ | | | | | | | | |
| 6 | | | | | | | | |
| | 6.3.1 | Sample | prepara | tion | | | | 109 |
| | 6.3.2 | | • | | | | | |
| | | | • | | | | | |
| | | | | | | | | |
| | 6.3.5 | | | | | | | |
| | 6.3.6 | • | | _ | | | | |
| | | | | | | | | |
| | | | | | | | • • • • • • • • • • • • • • • • • • • • | |
| | | | | | | | | |
| CC | NNECI | ING IEX | ١ | ••••• | •••••• | ••••• | • • • • • • • • • • • • • • • • • • • • | 126 |
| VII | | | | | ISTRUMENTA S CONTAINI | | TEXTURAL Y PROTEIN | 127 |
| _ | | | | | | | | |
| _ | | | | | | | ••••• | |
| _ | | | | | | | ••••• | |
| - | | | | | | | • • • • • • • • • • • • • • • • • • • • | |
| - 1 | 7.4 Rı <i>7.4.1</i> | 18/015 ANI 18/010 - 1 | oldina o | anacity on | d cooking loss | | | 134 |
| | 7.4.1 7.4.2 | Textura | ioiding C al analvsi | apaony am S | u cooking loss | | • • • • • • • • • • • • • • • • • • • • | 134 126 |
| | | . 5/11/01/0 | | | | • • • • • • • • • • • • • | • • • • • • • • • • • • • • • • • • • • | , 00 |

| 7.4.3 Porosity and pore size distribution | |
|-----------------------------------------------------------------------------------------|-----|
| ACKNOWLEDGEMENT | |
| 7.6 REFERENCES | |
| | |
| CONNECTING TEXT | 150 |
| VIII. POROSITY AND PORE SIZE DISTRIBUTION IN COOKED MEAT PATTIES CONTAINING SOY PROTEIN | 151 |
| 8.1 ABSTRACT | 151 |
| 8.2 Introduction | 152 |
| 8.3 MATERIALS AND METHODS | |
| 8.3.1 Materials 8.3.2 Sample preparation | |
| 8.3.2 Sample preparation | |
| 3.3.4 Heat treatment | |
| 8.3.5 Water activity | |
| 8.3.6 Cooking loss | |
| 8.3.7 Porosity and pore size distribution | |
| 8.3.8 Experimental design | |
| 8.4.1 Water holding capacity and water activity | |
| 8.4.2 Total cooking losses and water activity | |
| 8.4.3 Porosity | |
| 8.4.3.1 Pore size distribution | |
| 8.5 CONCLUSIONS | 177 |
| ACKNOWLEDGEMENT | 178 |
| 8.6 References | 179 |
| CONNECTING TEXT | 182 |
| IX PORE STRUCTURE CHARACTERIZATION OF DEEP-FAT FRIED CHICKEN MEAT | 183 |
| 9.1 Abstract | 183 |
| 9.2 Introduction | |
| 9.3 MATERIALS AND METHODS | |
| 9.3.1 Sample preparation | |
| 9.3.2 Frying | |
| 9.3.3 Freeze drying | |
| 9.4 RESULTS AND DISCUSSIONS | |
| 9.5 CONCLUSIONS | |
| 9.6 REFERENCES | |
| X. GENERAL SUMMARY AND CONCLUSIONS | 208 |
| 10.1 GENERAL SUMMARY AND CONCLUSIONS | 208 |

| 10.2 | CLAIMS OF CONTRIBUTION TO KNOWLEDGE | 211 |
|--------|---------------------------------------|-----|
| 10.3 | RECOMMENDATIONS FOR FUTURE RESEARCH | |
| GENER | AL REFERENCES | 214 |
| APPEN | DICES | 221 |
| APPE | NDIX 2: MERCURY POROSIMETRY UNIT | 232 |
| 2.1 | LOW PRESSURE SYSTEM | 232 |
| 2.1 | .1 Evacuation valves | 234 |
| 2.1 | .2 Gas inlet valve | 234 |
| 2.1 | .3 Mercury fill and drain valve | 235 |
| 2.1 | .4 Mercury reservoir evacuation valve | 235 |
| 2.1 | .5 Low pressure ports | 235 |
| 2.1 | · · · · · · · · · · · · · · · · · · · | |
| 2.1 | | |
| APPEN | IDIX 3: INDUSTRIAL FRYER | 238 |
| FAT AN | IAI YSIS | 239 |

LIST OF FIGURES

| Figure 2.1 Capillary action of wetting liquid in a capillary tube at atmospheric pressure. (Source: Moreira and Barrufet, 1999. Deep-fat frying: Fundamentals and Applications) | 10 |
|--------------------------------------------------------------------------------------------------------------------------------------------------------------------------------------|----|
| Figure 2.2 Pressure relationship for food product undergoing cooling. (Source: Moreira and Barrufet, 1999. Deep-fat frying: Fundamentals and Applications) | 11 |
| Figure 2.3 Interfacial tension between oil, water and food solid. (Source: Adamson (1990) Physical Chemistry of Surfaces | 16 |
| Figure 2.4 Illustration of different types of connectivity in a porous structure | 19 |
| Figure 2.5 Schematic diagram for a multi-volume helium pycnometer | 21 |
| Figure 2.6 Volume displacement pycnometer for measuring bulk volume of food stuff | 22 |
| Figure 2.7 Pore structure illustrating branches and node with a porous matrix. | 26 |
| Figure 2.8 Mercury in contact with the porous solid. | 30 |
| Figure 2.9 Illustration of an inkbottle pore. | 32 |
| Figure 2.10 Heat and mass transfer in an infinite slab representing a food product, where q, is defined as the heat flux, M, moisture loss, F, fat/oil uptake during deep-fat frying | 33 |
| Figure 3.1 Moisture loss as a function of frying times in chicken breast during deep-fat frying: (a) moisture loss at times <45 s and (b) moisture loss at times 0-900s. | 43 |
| Figure 3.2 Oil uptake as a function of frying times in chicken breast during deep-fat frying: (a) moisture in the range (<45 s) and (b) (>45 s). | 44 |
| Figure 3.3 Thermal histories of the chicken breast slab center for different oil temperatures during deep-fat frying. | 48 |
| Figure 3.4 Cook value at the chicken breast slab center as a function of frying time. | 49 |

| Figure 3.5 | Oil uptake as a function moisture loss in chicken breast meat during deep-fat frying | 50 |
|------------|-------------------------------------------------------------------------------------------------------------------------------------------------------------------|-----|
| Figure 4.1 | A typical moisture history during deep-fat frying of chicken breast meat slab. | 65 |
| Figure 4.2 | The effect of frying oil temperature on effective moisture diffusivity. | 68 |
| Figure 4.3 | Observed and predicted oil uptake at 180°C | 70 |
| Figure 4.4 | The effect of temperature on effective oil diffusivity | 72 |
| Figure 5.1 | Bulk density as a function of time for de-boned chicken meat deep-fat fried at 170, 180, and 190° C | 89 |
| Figure 5.2 | Apparent density as a function of time for de-boned chicken meat deep-fat fried at 170, 180, and 190° C | 90 |
| Figure 5.3 | Bulk and apparent densities as a function of moisture loss during deep-fat frying of de-boned chicken meat | 92 |
| Figure 5.4 | Experimental and predicted densities (bulk and apparent) of de-boned chicken meat as a function of water loss fraction during deep-fat frying. | 96 |
| Figure 5.5 | Volumetric shrinkage as a function frying time | 98 |
| Figure 5.6 | A typical apparent volumetric shrinkage of as a function of moisture loss for FOT 180°C. | 99 |
| Figure 6.1 | Change in porosity with frying time at different temperatures in de-boned chicken meat slabs. | 112 |
| Figure 6.2 | Porosity as a function of moisture loss at different frying temperatures in de-boned chicken meat samples during deep-fat frying | 114 |
| Figure 6.3 | Predicted vs experimental pore development as a function of moisture loss at different frying temperatures in deboned chicken meat samples during deep-fat frying | 118 |
| Figure 6.4 | Predicted vs experimental pore development as a function of oil uptake at different frying temperatures in de-boned chicken meat samples during deep-fat frying | 121 |

| Figure 7.1 | Cumulative pore volume (mL/g) of pan-fried beef patties extended with 5% different soy protein concentrations | 141 |
|------------|----------------------------------------------------------------------------------------------------------------------------------------------------------------------------------------------------------------------------------------------------------------------|-----|
| Figure 7.2 | Pore size distribution of pan-fried beef patties extended with 5% of different soy protein concentration | 143 |
| Figure 8.1 | Response surface graph of the effect extender concentration and cooking temperature at constant cooking time (10 min.) on porosity of beef patty samples extended with soy-protein flour. | 167 |
| Figure 8.2 | Response surface graph of the effect cooking temperature and cooking time at constant extender concentration (2%) on porosity of beef patty samples extended with soyprotein flour. | 168 |
| Figure 8.3 | Response surface graph of the effect cooking temperature and cooking time at constant extender concentration (5%) on porosity of beef patty samples extended with soy-protein flour | 170 |
| Figure 8.4 | Pore size distribution (total open volume mL/g) of beef patty extended with different concentration of soy-protein flour at different cooking temperature. | 172 |
| Figure 8.5 | Pore size distribution (total open volume mL/g) of beef patty extended with different concentration of textured soy-protein at different cooking temperatures. | 173 |
| Figure 8.6 | Pore size distribution (cumulative pore area m²/g) of beef patty extended with different concentration of soy-protein flour at different cooking temperatures. Pore size distributions obtained at 2%, 167°C; 5%, 167°C and 5%, 187°C were very close to each other. | 175 |
| Figure 8.7 | Pore size distribution (cumulative pore area m²/g) of beef patty extended with different concentration of textured soy-protein at different temperatures. Pore size distributions obtained at 2%, 187°C and 5%, 167°C were very close to each other. | 176 |
| Figure 9.1 | Mercury low pressure intrusion curve (normalized intrusion volume versus pressure) deep-fat fried chicken meat samples and the control. | 193 |

| Figure 9.2 | Pore volume distribution as a function of pore diameter of deep-fat fried chicken samples fried for 0, 4, 6, and 8 min | 194 |
|--------------|-------------------------------------------------------------------------------------------------------------------------------|-----|
| Figure 9.3 | Typical intrusion extrusion capillary hysteresis curve for the DFF (6 min) chicken sample. | 197 |
| Figure 9.4 (| Cumulative pore area as a function of pore diameter of deepfat fried chicken samples fried for 0, 4, 6, and 8 min | 199 |
| Figure 9.5 | Pore size distribution by volume distribution function D(r) as a function of pore diameter for deep-fat fried chicken meat | 200 |
| Figure 9.6 | Percent volume distribution function as a function of pore diameter for deep-fat fried chicken meat. | 201 |
| Appendix 2 | Figure 1 The Mercury Intrusion Porosimeter used in this study. | 232 |
| Appendix 2 | Figure 2 Schematic diagram of the low-pressure evacuation and filling system. (Source: Micromeritics operational manual) | 233 |
| Appendix 2 | Figure 3 Penetrometer assembly for sample holding. (Source: Micromeritics operational manual) | 234 |
| Appendix 2 | Figure 4 Schematic diagram of the high-pressure system of the mercury porosimetry. (Source: Micromeritics operational manual) | 237 |
| Appendix 3 | Figure 1 Photo of an industrial fryer Computron 7000 Pressure Fryer. | 238 |
| Appendix 3 | Figure 2 Photo of the Velp Scientific Soxhlet fat extractor used for determination of oil/fat uptake | 239 |

LIST OF TABLES

| Table 2.1 | Deep-fat frying oil quality parameters: phases oil passes through during the degradation process. | 14 |
|-----------|----------------------------------------------------------------------------------------------------------------------------------------------------------------------------|-----|
| Table 3.1 | Trends in oil uptake and moisture loss of chicken during DFF at different FOTs during the first phase of frying (0 to 360 s) | 46 |
| Table 3.2 | Regression equations for oil uptake as a function of moisture loss of chicken breast meat during deep-fat frying at different frying temperatures. | 51 |
| Table 4.1 | Parameters of the moisture diffusion model (Eq. 4.4) | 64 |
| Table 4.2 | Computed effective moisture diffusivity during deep-fat frying of chicken breast meat | 66 |
| Table 4.3 | Rate constants for oil uptake at different temperatures during deep-fat frying of chicken breast meat slab. | 69 |
| Table 4.4 | Computed effective oil diffusivity in chicken breast meat during deep-fat frying. | 71 |
| Table 4.5 | Comparison of predicted and observed oil uptake after 300 s frying at different FOT. | 73 |
| Table 5.1 | Pearson correlation coefficients matrix for bulk and apparent densities as a function of various process parameters | 93 |
| Table 5.2 | Estimated constant values from Equations 5.4 and 5.5 for the determination of bulk and apparent density parameters of de-boned chicken meat during deep-fat frying | 95 |
| Table 5.3 | Regression equations describing volumetric shrinkage as a function of moisture fraction for de-boned chicken meat during deep-fat frying | 100 |
| Table 6.1 | The Pearson correlation coefficient matrix between dependent and independent variables of de-boned chicken meat during deep-fat frying. (probabilities are in parentheses) | 115 |
| Table 6.2 | Pore development model parameters as a function of moisture loss in de-boned chicken meat during deep-fat frying and ANOVA statistics for the regression coefficients | 117 |

| Table 6.3 | Pore development model parameters as a function of oil uptake in de-boned chicken meat during deep-fat frying and ANOVA statistics for the regression coefficients | 120 |
|------------|--------------------------------------------------------------------------------------------------------------------------------------------------------------------|-----|
| Table 7.1 | Formulation of ground beef patties extended with soy-protein (soy protein flour and textured soy-protein) at different concentrations. | 131 |
| Table 7.2 | Mean comparison of types of soy-protein used on WHC and TCL on pan-fried beef patties extended with soy protein | 135 |
| Table 7.3 | Mean comparison of extender concentration on textural properties of pan-fried beef patties extended with SPF | 137 |
| Table 7.4 | Mean comparison of extender concentration on textural properties of pan-fried beef patties extended with TSP | 138 |
| Table 8.1 | Formulation of ground beef patties extended with soy-protein at different concentrations from 0 to 6%, for both the soy protein flour and textured soy-protein. | 155 |
| Table 8.2 | Selected factors and their levels for the first factorial design with the CCRD design. | 160 |
| Table 8.3 | Water holding capacity (WHC) of beef patties extended with soy-protein flour and textured soy-protein. | 162 |
| Table 8.4 | Total cooking losses and water activity data of the different treatments soy-protein flour and texture soy-protein | 163 |
| Table 8.5 | Structure of the experimental design and data of the dependent variables of the porosity of the samples extended with soy-protein flour and textured soy-protein | 165 |
| Table 9.1 | Pore structure properties measured by mercury Porosimetry of deep-fat fried chicken meat | 192 |
| Table 9.2 | Comparison of intrusion and extrusion volume and characterization of capillary hysteresis of deep-fat fried samples. | 196 |
| Appendix 1 | Table 1 Analysis of variance for the effects of time and frying oil temperature on moisture loss | 222 |
| Appendix 1 | Table 2 Analysis of variance of oil uptake as a function of time and temperature | 222 |

| Appendix 1 | Table 3 Analysis of variance of moisture diffusivity during deep-fat frying of chicken meat at different temperatures | 223 |
|--------------|------------------------------------------------------------------------------------------------------------------------------------------------------------|-----|
| Appendix 1 | Table 4 Analysis of variance of bulk density data for de- boned chicken breast meat deep-fat fried at 170, 180 and 190°C and at different times. | 224 |
| Appendix 1 1 | Fable 5 Analysis of variance of apparent density data for de- boned chicken breast meat deep-fat fried at 170, 180 and 190°C and at different times. | 224 |
| Appendix 1 7 | Table 6 Mean comparison of bulk density values by DMRT of de-boned chicken meat during deep-fat frying at different levels of frying temperatures | 225 |
| Appendix 1 | Table 7 Mean comparison of bulk density values by DMRT of de-boned chicken meat during deep-fat frying at different levels of frying times. | 226 |
| Appendix 1 | Table 8 Mean comparison of apparent density values by DMRT of de-boned chicken meat during deep-fat frying at different levels of frying temperatures | 227 |
| Appendix 1 | Table 9 Mean comparison of apparent density values by DMRT of de-boned chicken meat during deep-fat frying at different levels of frying times. | 228 |
| Appendix 1 | Table 10 Analysis of variance of volumetric shrinkage for de- boned chicken breast meat deep-fat at different FORs and time | 229 |
| Appendix 1 | Table 11 Mean comparison of volumetric shrinkage by DMRT of de-boned chicken meat during deep-fat frying at different levels of frying temperatures | 229 |
| Appendix 1 | Table 12 Mean comparison of volumetric shrinkage by DMRT of de-boned chicken meat during deep-fat frying at different levels of frying times. | 230 |
| Appendix 1 | Table 13 Effects of temperature (170, 180, and 190°C) and frying time (0, 5, 10 – 900 s) on porosity during deep-fat frying of de-boned chicken | 231 |

NOMENCLATURE

| ε | Porosity |
|-----------|----------------------------------------|
| γ | Interfacial tension for mercury (N/m) |
| θ | Contact angle between fluids (degrees) |
| ρ | Density (kg/m³) |
| σ | Interfacial tension (N/m) |
| τ | Tortuosity factor (m) |
| φ | Contact angle for mercury (130°) |
| ν | Cumulative volume (mL/g) |
| а | Regression constant |
| Α | Cumulative surface area (m²/g) |
| С | Oil uptake (% d.b.) |
| D | Diameter (m) |
| Ea | Activation energy (kJ/mole) |
| D_{eff} | Effective diffusivity (m/s²) |
| S_{v} | Shrinkage coefficient |
| b | Regression constant |
| g | Acceleration due to gravity (m²/s) |
| h | Capillary height (m) |
| k | Rate constant (/s) |
| 1 | Length (m) |

L Length (m)

O Oil

P Pressure (Pa)

r Radius (m)

R Universal gas constant (J/Kmol)

S Surface area (m²)

t Time (s)

T Temperature (°C)

V Volume (m³)

W Water

X Moisture loss (% w.b.)

DFF Deef-fat frying

MIP Mercury intrusion porosimeter

PSD Pore size distribution

TSP Texturized soy-protein

SPF Soy protein flour

WHC Water holding capacity

TCL Total cooking loss

ITPA Instrumental textural profile analysis

BCP Breakthrough capillary pressure

FOT Frying oil temperature

CCRD Central Composite Rotatetable Design

I. GENERAL INTRODUCTION

1.1 Background

Deep-fat frying (DFF) is considered to be one of the oldest methods of food preparation (Varela, 1988). It involves immersion of food in hot oil or fat for a given period of time, draining, cooling, and either further processing or consumption (Farkas et al., 1996). The processing conditions have significant influence on the quality attributes of the final product and on the inactivation of enzymes and microorganisms (Keller and Eseher, 1989). The frying medium also provides certain important nutritional elements, and renders an appealing texture and taste. Deep-fried (DF) snack foods are now popular worldwide for their distinct flavor and texture, as evidenced by the multi-billion dollar market products such as French fries, fried seafood, egg rolls, doughnuts, potato-, cornand tortilla chips and fried chicken. Canada alone, exports over 0.6 million tons of frozen French fries per year (Agriculture and Agri-Food Canada, 2000). Despite the fact that the deep-fat frying (DFF) industry is well established and highly automated, DFF is considered by many to be more of an art than a science (Blumenthal, 1991). However, there are some concerns as to the effects on health of consuming the additional oils, fats and degradation products that are absorbed by the food during the DFF process.

The oils used in DFF are usually blends of partially hydrogenated animal fats and vegetable oils (Brooks, 1991). They provide flavor, and increase the caloric content of the food (Gamble and Rice, 1987) and contribute nutritional

and physiological elements, such as fat-soluble vitamins, essential fatty acids, prostaglandin precursors, caloric energy and satiation (Perkins and Erikson, 1996). Because the oils are exposed to high temperature in open air they are subject to thermolytic and oxidative reactions (White 1991), causing their partial conversion to volatile chain-scission products, nonvolatile oxidative derivatives and dimeric, polymeric or cyclic substances (Blumenthal, 1991; Walter and Serbia, 1991). These degenerative reactions influence the viscosity of the frying medium over time, and the oils, fats and their by-products are a cause of public concern (Pinthus et al., 1995), due to links with cardiovascular diseases, obesity, colon cancer and other disorders. The National Heart Lung and Blood Institute (NHLBI) now recommends that the caloric intake of fats and oils should not exceed 30% of daily energy needs, thus fatty acid composition should consist of about >80% monosaturated, <10% saturates, and a maximum of 10% polyunsaturated fatty acids (Perkins and Erikson, 1996).

In face of the popularity, benefits and risks associated with DF foods, there is a need to develop a better understanding of how oils and fats are absorbed by foods that are deep-fried and how the processing conditions influence the quantities absorbed. DFF entails simultaneous heat and mass transfer, as does drying, but differs from the latter in that moisture loss is accompanied by oil intrusion and a desired crust formation. The heat transfer is initially due to a combined conduction and convection, the latter being caused by free water boiling at the surface (Singh, 1995) upon immersion of the moist food in hot oil. The further escape of moisture by vaporization results in the creation of

pathways, usually referred to as capillary pores (Gamble and Rice, 1987; Ufheil and Escher, 1996), through which hot oil enters the food. This situation is more complex than surface-to-center conduction in the traditional sense because the heat flow is accompanied by a heat-carrying mass flow towards the center. This is further complicated by the influence of oil uptake, crust formation, shrinkage and swelling, thus inducing macro- and micro-structural changes, which in turn influence vapor and liquid diffusion (Xiong et al., 1991). The relationships between changes in food microstructure due to deep-frying and food quality are very important, yet still not well understood (Nagai and Toshimasa 1990). However, information on pore development and the evolution of pore-size distribution during DFF may shed light on these relationships and lead to strategies that simultaneously ensure adequate heating for food safety assurance, and yield final products with the taste and textural characteristics expected by the consumer.

In this context, it is important to distinguish between types of foods that are deep-fried. Most foods are considered to be hygroscopic, with capillary porous matrices (Yamsaengsung and Moreira, 2002; Datta and Zhang, 1999). Insofar as heat and mass transfer during DFF are dependent on structural changes during the process, fundamental differences in the starting structure of different types of food can be expected to be important determinants in the evolution of the characteristics of the end product. Flour based products, such as doughnuts and tortilla, do not have a cohesive cellular structure since the base material was previously dried and ground, are low in protein and plant fiber.

and high in starch. Meat, fish and chicken patties are similar in the sense that the structure of the original material has been drastically altered, but are different in composition, being primarily composed of protein. Potatoes, for which there is ample literature, are also low in protein and high in starch but do have their original cell structure. However, it is quite different from muscle, which is mainly a hierarchical arrangement of protein fibers, which may relax and denature upon heating (Aguilera and Stanley, 1999; Atkins, 1987). To date, the literature on oil absorption in deep-fried foods is oriented mainly to plant-based foods and, due to the above considerations, cannot be directly adapted to meat products.

Given the intense popularity of deep-fried chicken parts and associated health concerns including microbiological safety, it was decided to investigate the relationships between frying oil temperature, cooking time, micro-structural change and oil absorption by chicken meat, while the ultimate goal of the research is to characterize pore structure in deep-fat fried food.

1.2 Hypothesis of the Research Project

This study is based on the hypothesis that porosity and pore size distribution of food product (porous medium) influence fat absorption during deep-fat frying. The assumption is that the intrinsic pore formation is the result of water diffusion out of the product forming capillary channels, which subsequently serves as pathways for fat transportation into the product during DFF.

1.3 Limitation of the Study

The scope of this study is to characterize porosity, pore size distributions and pore structure by using mercury intrusion porosimetry, liquid and helium displacement pycnometry.

1.4 Objectives

The main objective of this research project was to determine and quantify porosity and pore size distribution of deep-fat fried food products by mercury intrusion porosimetry and helium pycnometry. The characterization of pore structure requires the usage of the Washburn's model for estimation of pores in cylindrical capillary porous matrix.

The specific objectives are listed as follows:

- To establish the relationship between oil uptake and moisture loss during deep-fat frying and to explore the optimum cooking condition of the fried product using frying oil temperatures of 170, 180 and 190°C;
- To study the effect of moisture loss, oil uptake on pore development in chicken meat during deep-fat frying at frying oil temperatures 170, 180 and 190°C;
- To determine the physical properties such the bulk and apparent densities
 of fried foods as a function of time and moisture loss at frying
 temperatures of 170, 180 and 190°C;
- 4. To establish a relationship between instrumental textural analysis to pore structure on restructured meat extended with soy protein; and

5. To measure porosity, pore size distributions and pore structure by mercury porosimetry and evaluate their effect on oil uptake.

II GENERAL LITERATURE REVIEW

2.1 Chemistry of Frying Oil

Fat or oil used for deep-fat frying consists predominantly of triglycerides, which are three fatty acid molecules joined by glycerol (Stockwell, 1988) and are hydrophobic substances (Kalapathy and Proctor, 2000). The esterification of glycerol combined with fatty acids forms mono-, di-, and triglycerides. Frying oil is usually characterized based on the fatty acids present in the triglycerides. These components may be short or long chain fatty acids. Fatty acids with no double bond are referred to as saturated (eg. palmitic acid), those with one double bond are monounsaturated (eg. oleic acid); and those with more than one double bond between carbons are polyunsaturated (eg. linoleic acid). The stability of the oil depends on the molecular structure of these bonds.

Deep-fat frying is typically conducted in a temperature range of 120 to 180°C (Costa and Oliveira, 1999). The repeated and continuous use of oil at elevated temperature in the presence of air and moisture results in thermal and oxidative decomposition. As a result, volatile and nonvolatile decomposition products are formed within the medium. Foaming also occurs when products with high initial moisture content are fried. The development of surfactants by thermal alteration, results in the formation of cyclic monomers, dimers and polymers through polymerization. These cause increased viscosity (thickening). Hydrolysis, a chemical reaction that occurs in the presence of moisture and heat decomposes the triglycerides into free fatty acids (FFA) (Kalapathy and Proctor,

2000). This occurs when moisture escapes the frying food and mixes with the frying oil. Off-flavors and polar compounds are formed as a result of the decomposition of the frying oil, some of which are toxic or represent other health hazards (Romero et al., 2000). The sign of oil deterioration is the distinct odor and flavor of the frying oil. To minimize the rate of deterioration, soluble particulates and soluble components should be stirred and filtered periodically (Subramanian et al., 2000).

2.2 Theory of Fat Absorption

Deep-fat frying is a complex process that involves simultaneous heat and mass transfer. The process induces a variety of physiochemical changes in both the food and the frying medium. The principles underlying the mechanisms of water evaporation and oil absorption are intimately related. Fat absorption involves several mechanisms such as surface wetting, capillary action, and vacuum absorption (Perkins and Erikson, 1999). When the food product is immersed in hot oil, the initial fat absorption takes place through surface wetting, depending on the surface structure; some quantity of oil may be absorbed by capillary action. As the product heats up, moisture is converted to steam, migrates to the surface and eventually into the frying medium (oil) due to a pressure differential. This phase of the frying process, was regarded by Singh (1995) to be "surface boiling", during which the vapor being released from the product's surface impedes fat intrusion into the product. At the end of frying, when the product is cooled, the pressure gradient reverses and oil absorption

takes place by vacuuming the surface oil into the product (Gamble and Rice, 1987; Moreira and Barrufet, 1998; Perkins and Erikson, 1996). Moreira and Barrufet (1998) explained that as the product's temperature decreases, the interfacial tension between gas and oil increases, causing an increase in capillary pressure. This sucks the surface oil into the porous medium, thus increasing the final oil content. Sun and Moreira (1994) suggested that fat absorption is principally a post-frying phenomenon, having observed that 64% of total fat content of tortilla chips was absorbed during the cooling (post-frying) period. This phenomenon of fat absorption was related to a capillary pressure difference and the interfacial tension between the oil and gas within the pore spaces as described by Eq. 2.1 and shown Figure 2.1 and 2.2.

$$p_g = P_{alm} + \frac{2(\sigma \cos \alpha)}{r} - \rho g h \tag{2.1}$$

Where:

 $P_{\rm g}~=$ Gas pressure in the capillary tube;

 P_{atm} = Atmospheric pressure (Pa);

 σ = Interfacial tension between fluids above and below the meniscus (N/m);

 α = Contact angle between liquid and solid (rad);

 ρ = Density of fluid mixture underneath the meniscus (gas and oil) (kg/m³);

g = Acceleration of gravity (m/s²); and

h = Capillary height of fluid mixture (oil and /or gas) absorbed (m).

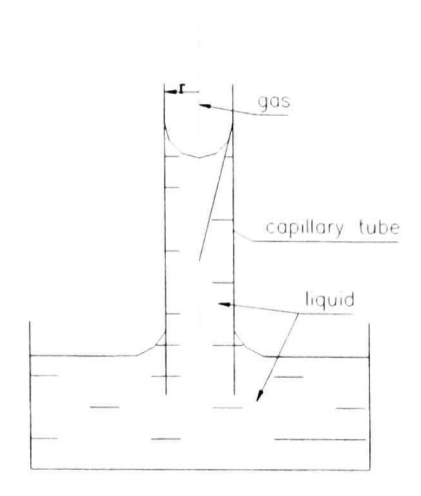


Figure 2.1 Capillary action of wetting liquid in a capillary tube at atmospheric pressure. (Source: Moreira and Barrufet, 1999.

Deep-fat frying: Fundamentals and Applications).

Mamur (1989) represented a two fluid phase model for capillary rise in a microscopically cylindrical porous medium by the following relationship:

$$h_0 = \frac{(1 - \varepsilon_o) S_0 \gamma_{ow} \cos \theta}{\rho g \varepsilon_o}$$
 (2.2)

where:

 h_0 = capillary rise;

 ε = overall porosity;

 S_0 = overall surface area;

 $\gamma_{\mbox{\tiny ow}}$ = interfacial tension between water and oil; and

 θ = contact angle,

Ufheil and Escher (1996) also suggested that the absorption theory was based on a surface phenomenon, which involves equilibrium between adhesion and drainage of oil during cooling. Fat absorption in chips due to surface adherence

was the result of steam condensation, as also suggested by Gamble and Rice, (1987).

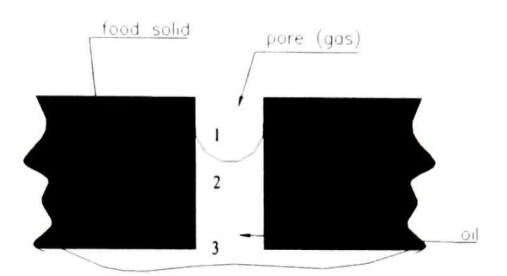


Figure 2.2 Pressure relationship for food product undergoing cooling.

(Source: Moreira and Barrufet, 1999. Deep-fat frying:

Fundamentals and Applications).

Many factors affect oil uptake during DFF. These are oil quality, frying temperature, residence time, product shape and size, product content (initial moisture content, solid, protein), pore structure (porosity and pore size distribution), and pre-frying treatments (drying, blanching, surface coating). Interfacial tension was also reported by Pinthus and Saguy (1994) to have a significant influence on oil uptake during deep-fat frying.

2.2.1 Factors that influence fat absorption

The quality of deep-fat fried products is affected by several factors. Those that influence fat absorption and mobility are discussed in the following subsections.

2.2.1.1 Frying time

Frying time is a significant parameter that affects fat absorption. Ufheil and Escher (1996) correlated oil uptake with frying time. Moisture content was also correlated with the square root of frying time (Gamble and Rice, 1987; 1988). The longer foods fries, the more their physical properties change, i.e., density, porosity, oil uptake, surface hardening, crispiness, and etc.

2.2.1.2 Frying temperature

Oil temperature during DFF alters the physiochemical properties due to the interaction of oil and water, which results in the formation of undesirable compounds (Blumenthal, 1991; Fritsch, 1981) and affects the viscosity. For example, viscosity is an important physical property, which significantly influences mass transfer. Viscosity decreases as temperature increases, but heating over a long period can result in an increase in viscosity. Singh (1995) reported that the kinematic viscosity of corn oil increases from 2.55 to 3.28 mm²/s as oil thermally degrades. Gupta et al. (2000) and Kassama and Ngadi (2000) reported a substantial increase in oil uptake at higher frying temperature due to lower viscosity. Potato chips fried at higher temperatures (177°C) have lower oil content than chips fried at (149°C), because the low viscosity at higher temperature facilitates drainage of fat from the chips (Shaw and Lukes, 1968). Oil temperature may significantly affect the rate of change of physical characteristics and microstructure of the food products due to different degrees

of thermal gelatinization of starch in potato products and denaturation of protein in meat products over a given period of time.

2.2.1.3 Moisture content

Moisture content plays a significant role in pore formation (Hussain et al., 2002; Rahman et al., 2002). Fat absorption is dependent on the initial moisture content of the food product being fried. Foods are hygroscopic materials and carry significant quantities of bound water in their porous matrix. As a result, as water diffuses from the matrix during frying, pathways usually referred to as 'capillary pores' are left. The formation of capillary pores enhances oil absorption, however, the occurrence of this process is still not fully understood. Many researchers have reported that the relationship between moisture loss and fat absorption is linear (Gamble and Rice, 1987; Krokida et al., 2000). Physical properties such as porosity and pore size distribution are modified as a result of physicochemical reactions between the food ingredients, such as solids and liquids within the food matrix during DFF (Kassama and Ngadi, 2001).

2.2.1.4 Oil quality

Oil quality is essentially the characteristic property that distinguishes the grade of excellence of fried products. The quality of oil influences the acceptability of the final product in terms of textural and sensory attributes. The frying oil changes with time (age). Oil contains high percentage (96-98%) of

triglycerides. The ideal oil quality is achieved at break-in (Table 2.1). However, extended use exposes the oil to diffused water, heat, light, and oxygen, which react with the triglycerides to form free fatty acids, polar and non-polar compounds and alkaline soaps as shown in Table 2.1. As the concentration of these materials increases, many physiochemical properties of the oil change: viscosity, thermal conductivity, dielectric properties, specific gravity, specific heat capacity, surface tension and interfacial tension. These changes influence fat absorption.

Table 2.1 Deep-fat frying oil quality parameters: phases oil passes through during the degradation process.

| Oil quality | Triglycerides (%) | Polar compound (%) | Polymers (%) | Free fatty acids (%) | Oxidized fatty acids (%) | Soaps (ppm) |
|-------------|-------------------|--------------------------|-----------------|-------------------------------|--------------------------|----------------|
| New oil | >96 | <4 | 0.5 | 0.02 | 0.01 | 0.7 |
| Break in | 90 | 10 | 2.0 | 0.50 | 0.08 | 10.0 |
| Fresh | 85 | 15 | 5.0 | 1.00 | 0.20 | 35.0 |
| Optimum | 80 | 20 | 12.0 | 3.00 | 0.70 | 65.0 |
| Degraded | 75 | 25 | 17.0 | 5.00 | 1.00 | >150.0 |
| Runaway | 65 | 35 | 25.0 | 8.00 | 2.00 | >200.0 |

Source: Blumenthal, M.M. and R.F. Stier 1991. Trend in Food Science and Technology.

2.2.1.5 Interfacial tension

Deep-fat fried food is assumed to consist of two liquid phases (water and oil) in its porous matrix. As a result, the contact angle can be used to determines which pores are to be filled by which liquid (Pinthus and Saguy, 1994). The interfacial tension between the fluid phases can determine whether external oil can overcome the energy barrier created by the pressure gradient, and infiltrate the porous structure. The fundamental equation relating contact angle and interfacial tension (Figure 2.3) is Young's equation:

$$\gamma_{OW} \cos \theta = \gamma_{WS} - \gamma_{OS} \tag{2.3}$$

where:

 γ = surface tension between solid and liquid (N/m),

Subscripts

S = solid;

W = water;

O = oil; and

 θ = contact angle.

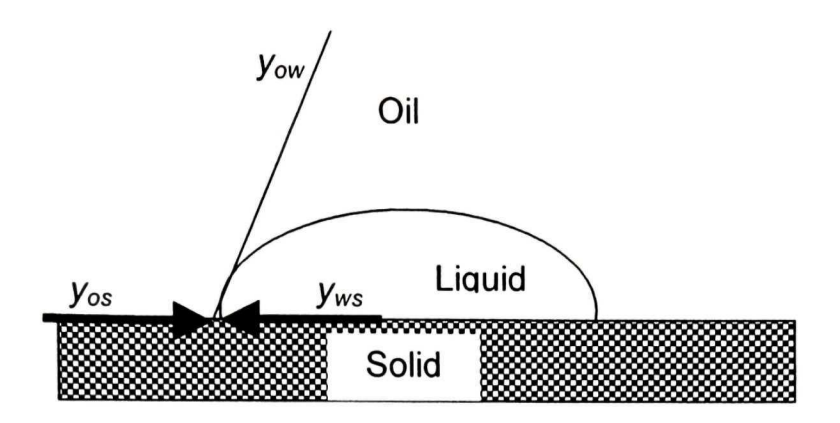


Figure 2.3 Interfacial tension between oil, water and food solid. (Source: Adamson, 1990. Physical Chemistry of Surfaces).

The formation of surfactants in the frying oil, as a result of chemical reaction between the product and the frying oil modifies the rheological properties of the frying media. This modification affects the contact angle and interfacial tension between the frying media, water, and the product. Pinthus and Saguy (1994) reported increasing interfacial tension with increasing oil uptake. The authors report a power law relationship between the initial interfacial tension and oil uptake. No information was reported on the effect of structural changes such as pore formation on the surface and interfacial tension on fat absorption.

2.2.1.6 Product geometry

Product shape and size affect the time needed to achieve the optimum center temperature during deep-fat frying. For example, the thinner the piece, the faster the optimum center temperature is attained. The moisture removal rate is usually faster than the center heating rate. Moreira et al. (1999)

compared the moisture loss rate of 2.6 mm and 1.6 mm deep-fried chips and concluded that the thicker chip (2.6 mm) took more than 100 s to acquire equilibrium moisture content (2% wb). The thicker material usually absorbs less fat during deep-fat frying. Fat absorption increases with higher-surface/mass ratio of fried products (Gamble and Rice, 1988). Although, thicker products are less likely to absorb more oil, but to achieve the optimal center temperature may prolong the frying time while quality may be compromised.

2.2.1.7 Pre-frying treatment

The effects of pre-frying treatments on oil uptake have been studied. Lamberg et al. (1990) blanched potatoes prior to frying. They found that oil uptake was lower when blanched potatoes were dried than when deep-fried with surface moisture remaining. Gamble and Rice (1987) compared the effects of pre-drying potatoes by microwaves, hot-air and freeze-drying on oil uptake. They found that microwave and hot-air drying reduced the oil uptake during DFF, whereas freeze-drying increased it.

Coating the surface of food products with batter, breading, and edible films prior to frying influence fat uptake. Mohamed et al. (1998) reported that coating with ovalbumin reduced fat absorption. William and Mittal (1999) coated various foods with edible films (gellan gum, methyl cellulose and hydroxypropyl cellulose) and reported that oil uptake during DFF was 50 to 90% lower than in the uncoated products. Huse et al. (1998) also reported significant reduction in oil uptake by deep-fried akara coated with edible film.

2.2.1.8 Post-frying oil penetration

The post-frying penetration of oil is a subject of controversy. Many researchers have suggested that fat absorption is primarily a post-frying phenomenon (Yamsaengsung and Moreira, 2002; William and Mittal, 1999; Perkins and Erickson, 1996), thus fat transfer occurs in food product during the cooling process. Gamble et al. (1987) and Ufheil and Escher (1996) suggested that the post-frying phenomenon of oil absorption is due to a vacuum pressure created by condensation of steam inside the product, resulting in a mass flow of oil from the surface and into the product. Moreira and Barrufet (1998) reported that 80% of the total oil content was absorbed in tortilla chips during the cooling period.

2.3 Pore Structure

Thermal processing of food causes physicochemical reactions that can affect food structure. As food cooks, the food moisture is converted to steam and releases under pressure, forming capillary voids. The type of process and the intensity of heating, coupled with the initial moisture content of the food product influence the final pore structure. For example, large diameter pores were observed in an over-cooked DFF tortilla chip, and the pores were saturated with oil (McDonough et al., 1993). Three types of pore structure could characterize void spaces formed in porous solids, namely: (a) interconnected pore segments, (b) isolated or non-interconnected pores and (c) dead-end or blind pores. The

interconnected pores are usually accessible from many directions (Figure 2.4). Blind or dead end pores are accessible from one direction only. Non-interconnected pore are inaccessible islands buried in the solid matrix of the porous material and behave as part of the solid (Dulien, 1992). Isolated pores therefore decrease the diffusivity characteristics of the porous medium.

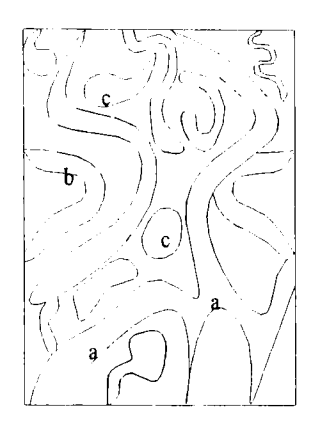


Figure 2.4 Illustration of different types of connectivity in a porous structure.

The pore structure of a fried food influences its mechanical properties and thus its acceptability in terms of texture (Clayton and Huang, 1984). Texture and friability are influenced by pore size distribution and sizes of the capillaries. Pore structure has a strong influence on the macro and microscopic properties of the porous medium. Pore parameters are usually classified as macroscopic and microscopic.

2.3.1 Macroscopic pore structure

Macroscopic pore structure is coined to distinguish the pores constituting the main skeleton of the pore network, as shown in Figure 2.4. The macroscopic

pore structure is more closely related to the transport characteristics of the porous medium. The most important macroscopic pore parameters are density, porosity, specific surface area and breakthrough capillary pressure.

2.3.2 Porosity and density

Density is the mass of a quantity of matter per unit volume of the same quantity. However, the density can be defined according to different perceptions. The true or skeletal or solid density, also referred to as absolute density, refers to that density calculated on the basis of the volume excluding both the pores that may be in the volume, and the interparticle spaces. The apparent density (envelope density) is based on the volume including the pores but excluding the interparticle spaces. The bulk density rests on the volume measurement including both the pores and the interparticle spaces.

Several researchers used either helium pycnometer or mercury porosimetry technique to measure absolute densities (Kassama et al., 2003; Kassama and Ngadi, 2001; Karathnaos et al., 1996). Helium pycnometry is a displacement technique and sample volume is calculated from the observed pressure change the gas undergoes when it expands from one chamber containing the sample into another chamber (expansion chamber) without the sample (Figure 2.5). Gas fills all open spaces including that of the pores. Helium is the preferred gas for measuring absolute density because it can penetrate most of the pores in food materials due to its minute atomic radius (3 Å)

(Karathanos et al., 1996; Karathanos and Saravacos, 1993; Chang, 1988). The general equation for computing the sample volume is,

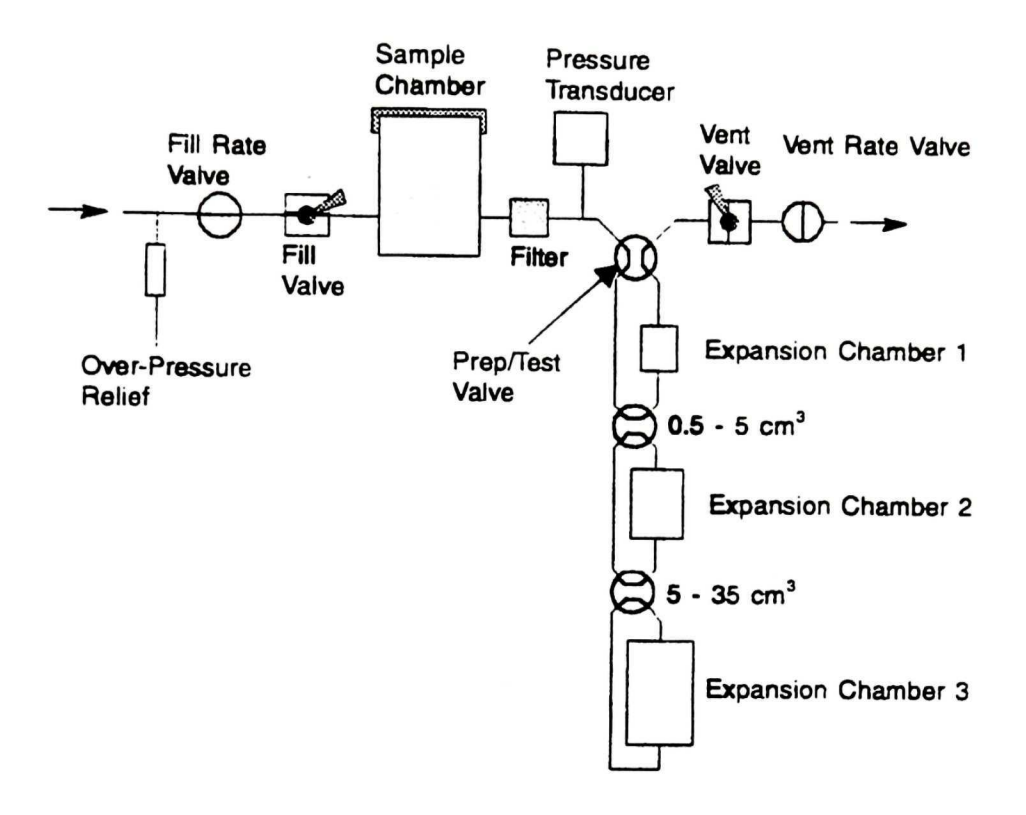


Figure 2.5 Schematic diagram for a multi-volume helium pycnometer.

$$V_{Samp} = \frac{V_{Cell} - V_{Exp}}{\left[\left(\frac{P_1}{P_2} \right) - 1 \right]}$$
 (2.4)

where $V_{\it Samp}$ is the sample volume being measured, $V_{\it Cell}$ the volume of the sample cell with the empty sample cup, $V_{\it Exp}$ is the expansion volume, $P_{\it l}$ is the initial

pressure of the sample volume chamber, and P_2 is the final pressure measure after expansion.

The bulk density is measured by liquid displacement. Krokida et al. (2000) used n-heptane, Moreira et al. (1999) used toluene and Hicsasmaz and Clayton (1992) used fine sand to measure the bulk densities of various foods. The apparatus shown in (Figure 2.6) consists of two compartments. The samples are immersed in the top compartment and sealed. When turned upside down the displaced volume is determined.

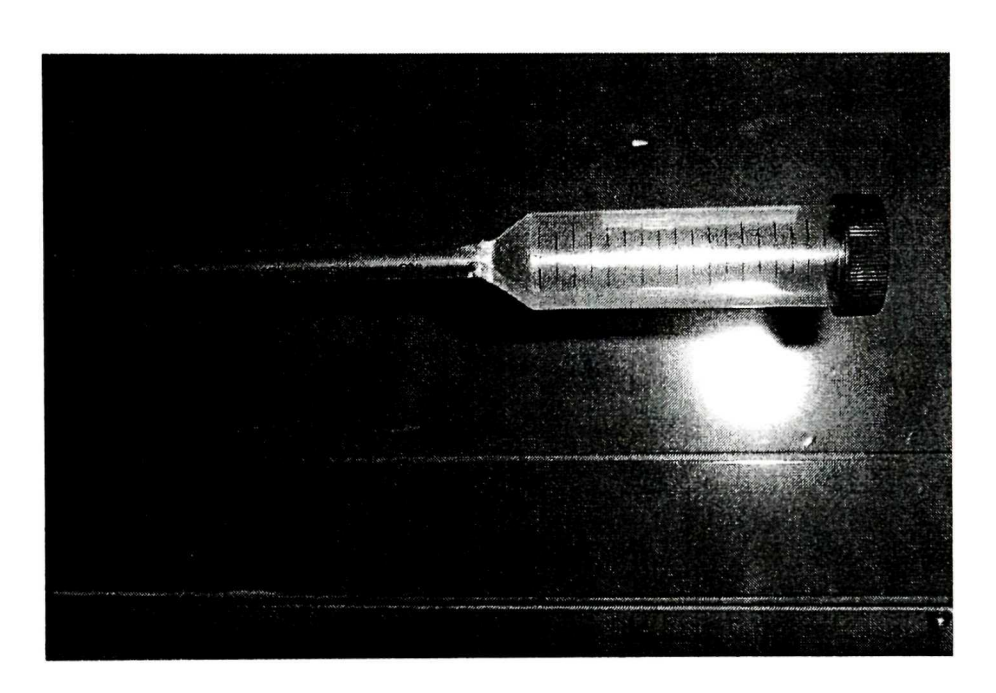


Figure 2.6 Volume displacement pycnometer for measuring bulk volume of food stuff.

Porosity, also referred to as voidage, is the fraction of the bulk volume of a porous medium that is occupied by pores or void spaces.

$$\varepsilon = 1 - \frac{\rho_b}{\rho_s} \tag{2.5}$$

where:

 ε = porosity,

 ρ_b = bulk density, and

 ρ_s = solid density.

Porosity may vary from near zero to unity. Pores are classified into two categories, those one that form a continuous phase within the porous medium (interconnected or effective pores), and isolated or non-interconnected pores. The interconnected pores contribute to the transport of fluid across the porous medium. Dead end pores may exist within the interconnected pore network; however their influence on flows is limited.

2.3.3 Specific surface area

The specific surface area is the interstitial surface area of the voids and is defined either by the per unit mass or per unit bulk volume of the porous material. It plays an important role in a variety of different applications of porous media. Specific surface area determines the adsorption capacity of various adsorbents, likewise it influences the effective fluid conductivity and permeability of porous media (Dullien, 1992).

2.3.4 Breakthrough pressure

The penetration of a non-wetting phase into networks of capillary tubes of randomly distributed diameters as a result of pressure, is called the capillary breakthrough pressure or the bubbling pressure. This is an important macroscopic parameter of a porous medium; it correspond to the appearance of a non-wetting phase i.e., mercury on the outlet phase of a sample. Dullien (1992) used mercury Porosimetry to determine the breakthrough pressure and the equivalent pore size for sandstone. Breakthrough pressure is deduced from Eq. 2.6 (Adamson, 1990).

$$P_{cb} = -\left(\frac{1}{P_c}\right) 4\gamma \cos \varphi \tag{2.6}$$

where P_{cb} is the capillary breakthrough pressure, P_c capillary penetration pressure, γ surface tension of the wetting fluid and φ contact angle of the wetting fluid. The breakthrough capillary pressure (BCP) is determined with the aid of a non-wetting fluid (mercury) and the data are used to characterize the pore structure of porous medium. The BCP is the pressure at which the penetrating fluid becomes hydraulically conductive in the macroscopic sample. The BCP can be used to compare the influence of different treatments on porous samples.

2.3.5 Microscopic pore structure

Mercury porosimetry, gas sorption or microscopic imaging, are used to determine microscopic pore structure. It must be noted that the characterization

of microscopic structure is extremely challenging due to the peculiar geometry of pore structures. Microscopic pore structure parameters are pore size (diameter, volume), pore size distribution and the volume distribution function (Dullien, 1992).

2.3.6 Topology of pore structure

The parameters that characterize pore topology are the dimensionality of the network and connectivity.

2.3.7 Connectivity

One of the most important topological parameters characterizing the interconnectedness of shapes or structure is the connectivity. Connectivity is a topological parameter that measures the number of times a pore structure is connected (Figure 2.7). It defines the number of non-redundant closed loops, and redundant loops that transform into another branch of pores and at some instances may terminate at some point without access to any new branch.

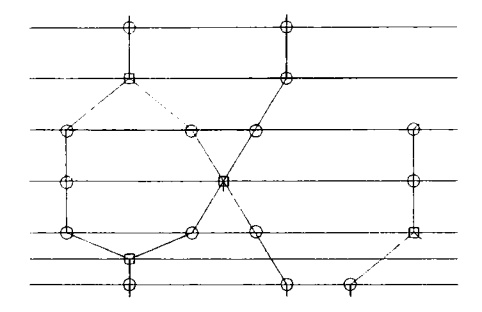


Figure 2.7 Pore structure illustrating branches and node with a porous matrix.

2.3.8 Pore size

Pore size may be defined as a portion of a pore pace bounded by solid surfaces; this could be analogously to a room defined by walls and a door opening to it. If the door is assumed to be the pore throat, while the hydraulic radius of the pore throat defines the pore's size, regardless of the shape of the pore (loannidis and Chatzis, 1993).

Hydraulic radius (r_H) $(r_H = r_m/2)$ is used as a measure of pore throat, and is useful in determining the cross sections of irregularly-shaped pores.

where r_m is the mean radius of curvature. Equation 2.7 is related to the capillary pressure P_c , a pressure difference across a fluid/fluid interface of r_m shown by Laplace's equation:

$$P_c = \frac{2\gamma}{r_m} \tag{2.7}$$

where γ is the interfacial tension. For non-zero contact angle fluids (mercury) the following relationship is used:

$$R = r_m \cos \theta \tag{2.8}$$

The pore radius R is determined by substituting Eq. 2.8 into Eq. 2.7.

2.3.9 Pore size distribution

Pore size distribution (PSD) is the table or graph of relative frequencies of pore sizes and is usually determined by fitting an experimental data to the Washburn's model (Dullien, 1992). PSD is commonly determined with a mercury porosimeter (Kassama et al., 2003; Rahman et al., 2002; Ngadi et al., 2001; Karathanos et al., 1996). The volume of mercury penetrating a sample is measured over a range of pressures. The pore size is calculated based on the capillary pressure obtained from the Laplace equation (Eq. 2.7) and using the bundle of capillary tubes (cylindrical) model of pore structure (Webb and Orr, 1997). Porosity and pore size distribution influences textural characteristics of dried foods (Huang and Clayton, 1990). Porosity and crispiness in extruded foods were correlated (Hussain et al., 2002).

2.3.10 Factors that influence pore structure

The dynamics of mass transfer and quality development are related to the development of microstructure in deep-fat fried food products. Most food materials are classified as hygroscopic and capillary porous media (Datta and Zhang, 1999). Vapor pressure build-up during deep-fat frying exerts stress on the pore walls and deforms the pore structure within the porous medium.

Changes in microstructure affect the bulk density and influences pore development and oil uptake. Moreira et al. (1995, 1997) reported that bulk density of tortilla chips decreases, while porosity and oil uptake increase as frying progresses. Hussain et al. (2002) associated stronger food agglomerates to high

apparent density and low porosity. The authors reported that the initial moisture content and particle size distribution of masa flour in tortilla chips affected the final oil content. The smaller the particle size (fine) of flour the more oil is absorbed in fried tortilla chips. Pinthus and Saguy (1994) reported that high initial porosity increases oil uptake during the initial stage of frying. At the end of the frying phase, porosity is lower as a result of the absorbed oil embedded in the pore spaces.

The MIP is used for quantifying food microstructure (Kassama et al., 2003; Ngadi et al., 2001; Kassama and Ngadi, 2001; Karathanos et al., 1996; Farkas and Singh, 1991) and measures micropore of up to 0.005 μ m pore diameter at a maximum pressure of 207 MPa.

2.4 Hierarchical Structure in Meats

In meats, the void structures are primarily the result of the hierarchical arrangement of muscle fibers and collageneous connective tissues. A single muscle fiber consists of many myofibrils, the contractile elements, sheathed by the endomysium, which is a composite structure of collagen fibers. The muscle itself is composed of bundles of muscle fibers, each fiber (10-100 µm) (Bailey and Light, 1989) held together by a collagen network, the perimysium, and the whole muscle structure held by a network called the epimysium (Flint, 1994). This type of arrangement is common to most vertebrates, i.e., poultry, beef and vertebrate fish. The water-holding capacity is highly dependent on pore structure (Ofstad, 1993). Meat, like most food materials, undergoes structural

(physicochemical) transformations as a result of thermal processing. When muscle is subjected to heat, the fibers begin to shrink in the transverse direction at 40-60°C (Offer et al., 1989). The collagen network shrinks at 60-70°C due to denaturation.

2.5 Mercury Intrusion Porosimetry

Mercury Intrusion Porosimetry (MIP) is a technique used in the study of pore structure and pore size distribution since in the 1960s. Pore sizes, pore volume, size range, areas and pore size distribution of porous media can be obtained with this technique. The method is only applicable to dehydrated solid samples that can withstand a high compressive stress without amalgamating or reacting with mercury. Mercury porosimeters are available in many configurations, can generate pressures up to about 414 MPa and can be used to determine pore diameters in the range of 360 to 0.005 μm.

Many researchers have used MIP to characterize pore structures of biological materials. Farkas and Singh (1991) reported a porosity value of 64% for freeze-dried chicken meat using MIP technique, while King et al. (1968) reported a range of about 70 – 80%, and a density of 1.33 g/mL. Karathanos et al. (1996) characterized pore structures of a number of agricultural plant products. The author suggested that the majority of the pores were smaller than 30 um based on volume distribution function analytical approach.

2.5.1 Principles of mercury porosimetry

The principle of mercury porosimeter is based on the capillary law. Washburn E. W. first characterized the behavior of non-wetting fluid in an inundated porous medium in the 1920s (Dullien, 1992). Mercury is one of the most suitable liquids for porosimetry, because it is non-wetting with most substances and will penetrate pores upon application of force but not by capillary action. The applied pressure is inversely proportional to the pore opening. Liquid mercury has a high surface tension (485 dyne/cm) and exhibits a high contact angle with solids. The advancing contact angles during porosimetry may range from 112 to 142° and the receding angles are usually reduced by 30° (Webb and Orr, 1997). When mercury is in contact with a pore of circular cross-section, the surface tension acts along the periphery of contact, which equals the perimeter of the circle, as shown in Figure 2.8.

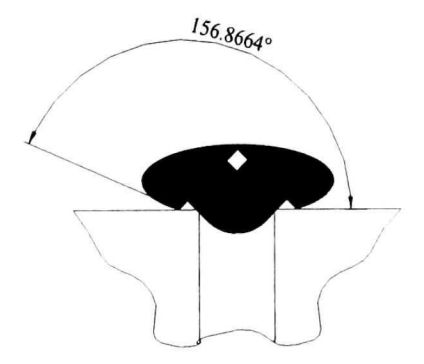


Figure 2.8 Mercury in contact with the porous solid.

The force resisting penetration is presented by the following relationship (Eq. 2.9):

$$F = -\pi D \gamma \cos \varphi \tag{2.9}$$

The intrinsically negative sign is the indication that the contact angle is greater than 90°. The external force required to achieve penetration (Eq. 2.10).

$$-\pi D \gamma \cos \varphi = \frac{\pi D^2 P}{4} \tag{2.10}$$

Combining Eq. 2.9 and 2.10, yields the Washburn equation (Eq. 2.11) which is commonly used for modeling pore sizes and PSD (Webb and Orr 1997; Orr 1969):

$$D = -\left(\frac{1}{P}\right) 4\gamma \cos \varphi \tag{2.11}$$

where:

D = pore diameter,

P =is the applied pressure at which the mercury is forced into the sample,

 γ = surface tension of mercury given as 0.485 N/m, and

 φ = solid-liquid contact angle (130°).

During the extrusion cycle, the high pressure generated is reduced sequentially to atmospheric pressure. Although, the reduction in pressure is in harmony with Eq 2.12, the receding contact angle is affected and is less than the advancing angle. This may be attributed to pore irregularities giving rise to an enlarged chamber and "ink-well" structure as shown in Figure 2.9.

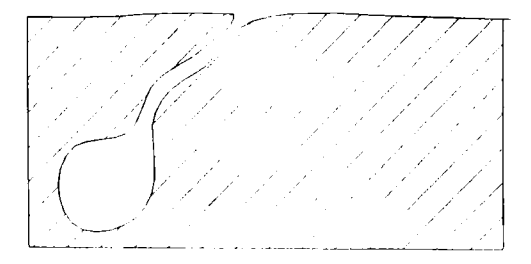


Figure 2. 9 Illustration of an inkbottle pore.

These phenomena give rise to the hysteresis phenomena, e.g., the difference between the intrusion and extrusion P-V curves. The pore volume distribution function $D_{\nu}(r)$ and the specific surface area (S) (Eq. 2.12 & 2.13) can be computed from the cumulative volume of intrusion vs pore radius data acquired from the porosimeter.

$$D_{\nu}(r) = \left(\frac{P}{r}\right) \left(\frac{d(V_{\iota} - V)}{dP}\right)$$
 2.12)

$$S = \left[\frac{1}{\gamma \cos \theta}\right] \int_0^{V_F} P_i dV = \left[\frac{1}{\gamma \cos \theta}\right] \sum_i P_i \Delta V_i$$
 (2.13)

2.6 Mass Transfer During Deep-fat frying

Moisture loss and oil absorption during frying may be considered to occur simultaneously (Figure 2.10), since they both appear to be linearly related to moisture diffusivity (Mittleman et al., 1984). Many researchers have assumed

the process to be diffusion controlled and therefore governed by Fick's second law (Eq. 2.14 and 2.15):

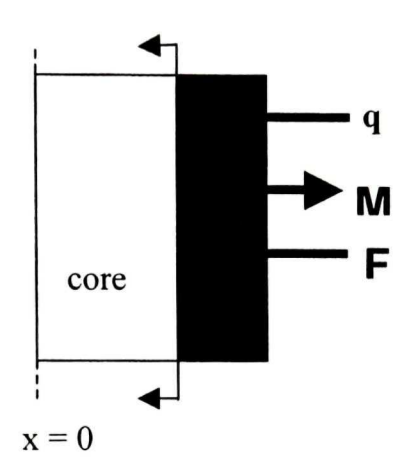


Figure 2.10 Heat and mass transfer in an infinite slab representing a food product, where q, is defined as the heat flux, M, moisture loss, F, fat/oil uptake during deep-fat frying.

$$\frac{\partial}{\partial l} \left[D_{w_{eff}} \frac{\partial X}{\partial l} \right] = \frac{\partial (X)}{\partial t}$$
 (2.14)

$$\frac{\partial}{\partial x} \left[D_{f_{eff}} \frac{\partial C_f}{\partial x} \right] = \frac{\partial (C_f)}{\partial t}$$
 (2.15)

Where:

 D_{eff} = effective diffusivity of liquid (m²/s);

X = moisture loss (% w.b.);

C = Oil uptake (%);

l =thickness of the test specimen; and

$$t = time(s)$$

The subscript w represents water and f represents fat.

One-dimensional Fick's mass diffusion on an infinite slab can be used. The solution to Fick's law for an infinite slab by Newman's analytical procedure (Eq. 2.16), as used by Crank (1975) is:

$$X = \frac{8}{\pi^2} \sum_{n=0}^{\infty} \frac{1}{(2n+1)^2} \exp\left[-(2n-1)^2 \frac{\pi^2}{4} \frac{D_{eff} t}{L^2}\right]$$
 (2.16)

where:

X = moisture loss (kg/kg- w.b.); or

C = oil uptake (%); and

L = half thickness of the infinite slab (m).

The Eq. 2.16 can be further simplified into Eq. 2.17 by assuming certain values negligible, this insignificant compared to values retained.

$$x = \frac{8}{\pi^2} \exp\left[-\frac{\pi^2 D_e t}{l^2}\right]$$
 (2.17)

The effect of temperature on effective diffusivity was expressed in terms of the Arrhenius equation (Eq. 2.18):

$$D_{eff} = D_0 \exp\left(-\frac{E_a}{RT}\right) \tag{2.18}$$

where:

 D_0 = effective diffusivity at high liquid concentration;

 E_a = activation energy;

T = absolute temperature; and

R = universal gas constant.

The effective diffusivity coefficient in a porous medium as shown in Eq. 2.19 (Datta and Zhang, 1999):

$$D_{eff} = D \frac{\varepsilon}{\tau} \tag{2.19}$$

where:

 ε = porosity;

D =diffusion coefficient at a references temperature; and

 $au = \frac{l_e}{l}$ = tortuosity factor and l_e is the effective average path length, and

l is the shortest distance.

Rice and Gamble (1989) reported effective moisture diffusivity to be in the range 1.40E-09 to 1.55E-08 m²/s for frying potatoes at 145 to 185°C for potatoes. Effective moisture diffusivity for chicken drums ranged from 1.32E-09 to 1.64E-08 m²/s during DFF (Ngadi, 1995). Both authors reported activation energy of 24 kJ/mole.

CONNECTING TEXT

Porosity and pore size distribution are physical properties that influence heat and mass transfer during deep-fat frying of food products. The understanding of these physical properties could lead to the development of better products. However, the literature review has revealed that there is a lack of information on the relationships between pore structure and transport phenomena occurring during deep-frying of meat products. While the focus of this thesis is pore development and pore structure characterization of fried foods, Chapter III gives an insight on the relationship between oil uptake and moisture loss during deep-fat frying of chicken breast meat. The effect of frying oil temperature and frying time are evaluated. A cook-value is established to estimate frying time in terms of quality and safe product.

III. RELATIONSHIP BETWEEN OIL UPTAKE AND MOISTURE LOSS DURING DEEP FAT FRYING OF CHICKEN BREAST MEAT

3.1 Abstract

The relationship between moisture loss and oil uptake at different combination of frying oil temperatures and time during deep-fat frying of chicken meat were investigated in this study. Chicken meat samples were diced and fried at different temperatures (170, 180, and 190°C) in an industrial fryer for periods varying from 5 to 900 s. Fat analysis was accomplished in a soxhlet extraction apparatus with petroleum ether solvent. Both fat and moisture analysis were conducted after freeze-drying. A cook value of 415 s was found to give the most ideal sensory characteristics. The relationship between moisture loss and oil uptake during the initial phase of frying (< 45 s) was erratic and appeared to be independent of frying oil temperature. A linear correlation existed (r = 0.97) between moisture loss and frying time. Oil uptake was positively correlated to moisture loss in the range of frying times 45 s to about 600 s. After 600 s, oil uptake tended to equilibrate while moisture loss continued. The relationship between moisture loss and oil uptake is an important phenomenon in the context of fried product. properties characterizing the physical of

3.2 Introduction

Despite the fact that excessive consumption of foods that are deep-fat fried has been linked to coronary disease and several forms of cancer (Browners et al., 1991), such foods remain popular due to their unique taste and rapidity of preparation. In consequence, there has been interest in determining how to minimize oil absorption while preserving the organoleptic characteristics that are favorable to the consumer, such as crispiness, color, and flavor (Saguy and Pinthus, 1995). Chicken is one of the most popular deep-fried foods. Raw chicken can contain from 1 to 5% saturated fats, depending on the part and whether with or without the skin. Although edible films coatings have been shown to reduce fat absorption by chicken meat (Balasubramaniam et al., 1997; Mallikarjunan et al., 1995), there is little information concerning fat absorption mechanisms of uncoated chicken.

Most of the research on the mechanism of fat absorption has been conducted on potatoes and plant-based products (tortillas, falafel balls, etc.), whereas little information is available for fat absorption of meat products. It has been shown that fat absorption by thin potato slices is directly related to moisture loss, that moisture loss is proportional to the square root of frying time and that frying oil temperature has an indirect affect on oil absorption (Gamble et al., 1987; Mittelman et al., 1982). These relationships have been studied for various foods (Krokida et al., 2000; Moreira et al., 1999; Singh, 1995; Keller and Escher, 1989; Gamble and Rice, 1987; Keller and Escher, 1986; Ashkenazi et al., 1984; Du Pont et al., 1982; Mittleman et al., 1982); however, there is some

disagreement as to the mechanisms of fat absorption. Moreover, fundamental differences in composition and structure of various food materials make it difficult to generalize results, even though foods in general are considered to be hygroscopic porous media.

Since chicken is one of the most popular deep-fried meat products, we chose to study the relationships between moisture loss and oil uptake at different combinations of oil temperature and frying time as a first step in elaborating the mechanisms of the combined heat and mass transfers involved.

3.3 Materials and Methods

3.3.1 Materials

Chicken breast samples supplied by a local chicken product manufacturer were used throughout this study. The stocks of samples were stored in a freezer at –20°C until used.

3.3.2 Sample preparation

Frozen samples were removed from a freezer and thawed in a refrigerator at 4°C for 24 h. The samples were diced into cubes of approximately 5 cm \times 3 cm \times 1 cm (\pm 0.5 cm). Minor departures from the target dimension were due to the irregular shape of the chicken breasts.

3.3.3 Frying

A programmable computerized pressure deep-fat fryer (Henny Penny Computron 7000 Pressure Fryer, Model 500C, Henny Penny Corporation, Eaton, OH.), with a fat holding capacity of about 30 L was used. A liquid shortening (Can Amera Food, Oakville, ON) was used for frying and the sample to oil weight ratio was about 1:480. The fresh oil was preheated at 170°C for 2 h and then adjusted to one of the three oil temperatures used for frying in this study (170, 180, 190°C). Three samples were fried at each of twenty frying times: 5, 10, 15, 20, 30, 45, 60, 90, 120, 150, 180, 210, 240, 300, 360, 420, 480, 540, 600, or 900 s. Frying times were randomly chosen within temperature and the triplicates were run sequentially at the given frying time. This procedure was preferred to a completely randomized approach, which would have resulted in significant time lapses for heating and cooling the oil. The fried samples were removed from the frying oil, cooled at room temperature, weighed using a TR-4102D scale, (Denver Instrument Co., Denver, CO), placed in plastic Zip-Lock sample bags, and frozen at -20°C in a freezer prior to further analysis.

3.3.4 Cook-value

The frying condition was adjusted to assure cooking at the center to attain a satisfactory texture. The center temperature of the chicken meat strip was measured with a T-type thermocouple (copper-constantan) placed at the geometric center of the product. The center temperatures were then used to

determine the cook-value (C-value), or cooking time equivalent at 100°C, as defined in Eq. 3.1 (Leonard et al., 1964, Dagerskog, 1977):

$$C = \int_{t}^{t} 10^{(T-T_r)/Z_c} dt \tag{3.1}$$

where, t_i is the beginning of the frying time, t_f time when frying is completed, T_r is the reference temperature (100°C), Z_c is the necessary temperature rise for a 10-fold increase in the reaction rate for chemical, physical or sensory change, taken as 24°C according to the value reported by Dagerskog (1977) for the rheological property of cooked meat.

3.3.5 Drying and moisture analysis

Drying of the fried samples was conducted using a freeze dryer (ModulyOD-115, Thermo Savant, Holbrook, NY) for 30 h. All the samples were dried at a temperature of –50°C and a pressure of 750 µm Hg. The initial mass of the samples prior to drying and the final mass of the dried product were determined using a TR-4102D scale (Denver Instrument Co., Denver, CO).

3.3.6 Fat analysis

The freeze-dried fried samples were ground using a blender (Proctor-Silex, model E160B, Picton, ON). The ground samples (2 – 4 g) were weighed with an electronic scale (TR-4102D, Denver Instrument Co., Denver, CO) and placed in a thimble. Some sea sand was added to the sample in the thimble and mixed with

a glass rod. Fat was extracted in a solvent extractor (SER148, Velp Scientifica, Usmate, Italy) using petroleum ether. The mass of the glass extraction cups with a few boiling stones was recorded and 50 mL of petroleum ether was added to each cup. The thimbles were then inserted to the magnetic connector of the extraction unit. Procedure followed as recommended by AOAC Method 960.39 (AOAC, 1990) and also (SER148, Operation manual). The thimbles were immersed in the boiling solvent for 30 min and then submitted to 60 min of reflux washing and 30 min of drying to recover the solvent. The extracts were further dried in a convectional oven (Isotemp 700, Fisher Scientific, Pittsburgh, PA) at 125 °C for 30 min. The sample cups were cooled in a desiccator and subsequently weighed. The oil content (*OC*) dry basis, was computed for each sample using the following relationship:

$$OC (\%) = \frac{\text{mass of oil extracted}}{\text{mass of dried sample}} \times 100$$
 (3.2)

3.3.7 Statistical analysis

The data were analyzed using SAS procedure using the General Linear Model (GLM) (SAS, V.8). Duncan's Multiple Ranges Test (DMRT) was used to estimate significant differences among the means at 5% probability level.

3.4 Results and Discussion

3.4.1 Moisture loss and oil uptake

The evolution of moisture loss is shown in Figure 3.1a,b, that of oil uptake in Figure 3.2a,b. Figures 3.1a and 3.2a focus on the first 45 s of frying, during which the behaviors tend to be erratic. In the case of moisture loss, the data exhibit a significant linear tendency at 180°C (r=0.89), but are random at the other temperatures (r=0.56 at 170°C, r=0.17 at 190°C).

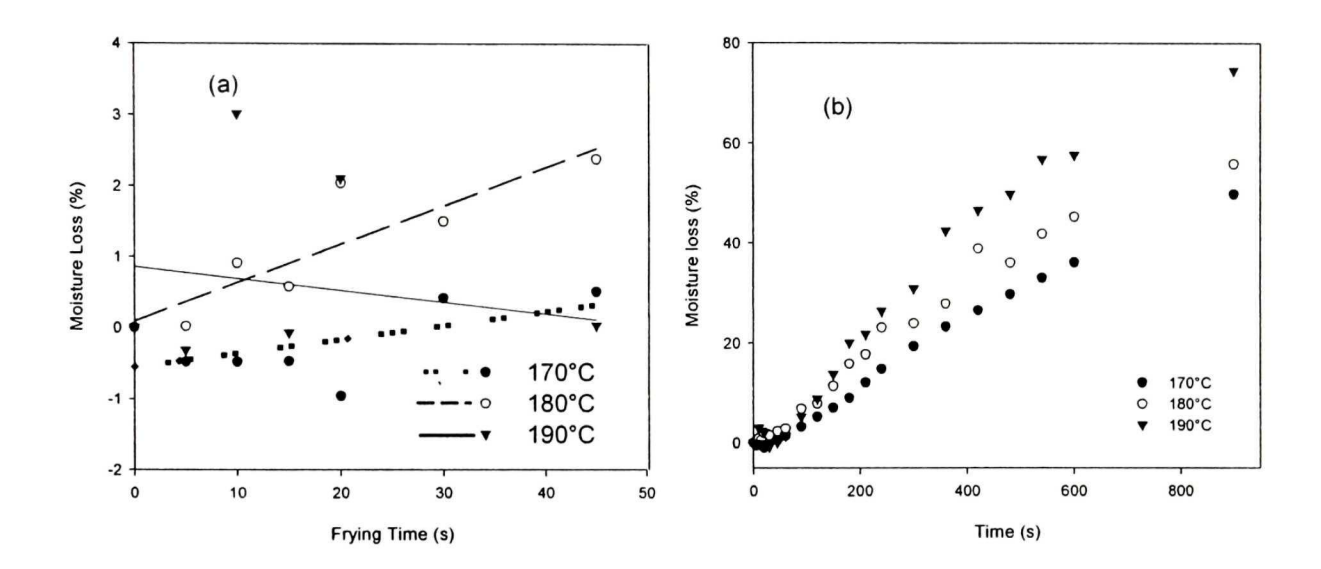


Figure 3. 1 Moisture loss as a function of frying times in chicken breast during deep-fat frying: (a) moisture loss at times <45 s and (b) moisture loss at times 0-900s.

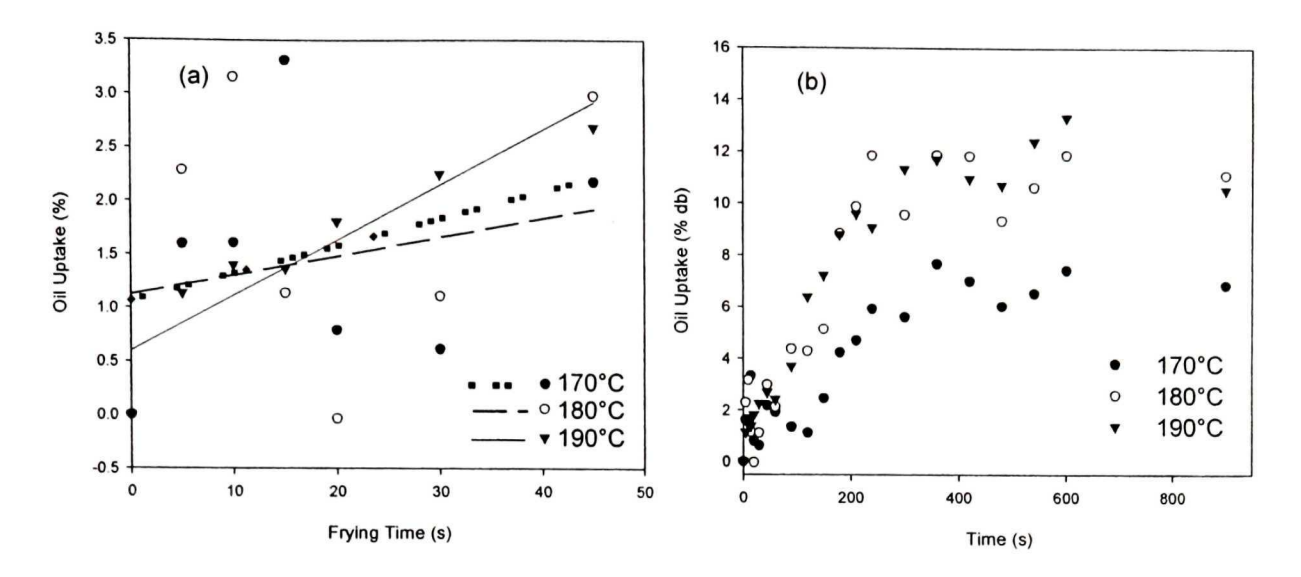


Figure 3.2 Oil uptake as a function of frying times in chicken breast during deep-fat frying: (a) moisture in the range (<45 s) and (b) (>45 s).

For oil uptake, the data was linear at 190°C (r=0.93) but random at 170°C and 180°C (r=0.24, 0.17 respectively). Singh (1995) has called this initial phase the surface-boiling phase. The instability is due to turbulence in the frying oil near the surface of the product, caused by boiling of surface water and bubbling up of water vapor from beneath the surface. Although the trend in oil uptake is significant at 190°C, the observations are within the scatter for the other temperatures; thus, it appears reasonable to conclude that oil uptake in this short lapse of time is mainly due to surface adhesion, penetration likely being inhibited by the movement of water in the surface layer. Lack of adequate heat energy to induce transport of moisture may also play a role. With respect to a similar phenomenon observed in a study of potato frying, Bouchon et al. (2001) also suggested that evaporative cooling at the surface could result in inadequate heat transfer in the initial phase.

In the second phase (>45s), moisture loss increases almost linearly (Figure 3.1b), as also reported for potato strips by Mittelman et al. (1982), with a slight convexity (>600 s) representing the onset of mass-transfer limitations. The effect of frying oil temperature (FOT) becomes more evident (separation of curves) after about 175 s, moisture loss being significantly affected by FOT. Oil uptake responds in a similar fashion to time and temperature up to about 400 s, after which the percent of oil declines for a short period and then recovers. This temporary expulsion of absorbed oil may be indicative that the forces tending to drive the remaining moisture out of the porous structure are reopening oil-blocked exits near the surface. Changes in pore structure in time and shrinkage may also contribute to the overall phenomenon. Another interpretation is that oil uptake may reach a quasi-equilibrium around which it fluctuates, although at these temperatures, frying for 900 s results in an inedible product: wet basis moisture losses were 50, 56 and 75% at 170, 180 and 190°C respectively.

The analysis of variance was conducted for moisture content and oil uptake for the first 360 s of frying, corresponding to the linear regions of the two sets of curves, and because cooking for longer times was observed to lead to the onset of deterioration of sensory qualities. The analyses are shown in Appendix Tables 1 and 2.

These analyses show that moisture loss and oil uptake change significantly in time, and are dependent on the FOT, and that the time trends are significantly influenced by the FOT (indicated by the significant interaction). The

effect of temperature on the slopes of the time trends (forced through the origin) is evident in Table 3.1.

Table 3.1 Trends in oil uptake and moisture loss of chicken during DFF at different FOTs during the first phase of frying (0 to 360 s).

| Variables | Frying Oil Temperature | Equation | |
|---------------|------------------------|------------|--|
| variables | (°C) | | |
| | 170 | X = 0.056t | |
| Moisture Loss | 180 | X = 0.083t | |
| | 190 | X = 0.099t | |
| | | | |
| | 170 | y = 0.021t | |
| Oil Uptake | 180 | y = 0.041t | |
| | 190 | y = 0.042t | |
| | | | |

where, X is moisture loss (%), y is oil uptake (%), t is time (s)

It is interesting to note that the effect of raising the FOT from 170°C to 180°C is far greater than the effect of the same incremental change to 190°C. In the case of moisture loss, the latter increment has, nevertheless, a noticeable effect on the slope, whereas in the case of oil uptake, the change in slope is negligible. Gamble et al. (1987) observed a similar decreasing effect of higher frying oil temperatures on oil uptake on potato slices.

At a frying time of 900 s, the mean fat uptakes by chicken breast were 6.84, 11.87 and 10.53% dry basis (db) at temperatures of 170, 180, and 190°C, respectively. Gupta et al. (2000) reported fat uptakes of 15 and > 15% in French fries after 14 min frying at temperatures of 170 and 180°C, respectively. Ang and Miller (1991) reported an oil content of 25.3% (wb) for deep-fat fried chicken.

Since samples fried for 900 s were too dry to be edible, we decided to establish cook values, C, to relate frying time to the organoleptic attributes of the material, prior to generating regression equations relating moisture loss and fat absorption to frying time and frying oil temperature.

3.4.2 Cook value

The evolution of temperature at the center of the chicken slabs is shown for the three frying oil temperatures in Figure 3.3. The frying oil temperature did not have a great influence on the center temperature, as also observed by Pravisana and Calvelo (1986) for deep-fat fried potatoes. Higher temperatures of the frying medium (oil) would certainly increase the boundary rate of advances but would maintain the same prescribed temperature on the boundary (T = 108°C). It was observed that even at the highest temperature (190°C), the center temperature tended to stabilize at 108°C. Introducing the experimental data of Figure 3.3 into Eq. 3.1, the temperature at the center of the slab was calculated as a function of time. Sensory observation of the color and crispiness of samples indicated that a frying time of 300 s was ideal at all frying oil temperatures. Based on this time and the reference temperature of 100°C,

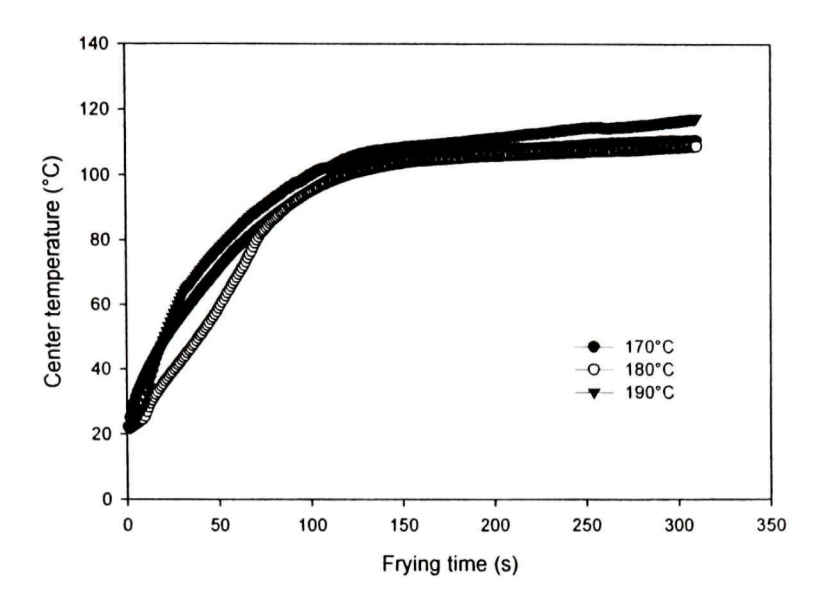


Figure 3.3 Thermal histories of the chicken breast slab center for different oil temperatures during deep-fat frying.

the C-value was calculated to be 415s, thus, ensures complete pasteurization. Frying for this amount of time would not only inactivate spoilage microorganism but also result in an acceptable texture. Results shown in Figure 3.4 allowed estimation of the minimum frying time needed to assure sufficient cooking at the center of the slab (once the center is cooked, the rest of the strip would certainly attain a c-value greater than 415 s). Therefore, as shown in Figure 3.4 the plot of C-value versus frying time indicates that the frying time for chicken breast pieces should not be shorter than 300 s. This result is independent of the oil temperature used. On the other hand, inspection of Figure 3.3 shows that about 30% of the frying time is required for the center temperature to reach 108°C. This is, of course, dependent on the thickness of the sample.

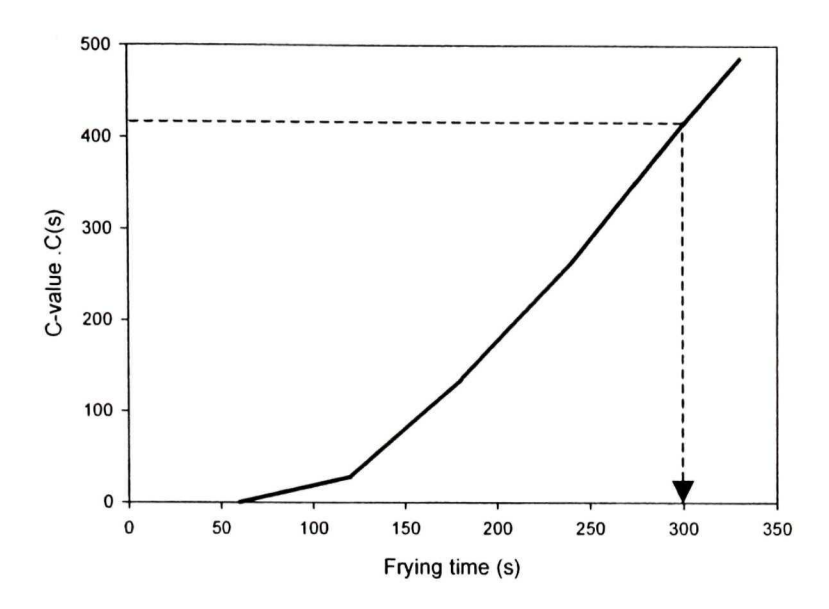


Figure 3.4 Cook value at the chicken breast slab center as a function of frying time.

3.4.3 Correlation between fat uptake and moisture content

The relationship between oil uptake and moisture loss (Figure 3.5a) closely resembles that between oil uptake and time (Figure 3.2b). This is to be expected since the relationship between moisture loss and time (Figure 3.1b) is reasonably linear, considered over frying times greater than 45s. Oil uptake is linearly related to moisture loss (or remaining moisture) at all frying oil temperatures until moisture loss reaches about 40% w.b. Oil uptake then appears to stabilize or fluctuate about a quasi-equilibrium (as mentioned earlier with respect to frying time), although moisture continues to leave the product.

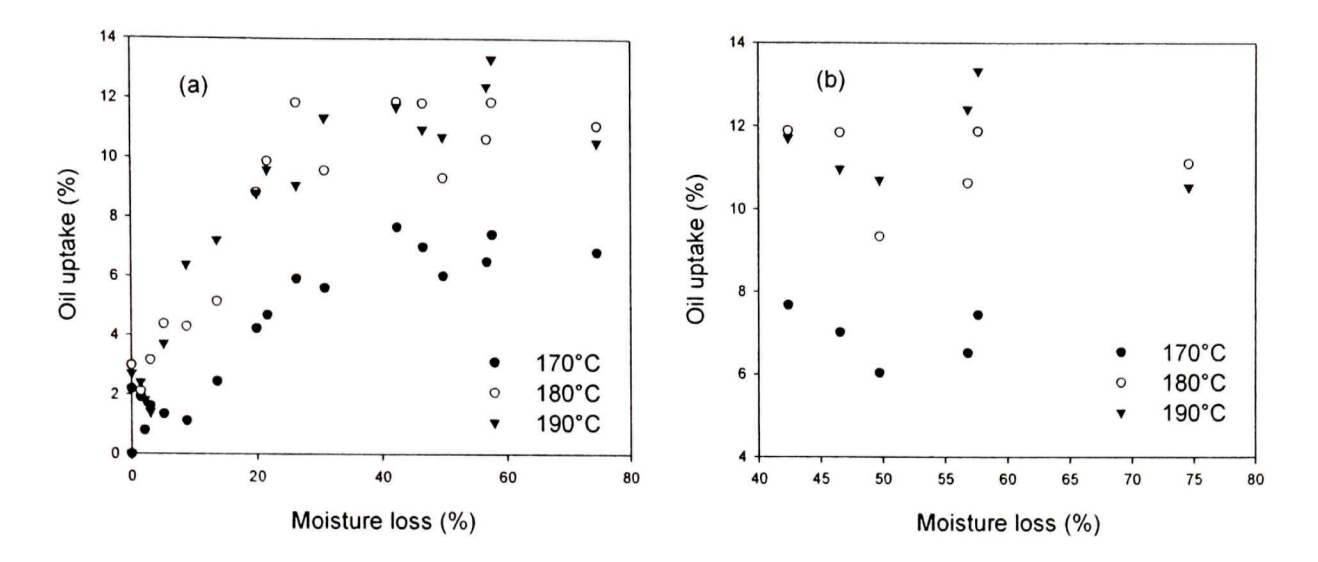


Figure 3.5 Oil uptake as a function moisture loss in chicken breast meat during deep-fat frying.

In contrast, Gamble et al. (1987) reported that oil uptake was directly proportional to moisture over a full range of moisture content (1 to 80%), in the case of 1.5 mm thick potato slices. Our results may differ from theirs due to inherent differences in pore structure and pore size distribution, and it is possible that limiting effects such as we observed may not be detectable in much thinner slabs.

The fluctuations in oil uptake at the later stages of frying (Figure 3.5b) may be due to a temporal interaction between oil intrusion and water vapor build-up. Infiltration of oil may permanently block capillary pores that are not connected to the deeper pore structure permanently, whereas oil blocking deeply connected structures may be repulsed once there is sufficient pressure build-up deeper in the tissue. Structural changes may also be involved, but were not monitored in this experiment.

The data at 180 and 190°C are quite similar, with those at 170°C showing that the rate of uptake of oil is lower at all moisture losses, as indicated by the slopes of the oil uptakes regressed on moisture content for the three frying oil temperatures (Table 3.2).

Table 3.2 Regression equations for oil uptake as a function of moisture loss of chicken breast meat during deep-fat frying at different frying temperatures.

| Temperature | | |
|-------------|---------------------|-------------------------|
| (°C) | Regression equation | Correlation coefficient |
| 170 | y = 1.35 + 0.24x | 0.73 |
| 180 | y = 1.64 + 0.39 x | 0.85 |
| 190 | y = 1.74 + 0.33 x | 0.92 |
| 100 | , | 0.02 |

y = oil uptake; x = moisture loss

Inspection of the slopes shows, as also noted by Gamble et al. (1987) regarding oil uptake by potato slices, that the rate of oil uptake is lower at lower FOT, and, that the increase due to an increment in FOT drops. They intimated that this might be indicative of the absence of any direct effect of frying temperature on oil uptake.

3.5 Conclusions

This study confirms that there is a strong relationship between oil uptake and moisture loss during deep-fat frying of chicken breast, as reported for other products by various researchers (Saguy and Pinthus, 1995; Singh, 1995; Kozempal et al., 1991; Rice and Gamble, 1989; Ashkenazi et al., 1984). The effect of frying oil temperature on oil absorption is significant but is likely close to a maximum at the frying oil temperatures used in this study. The data indicate that oil absorption reaches a plateau or quasi-equilibrium in the vicinity of 35-40% moisture loss. This is contrast to the linear relationship between oil uptake and moisture content over a full range of moisture content reported for thin potato slices by Gamble et al. (1987). The quasi-equilibrium or fluctuations in oil uptake as moisture loss progresses beyond 40% warrants further study on changes in structure of the chicken meat during deep-fat frying.

3.6 References

- Ang, J. F. and W. B. Miller. 1991. Multiple functions of powdered cellulose as a food ingredient. Cereal World. 36 (7): 558-564.
- AOAC. 1990. Official methods of analysis. Association of Official Analytical Chemists, Washington, DC.
- Ashkenazi, N., Mirzrahi, S. and Z. Berk 1984. Heat and mass transfer in frying. In "Engineering and Food, Vol. 1, Engineering Sciences in the Food Industry," ed. B. Mckenna, pp. 109-116. Elsevier Press, London.
- Balasubramaniam, V. M., M. S. Chinnan, P. Mallikararjunan and R. D. Phillips. 1997. The effect of edible film on oil uptake and moisture retention of a deep-fat fried poultry product. Journal of Foof Engineering 20: 17-29.
- Bouchon, P., P. Hollins, M. Pearson, D. L. Pyle, and M. J. Tobin. 2001. Oil distribution in fried potatoes monitored by infrared microspectroscopy. Journal of Food Science 66 (7): 918-923.
- Browner, W. S., J. Westenhouse, and J. A. Tice. 1991. What if Americans ate less fat? A quantitative analysis estimate of the effect on mortality. Journal of American Medical Association 265:3285-3291.
- Dagerskog, M. 1977. Time-temperature relationships in industrial cooking and frying. In "Physical, Chemical and Biological Changes in Food Caused By Thermal Processing" ed. T. Hoyem and O. Kvale, pp. 77-100.Applied Science Publishers Ltd, London.

- Du Pont, M. S., A. B. Kirby, and A. C. Smith. 1992. Instrumental and sensory tests of cooked frozen French fries. International Journal of Food Science and Technology. 27: 285-295.
- Gamble, M.H., and P. Rice. 1987. Effect of pre-fry on oil uptake and distribution in potato chip manufacture. International Journal of Food Science and Technology. 22: 535-548.
- Gupta, P., U. S. Shivhare, and A. S. Bawa. 2000. Studies on frying kinetics and quality of French fries. Drying Technology 18 (1 & 2): 311-321.
- Keller, C. and F. Escher. 1986. A method for localizing fat distribution in deep-fat fried potato products. Lebensmittel-Wissenschaft und. Technologie 19: 346-348.
- Keller, C. and F. Escher. 1989. Heat and mass transfer during deep fat frying of potato products. International Congress on Engineering and Food 5.Cologne, Germany, May 25 June 1.
- Kozempel, M. F., P. M. Tomasula, and J. C. Craig. 1991. Correlation of moisture and oil concentration in French fries. Lebensmittel-Wissenschaft und. Technologie 24: 445-448.
- Krokida, M. K., V. Oreopoulou, and Z. B. Maroulis. 2000. Water loss and oil uptake as a function of frying time. Journal of Food Engineering 44: 39-46.
- Leonard, S., B. S. Luh and M. Simone. 1964. Aseptic canning of foods: 1.

 Preparation and processing procedures. Food Technology 18: 81.
- Mallikararjunan, P., M. S. Chinnan, and V. M. Balasurbramaniam. 1995. Mass transfer in edible film coated chicken nuggets: influence of frying

- temperature and pressure. In advances in food engineering proceedings of the 4th conference in Food Engineering, ed, Narsimhan. Okos, and Lombrado, 107-111.
- Mittelman, N., S. H. Mizrahi, and Z. Berk. 1982. Heat and mass transfer in frying. In: Engineering and Food (edited by B. M. Mckenna). Pp. 109-116. UK: Elsevier Applied Science Ltd.
- Moreira, R. G., M.E. Castell-Perez, and M. A. Barrufet. 1999. Deep-Fat Frying: Fundamentals and Applications. MD: Aspen Publishers Inc.
- Pravisani, M. F., and A. Calvelo. 1986. A minimum cooking time for potato strip frying. Journal of Food Science 51:614-617.
- Rice, P., and M. H. Gamble. 1989. Modeling moisture loss during potato slice frying. International Journal of Food Science and Technology. 24: 183-187.
- Saguy, I. S. and E. J. Pinthus. 1995. Studies designed to gain an understanding of how oil is absorbed by foods during deep-fat frying can lead to improved products and processes. Food Technology. Presented at a symposium sponsored by the IFT Food Engineering Division.: 142-145
- Singh, P. R. 1995. Heat and mass transfer in foods during frying. Food Technology. Presented at a symposium sponsored by the IFT Fodd Engineering Division: 134-137.

CONNECTING TEXT

The results of the investigations in chapter III confirm the existence of a relationship between moisture loss and oil uptake. The relationship is not linear throughout a full range of moisture loss and there is a dependence on frying oil temperature. Oil uptake stabilizes after a certain time while moisture continues to leave the porous matrix more or less linearly for a longer time. This is an indication that there is a mechanistic interaction between moisture loss and oil uptake. The dependence of both mass transfers on temperature and time can be described by their diffusivities. Thus, in Chapter IV, thinner pieces of chicken meat are fried for different time-temperature combinations to permit calculation of the moisture and oil diffusivities according to the one-dimensional transport model based assumption of infinite slab. the an on

IV. MOISTURE DIFFUSIVITY DURING DEEP-FAT FRYING OF CHICKEN MEAT

4.1 Abstract

The effects of frying oil temperature on the effective moisture and oil diffusivities were investigated in this study. Liquid and vapor diffusivity were lumped. Samples of chicken meat were diced into 5 x 3 x 0.3 cm slabs. One-dimensional mass diffusion was assumed on an infinite slab. Chicken meat samples were fried at different temperatures (170, 180, and 190°C) in an industrial fryer for periods varying from (5 to 900 s). Fried samples were freeze-dried prior to fat and moisture analysis. The effective moisture and oil diffusivities increased with frying oil temperature. Over the range 170 to 190°C, the effective moisture diffusivity increased from 3.65E-09 to 7.42E-09 m²/s and the effective oil diffusivity increased from 9.12E-09 to 3.32E-08 m²/s, based on data from 5 to 900 s frying time. The activation energies were calculated to be 59.5 and 107 kJ/mol for moisture and oil diffusion, respectively.

4.2 Introduction

Deep-fat frying is a simultaneous heat and mass transfer process in which the food product is subjected to high heat treatment at high initial moisture content. During this process, heat is transferred to the product by the hot oil, resulting in the vaporization of the product's surface moisture. Heat is conducted from the surface contact as well as by penetration of the hot oil into the product. The oil may also serve as an active ingredient for supplementary nutrients (Perkins and Erickson, 1996) and influences texture and sensory quality. The parameters influencing the rate and efficiency of the frying process are oil temperature, product moisture content, frying time (Kassama and Ngadi, 2001; Moreira et al., 1999; Perkins and Erickson, 1996; Mittelmann et al., 1982) and surface coatings (El-Dirani, 2002; Balasubramaniam et al., 1997; Mallikarjunan et al., 1995). Oil type and quality are also important to consider as these factors may influence the physicochemical composition of the product. For example, additives and contaminants in oils can have a marked effect on the organoleptic attributes of the fried products (Blumenthal, 1991). The characteristics of the food product, i.e. initial moisture content, shape and size, sample weight/frying oil volume and sample surface area/volume ratio are factors that influence oil penetration and absorption, and, in consequence, may destroy heat labile constituents and influence the interactions between nutrients in food and those in the frying oil (Varela et al., 1988).

Many authors associate frying to drying (Krokida et al., 2001; Costa and Oliveira, 1999; Singh, 1995; Mohan Rao and Delaney, 1995). The drying

process is divided into 2 distinct phases: the constant rate period and the falling rate period. The initial phase, when the surface moisture vaporizes into the cooking medium (oil) has been related to the constant rate period, which causes a considerable amount of turbulence due to boiling at the surface (Singh, 1995). Throughout the falling rate period, the movement of moisture to the drying surface occurs by diffusion and by capillarity. In this period the boiling front moves towards the internal core of the product. As a result, physicochemical changes such as solubilization of proteins, denaturation of protein, shrinkage, and pore formation can occur.

Kinetic modeling can elucidate the transport phenomena involved, and thereby complement the understanding of how the physical properties of the product may change at different combinations of the process variables. This may lead to optimization for a safer product. Several researchers have used kinetic modeling to describe desorption and absorption of moisture and oil, respectively, during deep-fat frying and other processes (Krokida et al., 2001; van Boekel et al., 2001; Gupta et al., 2000; Geka and Lamberg, 1991; Moreira et al., 1991). Kinetic modeling quantifies rate change, thus correlating the rate parameter to the physical changes that occur as the result of a process.

The objective of this study is to determine the effect of frying temperature and time on effective moisture diffusivity and the oil uptake rate constant in chicken breast slabs, and to develop an empirical model for fat absorption by deep-fried chicken breasts.

4.2.1 Moisture diffusion model

Mass diffusion from the chicken breast meat slab was modeled using governing equation of Fick's second law of mass diffusion:

$$\frac{\partial C}{\partial t} = D_e \frac{\partial^2 C}{\partial l^2} \tag{4.1}$$

where C is the mass concentration of moisture (%) or oil (kg/kg wb), D_e is the effective diffusivity of the liquid in question (m²/s) and I is the thickness of the sample slab (m). In this study the resistance to moisture transfer at the surface, normally due to convective moisture transfer, was assumed to be negligible since water vapor was rapidly lost from the surface of the frying food. Furthermore, a one-dimensional mass diffusion was assumed on an infinite slab (i.e. the lateral dimensions are much greater than the thickness) of thickness I as shown in Eq (4.1). The solution to Eq. 4.1 (Crank, 1975) is based on the following assumptions: uniform initial moisture content, negligible external resistance to moisture transfer. Many authors used Newman's analytical procedure to obtain a solution for Eq. 4.1. The Newman solution is:

$$x = \frac{8}{\pi^2} \sum_{n=0}^{\infty} \left\{ \frac{1}{(2n+1)^2} \left[\exp\left(-\frac{(2n+1)^2 \pi^2}{4} \frac{D_e t}{l^2} \right) \right] \right\}$$
 (4.2)

where x is moisture content, C in place of x would be the oil concentration, l is the half thickness of the slab (m) and n is an integer. Equation 4.2 was further

simplified by assuming that the missing terms are relatively small. Thus, the expression reduces to:

$$x = \frac{8}{\pi^2} \exp\left[-\frac{\pi^2 D_e t}{l^2}\right] \tag{4.3}$$

4.3 Materials and Methods

Samples used for the study were chicken breast. The chicken breast meat was acquired from a local chicken product manufacturer and was stored in a freezer at -20° C until used. Frozen samples were thawed in a refrigerator at 4° C for 24 to 36 h. The samples were diced into approximately 5 cm (length) x 3 cm (width) x 0.3 cm (thickness) pieces. Sizing was difficult due to the irregular nature of chicken breast pieces and, as a result, the length and width dimension may vary by approximately \pm 3 mm.

4.3.1 Frying

Frying was done in a commercial programmable computerized pressure deep-fat fryer (Henny Penny Computron 7000 Pressure Fryer, Model 500C, Henny Penny Corporation, Eaton, OH), with a fat/oil holding capacity of about 30 L. A liquid shortening (Can Amera Food, Oakville, ON) was used. A sample to oil weight ratio of 1:480 was maintained, and samples were placed in a wire basket to ensure good contact between the sample and the oil. The fryer was preheated to

170°C for 2 h prior to frying. Samples were fried for a specific period of time, after which they were removed from the fryer, cooled at room temperature, weighed, placed in plastic Zip-Lock sample bags and frozen at –20°C in a freezer prior to further analysis.

4.3.2 Analytical methods

4.3.2.1 Moisture content

Moisture content was determined by freeze-drying the fried samples to constant weight in a ModulyOD-115 freeze dryer (Thermo Savant, Holbrook, NY) for 30 h at -50° C and 750 μ m Hg, according to the procedure outlined in chapter III.

4.3.2.2 Fat content

Fat content was determined using a soxhlet extractor, and according to method Aa 4-38 (AOCS, 1993). The fried chicken breast samples were freezedried and ground in a blender (Proctor-Silex, model E160B, Picton, ON). The ground samples were placed in thimbles, which were loaded into the solvent extractor (SER148, Velp Scientifica, Usmate, Italy). Petroleum ether was the solvent used. (Detailed procedure given in chapter III).

4.3.3 Experimental design and statistical analysis

Frying times were randomized within each temperature and triplicates were run sequentially at each time. There were three frying oil temperatures (170, 180, and 190°C), and 14 frying times (5, 10, 15, 20, 30, 45, 60, 90, 120, 150, 180, 210, 240, 300, 360, 420, 480, 540, 600, or 900 s). Initial fat content was determined on three samples (control). Regression analyses were conducted using SAS software (SAS v.8, Nashville). Duncan's multiple range test (DMRT) was used to separate treatment means (5% level of significance) (Gomez and Gomez, 1984).

4.4 Results and Discussion

4.4.1 Moisture diffusivity

Experimental moisture content data was fitted as an exponential function of frying time according to Eq. 4.4:

$$x = ae^{-bt} (4.4)$$

where a and b are constants. The values of a and b obtained at each temperature are given in Table 4.1. The rate constant, b, is related to moisture diffusivity by the following relationship:

$$b = \frac{\pi^2 D_e}{I^2} \tag{4.5}$$

The rates of moisture loss tend to be higher at greater FOT. The temperature dependence of the rate constant is to be expected due to energy considerations, as reported in studies of fried potatoes (Costa and Oleveira, 1999) and deepfried chicken drums (Ngadi, 1995).

Table 4. 1 Parameters of the moisture diffusion model (Eq. 4.4) .

| | | Mode | l Parameters | | |
|------|----------------|----------|-----------------------|--------|------|
| Temp | a (kg/kg we | t basis) | b (s ⁻¹ |) | R² |
| (°C) | Estimate | SE | Estimate | SE | |
| 170 | 0.81 | 0.0051 | 0.0010 | 0.0001 | 0.99 |
| 180 | 0.82 | 0.0085 | 0.0014 | 0.0001 | 0.98 |
| 190 | 0.84 | 0.0150 | 0.0020 | 0.0002 | 0.97 |

Legend: Temp = Frying temperature; SE = Standard error; $R^2 = Coefficient of determination, a and b are the parameters in Equation 4.$

The observed moisture history at a frying oil temperature of 180°C is shown in Figure 4.1 along with the model predictions. The experimental model adequately described the data as indicated by the high R² and low variability of the parameter estimates (SE's <11% of parameters). The moisture change with respect to time during deep-fat frying is analogous to that obtained during dehydration of food materials (Karathanos et al., 1991; Hallstrom, 1992).

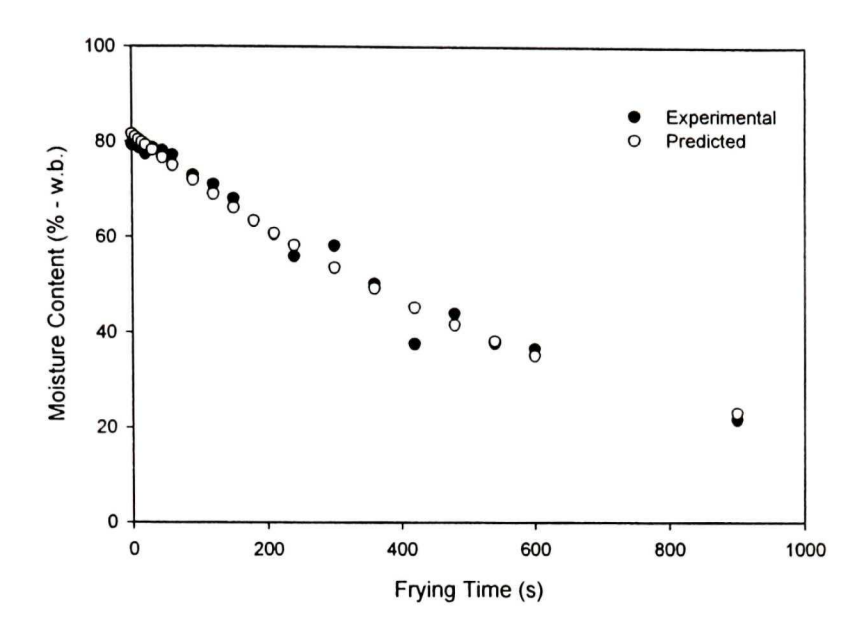


Figure 4.1 A typical moisture history during deep-fat frying of chicken breast meat slab.

The effective moisture diffusivities were calculated according to the following relationship and are presented in Table 4.2:

$$D_e = \frac{b^* l^2}{\pi^2}$$
 (4.6)

Table 4.2 Computed effective moisture diffusivity during deep-fat frying of chicken breast meat.

| Temperature (°C) | Effective moisture Diffusivity (m²/s) | Std Deviation |
|------------------|---------------------------------------------|---------------|
| 170 | 3.65E-09 a | 3.64E-10 |
| 180 | 5.23E-09 b | 5.57E-10 |
| 190 | 7. 42 E-09 c | 2.11E-10 |

Means with the same letter in the same column are not significantly different at 5% level.

The effect of temperature on moisture diffusivity was evaluated by analysis of variance (ANOVA) (Appendix Table 3). The moisture diffusivity at different frying oil temperatures were found to differ significantly (P < 0.01), thus diffusivity increases with increase in FOT. The D_{e} ranged from 3.65E-09 to 7.42E-09 when chicken meats were deep-fat fried at FOT of 170 to 190°C for 900 s. Ngadi (1995) reported diffusivity coefficients of 1.32E-09 and 1.64E-08 m²/s for deep-fat fried chicken drums at 120 and 180°C, respectively. The diffusivity obtained at 180°C is an order of magnitude greater than that observed in this study. This may be due to a number of factors, such as different structures of chicken drum compared to breast meat, and heat conduction along the bone to the inner surface of the muscle mass. El-Dirani (2002) obtained values of 2.1E-09 to 2.9E-09 m²/s for breaded deep-fried chicken nuggets, which are close to our values. The differences may be the result of the effect of batter. The variations in effective moisture diffusivity are a complex function of the physical properties of the material, such as porosity and pore structure (Saravacos, 1986; Karathanos

et al., 1991), and of temperature (Ngadi, 1995; Schoeber, 1976). Since it is very difficult to measure liquid and vapor diffusion independently the effective moisture diffusivity accounts for both phases. Changes in the physical structure i.e. volumetric shrinkage, may introduce error in the calculated values of apparent diffusivity. Since chicken muscle consists primarily of moisture and protein (Kropf and Bowers, 1992), denaturation of protein is another factor, which may lead to increases in moisture diffusion due to less water binding capacity at higher temperatures. The rapid increase in moisture loss from the denatured muscle as a result of FOT may have contributed to shrinkage, increased porosity and thus increased moisture diffusivity (Ngadi, 1995; Karathanos et al., 1991; Xiong et al., 1991). Another factor could be the loss of structural integrity of muscle myofibrils at temperatures above 97°C, hence at higher FOT would increase the rate of heat transfer thus may increase its deterioration rate.

The dependence of the effective moisture diffusion coefficient on temperature was assumed to follow the Arrhenius type model:

$$D_e = D e^{\left(-\frac{E_a}{RT}\right)} \tag{4.7}$$

where D is the apparent diffusivity, E_a is the activation energy, R (8.1814 J/K mol) is the universal gas constant, and K in (°K). The effective diffusivity is plotted against the inverse of temperature in Figure 4.2. The slope of the line is the activation energy and the intercept is the apparent diffusivity. The ratio of the activation energy to the gas constant (R) is 7275°K, and the apparent moisture

diffusivity as 5E-07 m²/s. The activation energy for effective moisture diffusivity was calculated to be 59.5 kJ/mol during DFF of chicken breast meat. Activation energies of 24 kJ/mol for DFF of chicken drums and 26 kJ/mol for deep-fried chicken nuggets were reported by El-Dirani (2002) and Ngadi (1995), respectively. Motarjemi (1989) reported activation energies ranging from 34 to 54 kJ/mol (at 5 to 30°C) for moisture diffusion in mincemeat during oven frying. Low activation energy is an indication of greater ease of moisture transfer and is therefore dependent on the structure of the material and FOT.

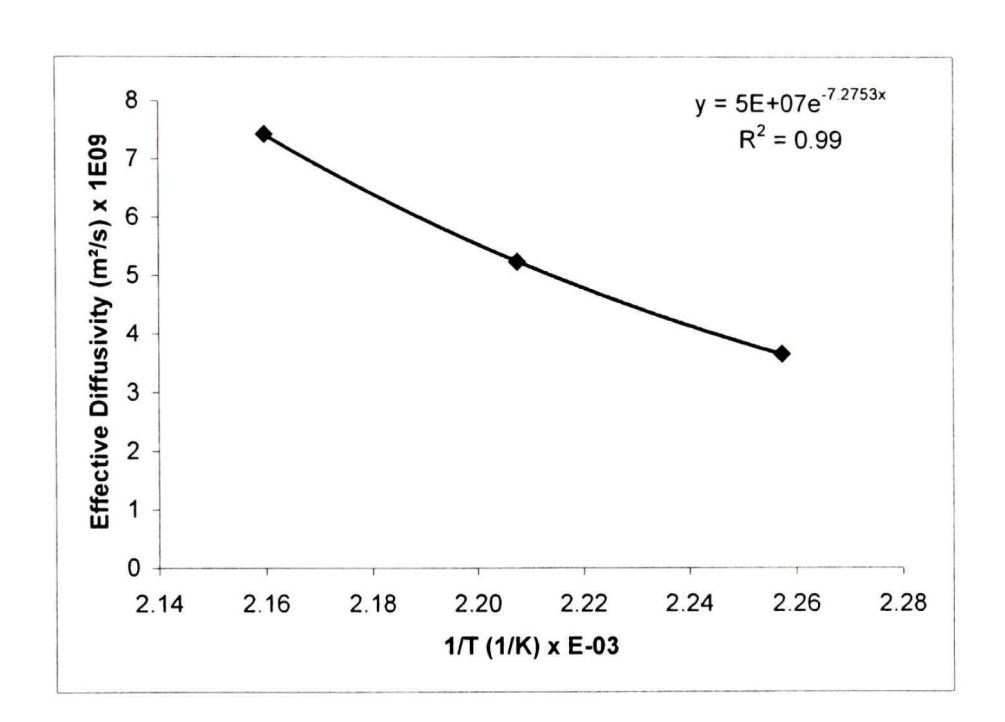


Figure 4.2 The effect of frying oil temperature on effective moisture diffusivity.

4.4.2 Fat uptake

The rate of oil uptake was computed from the following kinetics equation:

$$C = C_0 \left[1 - \exp\left(-k_c t\right) \right] \tag{4.8}$$

where, k is the rate constant, C is the oil uptake and C_0 is the initial oil uptake. The results of the estimated kinetic parameters were estimated by non-linear regression and are shown in Table 4.3. The rate of oil uptake tends to increase with frying temperature (Krokida et al., 2000, 2001; Gamble et al., 1987). Frying oil temperature significantly (P<0.05) affected the rate of oil absorption. The rate constants for oil uptake were 0.0025, 0.0046, and 0.0091% oil uptake per second at frying temperatures of 170, 180, and 190°C, respectively.

Table 4.3 Rate constants for oil uptake at different temperatures during deep-fat frying of chicken breast meat slab.

| | | Mode | el Parameters | | |
|--------------|---------------------------|------|------------------------------------|--------|------|
| Temp (°C) | k (Oil Uptake basis | | C ₀ (s ⁻¹ |) | R² |
| (0) | Estimate | SE | Estimate | SE | |
| 170 | 8.13 | 1.90 | 0.0025 | 0.001 | 0.88 |
| 180 | 10.85 | 1.34 | 0.0046 | 0.0014 | 0.92 |
| 190 | 9.99 | 0.62 | 0.0091 | 0.0019 | 0.94 |

The rate of oil absorption increases with increase in FOT. Figure 4.3 shows a typical experimental and predicted oil uptake history for samples fried for 180°C. The mathematical model seems to be well fitted to the experimental data as shown by the low standard errors.

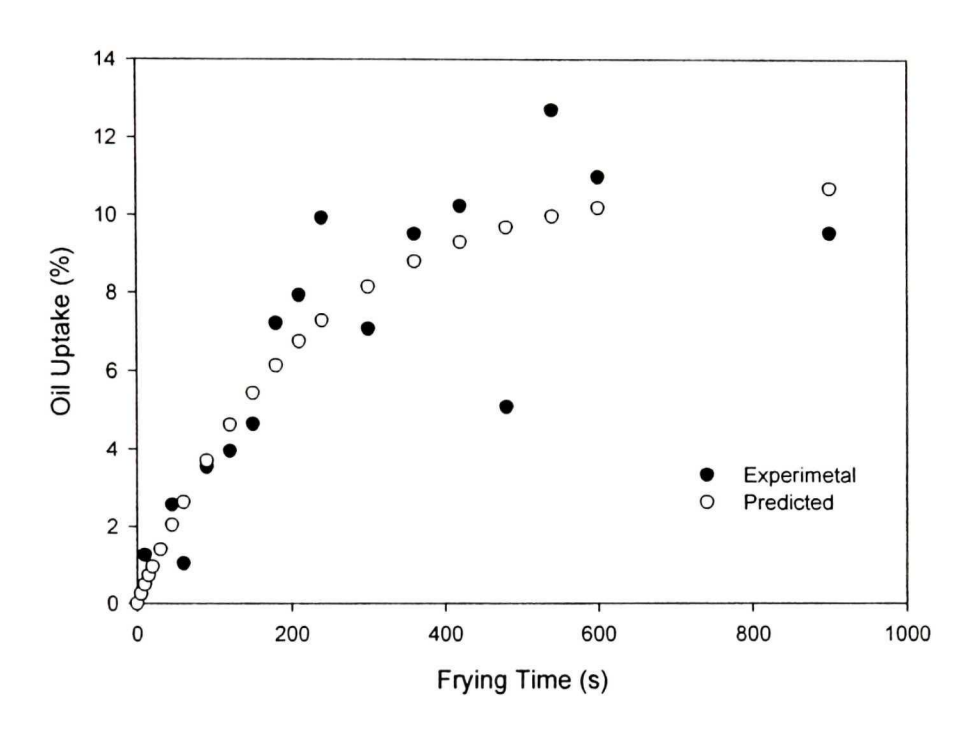


Figure 4.3 Observed and predicted oil uptake at 180°C.

The effective oil diffusivities were computed based on Eq. 4.6 and are shown in Table 4.4. The effect of frying oil temperature is significant (P<0.01) on oil diffusing into the chicken meat during deep-fat frying. The fact that moisture loss and oil uptake are positively correlated is an indication that oil diffusivity in chicken may be dependent on moisture diffusivity. The effective oil diffusivity is almost an order of magnitude greater than that of moisture diffusivity computed from the experimental data. This may be due to the fact that the moisture

diffusivity involves two phases (liquid and vapor), most of the moisture movement being due to diffusion of the vapor phase. The diffusion of oil during deep-fat frying is also dependent of the formation of capillary pores, which occurs as a result of moisture diffusion. Therefore, It is apparent that oil would diffuse with much ease through the capillaries. However, information regarding oil diffusivity is scanty.

Table 4.4 Computed effective oil diffusivity in chicken breast meat during deep-fat frying.

| - | | Effective Oil | |
|---|------------------|---------------|---------------|
| | Temperature (°C) | Diffusivity | Std Deviation |
| | | (m²/s) | |
| • | 170 | 9.12E-09 a | 1.70E-10 |
| | 180 | 1.68E-08 b | 1.30E-09 |
| | 190 | 3.32E-08 c | 2.3E-09 |
| | | | |

Means with the same letter in the same column are not significantly different at 5% level.

The apparent oil diffusivity was determined from the graph (Figure 4.4). The parameters were estimated using Eq. 4.7. The apparent oil diffusivity was 7.0E-12 m²/s and the activation energy for oil absorption in chicken meat was found to be 107 kJ/mol.

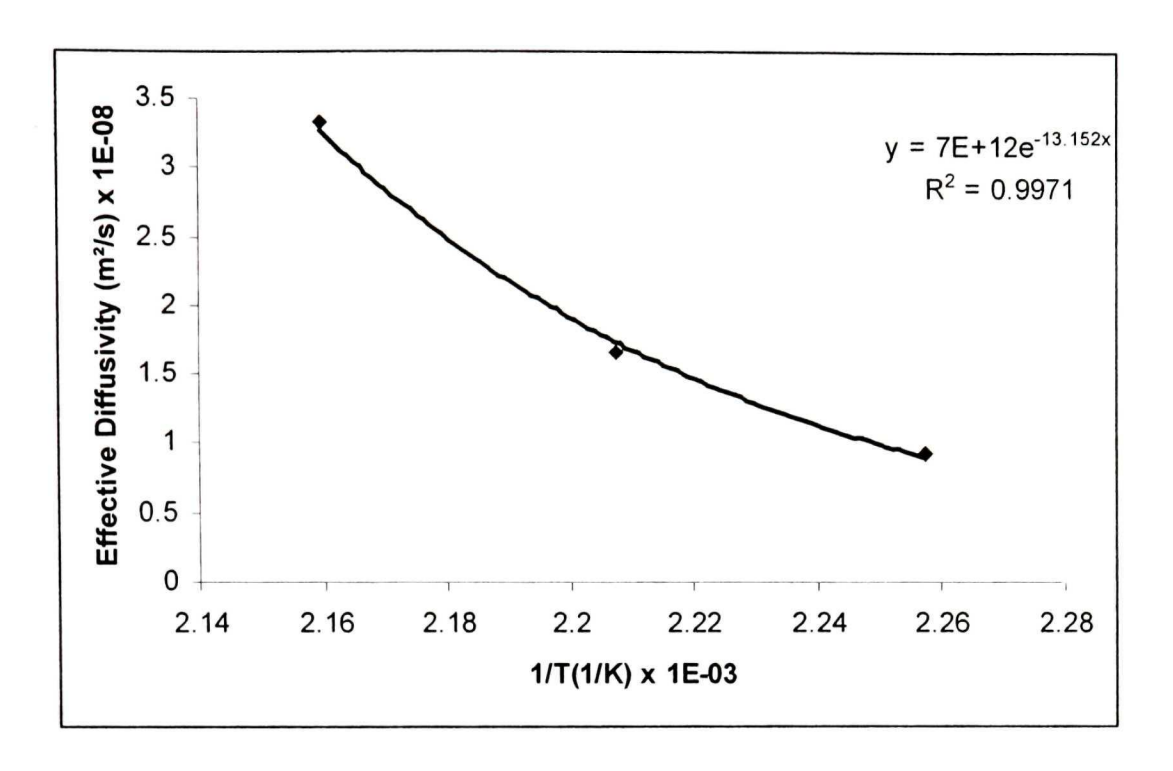


Figure 4. 4 The effect of temperature on effective oil diffusivity.

Moisture loss and oil uptake were found to be positively correlated through the first 360 to 420 s in Chapter III, Table 3.2. Comparison of predicted oil uptake values using Eq. 4.8 and the experimental values reported in chapter III are presented in Table 4.5. Values predicted by the model were smaller (15 and 40%) than the actual experimental values for the FOT 180, and 190°C respectively. This discrepancy may have been due to the change in physical properties as a result of pore development and shrinkage. The effect of the erratic nature of oil uptake after 300 s of frying shown in Figure 4.3 may have induced some error in the estimates of the model parameters.

Table 4.5 Comparison of predicted and observed oil uptake after 300 s frying at different FOT.

| Temperature | Oil Uptake | | |
|---------------|------------|--------------|--|
| remperature _ | Predicted | Experimental | |
| 170°C | 4.66 | 4.28 | |
| 180°C | 7.06 | 8.14 | |
| 190°C | 9.34 | 10.04 | |

The relationship between moisture loss and oil uptake was investigated in chapter III, and they were positively correlated for up to about 360 s frying time. Therefore, it is possible to predict oil uptake from moisture loss using moisture diffusivity. Both parameters may be dependent on the physical properties of the food product being fried. Pore formation due to moisture loss was elucidated by the capillary theory of drying (McDonough et al., 1992). The creation of capillary pathways enables oil uptake to occur (Guillaumin, 1988). However, it is apparent that increases in moisture diffusivity and pore formation will likely increase the rate of oil uptake.

4.5 Conclusions

Moisture loss and oil uptake are mass transfer phenomena that occur during deep-fat frying and are described by an empirical first order kinetic model. Based on the regression models, the effective moisture diffusivity was found to vary from 3.65E-09 to 7.42E-09 m²/s, while the oil diffusivity ranged from 9.12E-09 to 3.32E-08 m²/s at temperatures ranging from 170 to 190°C during deep fat frying of chicken breast meat slab for 900 s. The activation energy was calculated to be 59.5 and 107 kJ/mol for moisture and oil diffusion, respectively. Frying temperatures significantly (P < 0.01) affect moisture and oil diffusivity. The intensity of moisture loss and oil uptake increases with frying oil temperature. Better prediction of oil uptake was given during the first 300 s of frying. Change in the physical properties of the food product during deep-fat frying may have influenced the mass transport. The effect of shrinkage on pore formation during deep-fat frying of meat products needs further investigations.

4.6 References

- Balasubramaniam, V. M., M. S. Chinnan, P. Mallikararjunan and R. D. Phillips. 1995. The effect of edible film on oil uptake and moisture retention of a deep-fat fried poultry product. Journal of Foof Engineering 20: 17-29.
- Blumenthal, M. M. 1991. A new look at the chemistry and physics of deep-fat frying. Food Technology 45(2): 68-71, 94.
- Costa, R. m. and F. A. R. Oliveira. 1999. Modeling the Kinetics of Water Loss During Potato Frying with a Compartmental Dynamic Model. Journal of Food Engineering, 41: 177-185.
- Crank, J. 1975. The mathematics of diffusion, 2nd edition, Oxford University Press, Oxford, UK.
- El-Dirani, K. 2002. Testural and mass transfer characteristics of chicken nuggets during cooking. M.Sc thesis, McGill University, Montreal, Canada.
- Gamble, M. H., P. Rice, and J. D. Seldman. 1987. Relationship between Oil Uptake and Moisture Loss During Frying of Potato Slices from c.v. Record UK Tubers. International Journal of Food Science and Technology, 22: 233-241.
- Geka, V. and I. Lamberg. 1991. Determination of Diffusion Coefficient in Volume-Changing Systems-Application in the Case of Potato Drying. Journal of Food Engineering 14: 317-326.
- Gomez, A. K., and A. A. Gomez. 1984. Statistical Procedures for Agricultural Research, 2nd Edition, NY: John Willey and Sons Inc.

- Guillaumin, R. 1988. Kinetics of Fat Penetration in Food. In: Frying of Food, Principles, Changes and New Approaches (edited by G. Varela, A. E. Bender and I. D. Morton), pp 82-89, Chichester: Ellis Horwood.
- Gupta, P., U. S. Shivhare, and A. S. Bawa. 2000. Studies on Frying Kinetics and Quality of French Fries. Drying Technology 18(1and 2): 311-321.
- Hallstrom, B. 1992. Mass transfer in food: In handbook of food engineering, ed. By D. R. Heldman and D. B. Lund. Ch.7, 317-339. Marcel Dekker, Inc., New York.
- Karathanos, V. T., G. K. Vegenas, and G. D. Saravacos. 1991. Water diffusivity in starches at high temperatures and pressures. Biotechnology Progress 7(2): 178-184.
- Kassama, L. S. and M. O. Ngadi. 2001. Development of Pores and Pore Size Distribution in Chicken Meat During Deep-fat Frying. Canadian Society of Agricultural Engineering, Mansonville, QC, Paper No. 01-322.
- Krokida, M. K., V. Oreopoulou, and Z. B. Maroulis. 2000. Water Loss and Oil Uptake as a Function of Frying Time. Journal of Food Engineering, 44: 39-46.
- Krokida, M. K., V. Oreopoulou, Z. B. Maroulis and D. Marinos-Kouris. 2001. Deep-fat Frying of Potato Strips-Quality Issues. Drying Technology, 19(5): 879-935.
- Kropf, D. and Bower, J. 1992. Meat and meat products. In Food Theory and Application, 2nd, ed, J. Bowers (Ed), 505-686. Macmillan Publishing Co., New York, NY.

- McDonough, C. M., J. K. Lee, m. H. Gomez, R. D. Waniska and L. W. Rooney. 1992. Institute of Food Technologists Annual Meeting, New Orleans, LA.
- Mallikararjunan, P., M. S. Chinnan, and V. M. Balasurbramaniam. 1995. Mass transfer in edible film coated chicken nuggets: influence of frying temperature and pressure. In advances in food engineering proceedings of the 4th conference in Food Engineering, ed, Narsimhan. Okos, and Lombrado, 107-111.
- Mittelman, N., S. H. Mizrahi, and Z. Berk. 1982. Heats and Mass Transfer in Frying. In: Engineering and Food (edited by B. M. McKenna). Pp. 109-116. UK: Elsevier Applied Science Ltd.
- Mohan Rao, V. N. and R. A. M. Delaney. 1995. An Engineering Perspective on Deep-fat Frying of Breaded Chicken Pieces: Mathematical Modeling of Heat and Mass Transfer During Deep-fat Frying of Chicken Parts can Lead to Improved Quality and Consumer Value. Food Technology. Presented at a symposium sponsored by the IFT Food Engineering Division: 138-141.
- Motarjemi, Y. 1989. Determination of moisture diffusivity in foodstuffs. In Trend in food Science, W. S. Lien (Ed), 139 143. Singapore Institute of Food Science and Technology, Singapore.
- Moreira, R. G., M.E. Castell-Perez, and M. A. Barrufet. 1999. Deep-Fat Frying: Fundamentals and Applications. MD: Aspen Publishers Inc.
- Ngadi, M. O. 1995. Finite element modeling of heat and mass transfer during deep-fat frying of chicken drums. Ph.D thesis. Technical University of Nova Scotia, Halifax, Nova Scotia.

- Perkins, E. G., and M. D. Erickson. 1996. Deep Frying: Chemistry, Nutrition, and Practical Applications. IL: AOCS Press.
- Saravacos, G. D. 1986. Mas transfer properties of foods. In Engineering properties of foods, M. A. Rao and S. S. H. Rizvi (Ed.), 89-132. Marcel Dekker, Inc., New York, NY.
- Schoeber, W. J. A. H. 1976. Regular regimes in sorption processes. Calculation of drying tares and determination of concentration dependent diffusion coefficients. Ph.D Thesis, Eindhoven University and Technology, Netherlands.
- Singh, P. R. 1995. Heat and Mass Transfer in Foods During Frying. Food Technology. Presented at a symposium sponsored by the IFT Food Engineering Division: 134-137.
- Van Boekel, M. A. J. S., and L. M. M. Tijskens. 2001. Kinetics Modeling, In Food Process Modeling. Ed. By L. M. M. Tijsken, M. L. A. T. M. Hertog and B. M. Nicolai. Woodhead Publishing Ltd. Cambridge, England.
- Varela, G., Bender, A. E., and I. D. Morton. 1988. Frying of foods: Principles, Changes, New Approaches. New York: VCH publishers.
- Xiong, X., Narsimhan, G. and Okos, M. R. 1991. Effect of composition and pore structure on binding energy and effective diffusivity of moisture in porous food. Journal of Food Engineering 15(3): 187-208.

CONNECTING TEXT

Frying oil temperature significant influences moisture and oil diffusion through the pore matrix of deep-fried chicken meat as demonstrated by the result of the investigation in Chapter IV. The rate of diffusion increases with increasing frying oil temperatures. The predicted oil uptakes were smaller than the experimental values of the different frying oil temperatures. This discrepancy was attributed to the physicochemical changes that may have occurred as a result of intense heating. Therefore, it is imperative to investigate the effect of process variable on physical properties such as shrinkage, and changes in densities during deep-fat frying.

V. Shrinkage and Density Change of Chicken Meat During Deep-fat Frying

5.1 Abstract

The effects of frying oil temperature and time on densities and shrinkage in chicken breast meat during deep-fat frying were investigated. Chicken meat samples were diced and fried at different temperatures (170, 180, and 190°C) in an industrial fryer for periods varying from 5 to 900 s. Bulk and apparent densities were determined with a fluid displacement pycnometer, and fat analysis was conducted using soxhlet extraction with petroleum ether solvent. The physical structure of chicken meat changed significantly with time of frying and frying oil temperature (P < 0.001). Bulk density was 1.15 g/cm³ in the raw product and decreased to 0.98, 0.95, and 0.93 g/cm³ after 900 s of deep-frying at 170, 180 and 190°C, respectively. Similarly, apparent density changed from 1.13 to 1.25, 1.24 and 1.22 g/cm³. Moisture loss was linearly correlated with both densities. Volumetric shrinkage also appeared to be significantly affected by the process variable and was also correlated to moisture loss.

5.2 Introduction

During deep-fat frying, the transfer of heat to the product results in opposite mass transfers namely: expulsion of water, and intrusion of oil – as mediated by the food product's physical characteristics (Hough, 1993). This distinguishes it from a similar process – drying. In drying, moisture loss causes shrinkage, which manifests as changes in bulk density and porosity (Sjoholm and Gekas, 1995; Lozano et al., 1983; Roman et al., 1982; Misra and Young, 1980), which in turn influence thermal properties and transport phenomena (Karathanos et al., 1996; Mattea et al., 1990; Sereno and Mediros, 1990). Since moisture loss is accompanied by oil intrusion over a certain range of dehydration (Kassama and Ngadi, 2001), the connections between the changes in properties require investigation in the case of deep-fat frying.

In meat, the change in the connective muscle tissues during cooking may be attributed to shrinkage phenomenon resulting from water loss and changes in other intrinsic preperties. Perez and Calvelo (1984) reported apparent densities for beef of 0.920 and 1.053 g/cm³ at moisture contents of 4.7 and 74% w.b., respectively. They reported the densities of meat at water contents of 0.5 and 74% w.b. to be 1.180 and 1.053 g/cm³, respectively, i.e. meat density increases with increase in moisture content. Deep fat frying improves product quality and stability, thus modifying its physicochemical properties. Volume changes are dependent on several factors, such as geometry (Moreira et al., 2000; Mulet et al., 2000), drying methods (Krokida and Maroulis, 1997) and experimental conditions (McMinn and Magee, 1996).

Porosity changes as result of shrinkage during thermal processing and is dependent on initial moisture content, composition and size of food materials, type of drying (freeze-dried or air dried) and drying conditions such as temperature and relative humidity (Rahman, 2001; Marousis and Saravacos, 1990).

Rahman et al. (1996) reported that the apparent density of calamari meat was found be in the range of 1063 to 1356 kg/m³. The authors observed that the apparent density's deviation from the bulk density was the result of pore formation due to significant shrinkage during dehydration. A linear relationship of bulk shrinkage over a full range of moisture levels was proposed by Kilpatrick et al. (1955) while Lozano et al. (1983) incorporated a correction factor at the lower moisture levels for food products. In garlic shrinkage due to moisture loss is linear from the fresh state to about 20% moisture loss during drying, similar relationships were found for other food products (soybean: Misra and Young, 1980; fruits and vegetables: Kilpatrick et al., 1955), while a non linear-behavior was found at the lower moisture range (Rahman and Potluri, 1990 for fish muscles; Lozano et al., 1983 for fruits). Moreira and Sereno (2003) showed that volumetric shrinkages could be estimated based on the change in moisture content of a sample, independent of drying rate, and that conversely, determination of the volumetric shrinkage could give an indirect indication of the product's change in moisture content.

Shrinkage and density are physical properties widely used in the modeling of transport phenomena. In developing mathematical models, density,

shrinkage, and porosity are crucial to the adequacy of the model to predict and/or optimize certain processes. Balaban and Pigott (1986) studied shrinkages of ocean perch while Kilpatrick et al. (1955), Suzuki et al. (1976), and Misra and Young (1980) studied shrinkage of fruits, vegetables, and grains. Lozano et al. (1983) formulated an empirical model for the apparent densities of fruits and vegetables as a function of moisture content. Rahman and Potluri (1990) fitted the mathematical model developed by Lozano et al. (1983) to apparent density of squid meat during air-drying. A polynomial model (third and fourth degree) was used to predict the density of corn, wheat and starchy materials (Marousis and Saravaco, 1990; Nelson, 1980). Balaban and Pigott (1986) reported a linear relationship between apparent density and moisture content of pigeon peas while Shepherd and Bhardwaj (1986) reported a similar finding for grain and rewetted high moisture grain (Brusewitz, 1975).

Density can be measured by the pycnometric method. Several researchers have used fluid displacement methods (Rapusas and Driscoll, 1995; Wang and Brennan, 1995). Ngadi et al. (2001) used a pycnometer to measure the skeletal density of meat patties extended with soy protein.

The objective of this investigation was to study the relationships between moisture loss and physical properties such as density and shrinkage, and to develop baseline data for the study of pore development in de-boned chicken meat during deep-fat frying.

5.3 Materials and Methods

5.3.1 Materials

Fresh de-boned chicken breast was used throughout this study. Samples were purchased from a local supplier. The stock was stored in a freezer at – 20°C until used. It was then thawed in a refrigerator at 4°C for 24 to 36 h before the commencement of the experiment.

5.3.2 Sample preparation

The thawed chicken breast meat was cut into approximately 10 X 20 X 15 mm slabs. The sample slabs were individually deep-fat fried in a liquid shortening (Can Amera Food, Oakville, ON) in a commercial programmable computerized pressure deep-fat fryer (Henny Penny Computron 7000 Pressure Fryer, Model 500C, Henny Penny Corporation, Eaton, OH). The fryer was preheated at 170°C for 2 h prior to the commencement of frying. Samples were placed in a wire basket to ensure good contact between the sample and the oil. Fried samples were cooled at room temperature, weighed, and placed in plastic Zip-Lock sample bags until the density measurements were to be executed.

5.3.3 Moisture content measurement

The moisture content was determined at the end of each frying period.

The final moisture removal of the fried samples was conducted by freeze-drying in a ModulyOD-115 (Thermo Savant, Holbrook, NY) for 30 h. Prior to freeze

drying, all samples were frozen overnight in a freezer at -20° C. The freezedryer's refrigerating system and vacuum chamber were operated at -50°C and 750 μm Hg, respectively. This approach was adopted to minimize major changes in the sample's microstructure as a result of shrinkage during frying (Ngadi et al., 2001).

5.3.4 Fat analysis

The fried, freeze-dried samples were ground using a blender (Proctor-Silex, model E160B, Picton, ON), and fat was extracted with a solvent extractor (SER148, Velp Scientifica, Usmate, Italy) using petroleum ether. Ground samples were weighed and placed in thimbles (procedure followed as recommended by (SER148, Operation manual) for details). The oil content (*OC*) dry basis was computed for each sample based on the following relationship (Eq. 5.1).

$$OC (\%) = \frac{\text{mass of oil extracted}}{\text{mass of dried sample}} \times 100$$
 (5.1)

5.3.5 Density Measurements

5.3.5.1 Bulk density

Bulk or total density of the samples was measured using the liquid displacement technique with water. The method requires immersing the sample in a volume displacement (Archimedes) pycnometer. The apparatus was filled

with water and the samples were immersed in the sample compartment, which was then hermetically sealed with the lid. The volume displacement was measured by turning the apparatus upside down twice, the first time without the samples and the second time with the samples immersed in the liquid. The volume displacement was computed based on the follow relationship (Eq. 5.2).

$$V_s = V_f - V_i \tag{5.2}$$

where V_s is the volume of the samples, V_f is the final volume of the with the samples immersed in the liquid, and V_i is the initial volume without the samples. The shrinkage volume was measured using the same method.

5.3.5.2 Apparent density

The apparent or skeletal density was measured using a helium pycnometer (Model 1305 Multivolume, Micromeritics Instrument Corporation, Norcross, GA). The fried samples were weighed prior to analysis. The solid volume of the samples excludes pores within the sample material. Using the pycnometry method, the sample was placed in the $35~\rm cm^3$ sample chamber. The samples were subjected to cyclic action (purging) by a pressurizing and depressurizing with helium gas prior to analysis in order to expel all the air and vapors trapped in the pores and crevices. The analysis was conducted at a room temperature with pressure of $134 \pm 1.4~\rm kPa$ ($19.5 \pm 0.2~\rm psi$). Initially, all valves

were closed while the system equilibrated to the atmospheric pressure. When valve 1 was opened, the sample chamber was filled with helium at an elevated pressure and closed for 15 s of pressure equilibrium, after which time the pressure was recorded as P_1 . Then valve 2 was opened, allowing the trapped helium to flow into the expansion chamber, and pressure P_2 was measured. Valve 3 was then opened to release the spent helium gas from the system. The following general equation (Eq. 5.3) was used to compute the volume of the samples. For detailed methodology and procedure, refer to the standard protocol (Micromeritics, 1992).

$$V_{Samp} = V_{Cell} - \frac{V_{Exp}}{[(P_1 - P_2) - 1]},$$
(5.3)

Where: V_{Samp} = the volume of the samples of interest;

 $V_{\it Cell}$ = volume of the sample cell with the empty sample cup in place;

 $V_{\it Exp}$ = the volume of the expansion chamber;

 P_1 = sample chamber initial pressure with the expansion chamber closed; and

 P_2 = final chamber pressure with the expansion chamber open.

5.3.6 Definitions of Terms

Density is a physical property of all matter; it is simply the unit quantity of matter per volume of the same quantity (kg.m⁻³). The densities used in this study are defined as follows:

Bulk density: the measurement of bulk density includes all pores, interparticle spaces, moisture, and air in the material.

Apparent density: the measurement includes blind and non-interconnected pores of the material and that excludes open, interconnected and interparticle pore spaces.

5.3.7 Experimental Design

Three frying oil temperatures (FOT) (170, 180, and 190°C) were used in this study. The samples were fried randomly at each 20 frying times (5, 10, 15, 20, 30, 45, 60, 90, 120, 150, 180, 210, 240, 300, 360, 420, 480, 540, 600, or 900 s) in 3 replicates within each FOT. The analysis of variance (ANOVA) and nonlinear regression were conducted using SAS software (SAS V8). All mean comparisons were performed by using Duncan's multiple range test (DMRT), at the 5% level of significance.

5.4 Results and Discussions

5.4.1 Densities

Bulk and particle densities of deep-fat fried de-boned chicken meat samples are shown in Figure 5.1 and 5.2, respectively. The figures indicate that bulk density decreased with frying time, whereas the apparent density increased with frying time. Air-drying of potato displayed a similar trend (Wang and Brennan,1995). The analyses of variance (ANOVA) of the two densities (Appendix Tables 4 and 5) show that the temporal changes were influenced by frying oil temperature (FOT), as indicated by the significant interaction terms (P<0.01) in both tables.

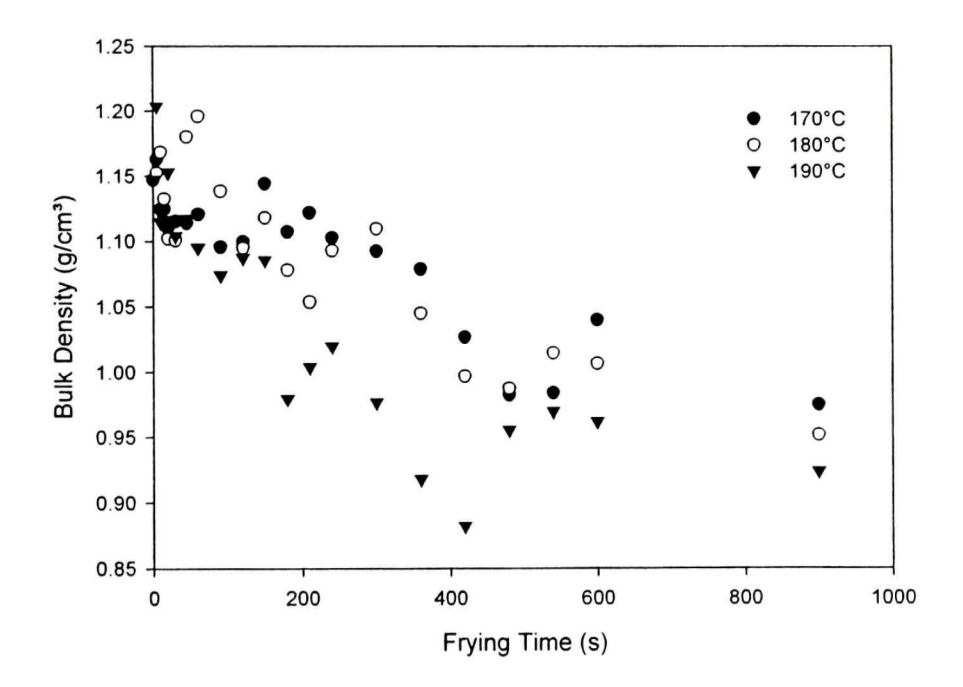


Figure 5.1 Bulk density as a function of time for de-boned chicken meat deep-fat fried at 170, 180, and 190° C.

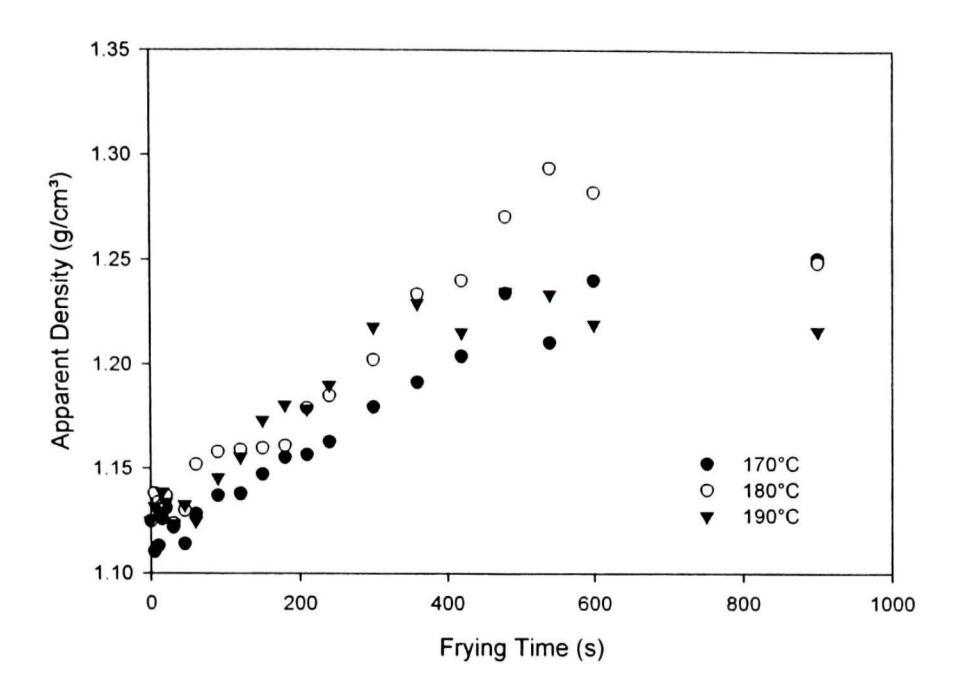


Figure 5.2 Apparent density as a function of time for de-boned chicken meat deep-fat fried at 170, 180, and 190° C.

The differences between means, analyzed using Duncan's mean comparison test (DMCT) are presented in Appendix Table 6, 7, 8 and 9 for bulk and apparent densities, respectively. The mean apparent density are not significant different at frying oil temperatures 180 and 190°C. The bulk density values decrease from 1.15 g/cm³ for the control, for which there is no moisture loss, to 0.98, 0.95, and 0.92 g/cm³ after 900 s of frying at the following FOTs 170, 180 and 190° C and final moisture contents of 33, 25, and 16% wet basis (wb), respectively. Frying at a higher temperature resulted in a lower bulk density. This is probably due to the effect of aggravated water loss resulting in shrinkage and pore formation, as also observed by Rahman et al. (1996) in drying fish muscles. In contrast, the apparent density increased from 1.13 g/cm³ for the control to 1.25, 1.24 and 1.22

g/cm³. The apparent density increased consistently when fried for 540 s, and the mean values were 1.21, 1.29 and 1.23 g/m³ at 170, 180 and 190° C, respectively, after which it tended to equilibrate. This behavior was analogous to the oil absorption curves during deep-fat frying as shown in Chapter III. The changes in densities could also be attributed to physicochemical reaction, which induce changes such as deterioration of solid content and collageneous connective tissues, likewise denaturation of protein may contribute to alteration of the physical properties, thus change in densities. The change in state could possibly be due to oil saturation into the empty voids. The volume gain due to oil uptake in place of voids evacuated by moisture may explain the decreasing trend of the apparent density. Krokida et al. (2001) made similar observations for deep-fat fried potato strips.

Figures 5.3a to 5.3c show bulk and apparent densities as functions of moisture loss during deep-fat frying. Bulk density decreases while apparent density increases, as moisture loss increases. These results agree with the observations of various researchers (Krokida et al., 2000; Wang and Brennan, 1995; Karathanos et al., 1996; Rahman and Potluri, 1990; Balaban and Pigott, 1986). The relationships between distinct parameters such as the moisture content, bulk and apparent density and the process variables are shown in the Pearson correlation coefficients matrix (Table 5.1). A weak linear correlation (r = 0.66; P < 0.01) exists between moisture content and bulk density.

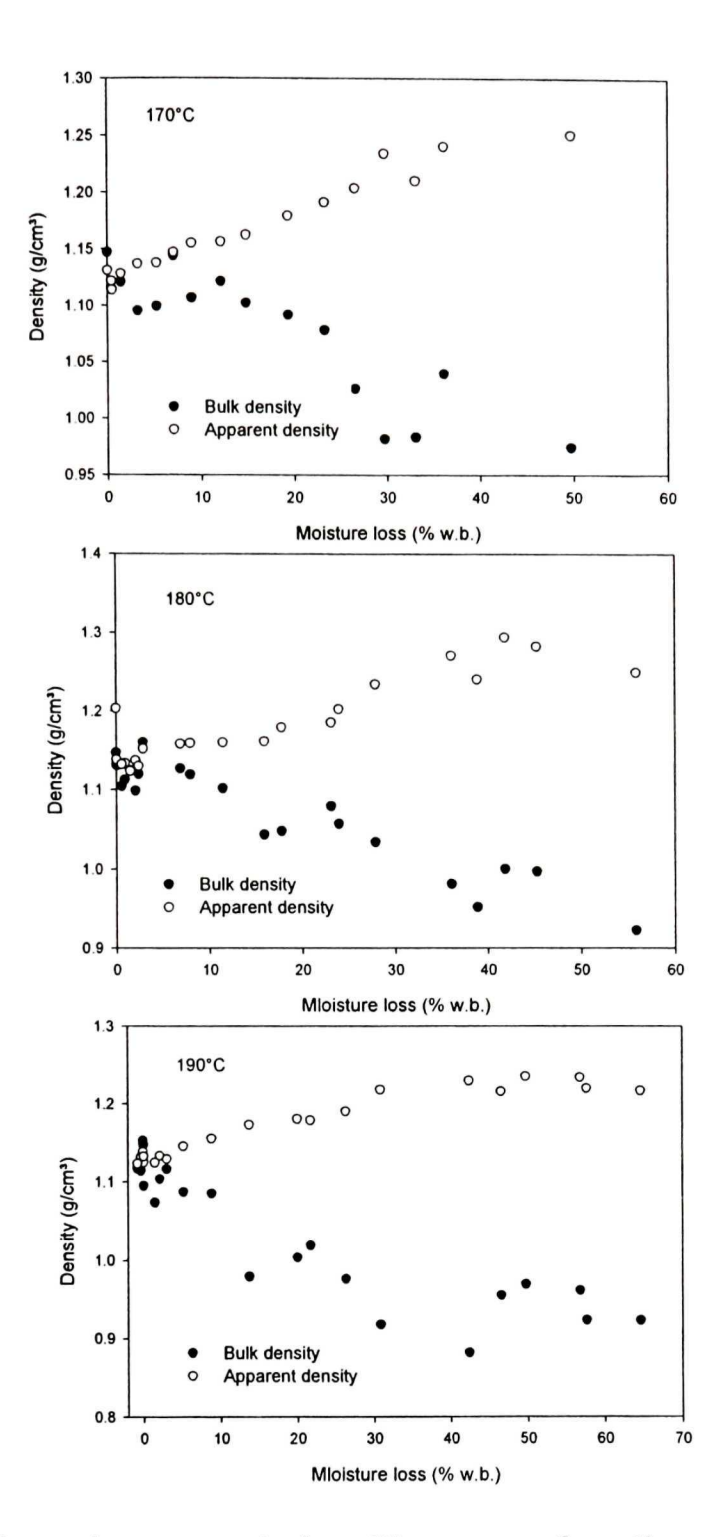


Figure 5.3 Bulk and apparent densities as a function of moisture loss during deep-fat frying of de-boned chicken meat.

Table 5.1 Pearson correlation coefficients matrix for bulk and apparent densities as a function of various process parameters.

| | Temperature | Time | Bulk | Apparent | Moisture |
|--------------|---------------------------------------|-------|---------|----------|----------|
| | | | density | density | Content |
| Temperature | 1.00 | 0.00 | -0.27 | 0.10 | 0.13 |
| Time | 0.0 | 1.00 | -0.70 | 0.83 | -0.94 |
| Bulk density | -0.27 | -0.70 | 1.00 | -0.66 | 0.66 |
| Apparent | 0.01 | 0.83 | 0.00 | 1.00 | 0.83 |
| density | | | -0.66 | | |
| Moisture | 0.40 | | | | 4.00 |
| Content | 0.13 | -0.94 | 0.66 | -0.83 | 1.00 |
| D +0.04 | · · · · · · · · · · · · · · · · · · · | | | | |

P < 0.01.

The apparent density peaked at the low moisture region, while the bulk density peaked at the high moisture region. There was a linear relationship (r = 0.83; P < 0.01) between moisture loss and apparent density. The frying oil temperature was poorly correlated to both the bulk and apparent density, while frying time was high positively correlated. A medium correlation (r = -0.66; P < 0.01) was achieved between the bulk and apparent density of de-boned chicken meat during deep-fat frying. Therefore, the bulk and apparent density may be adequately predicted by a linear equation with a higher degree of accuracy as a function of moisture loss in de-boned chicken meat during the deep-fat frying process. Balaban and Pigott (1986) reported a best fit with the R²- value of >0.86

for density for fish muscle during drying by assuming linearity in their application of the drying model equation which will be appropriate to our study.

The experimental data were fitted to the following empirical equations (Eq. 5.4 and 5.5) to predict the bulk and apparent density of chicken meat during deep-fat frying.

$$\rho_B = \rho_{oB} + a * X \tag{5.4}$$

$$\rho_A = \rho_{oA} + a * X \,, \tag{5.5}$$

Where $\rho_{\scriptscriptstyle B}$ is the bulk density, $\rho_{\scriptscriptstyle 0B}$ is the initial bulk density, $\rho_{\scriptscriptstyle A}$ is the apparent density, $\rho_{\scriptscriptstyle 0A}$ is the initial density, a is a constants and X is the moisture loss.

Table 5.2 shows the corresponding values of the constants and the coefficient of determination (R²) obtained from a linear regression analysis. The estimation of density parameters by Eq 5.4 and 5.5 shows a good fit, and thus the coefficients of the determinations are relatively high for all ranges of the FOT as seen in Figure 5.4 the experimental and predicted curves as a function of moisture loss.

Table 5.2 Estimated constant values from Equations 5.4 and 5.5 for the determination of bulk and apparent density parameters of deboned chicken meat during deep-fat frying.

| | <u> </u> | Model Parameters (Bulk Densities) | | | |
|------|------------------|-----------------------------------|---------------|--------|------|
| Temp | $ ho_{0B}$ | $ ho_{0B}$ | | a | |
| (°C) | Estimate | SE | Estimate | SE | R² |
| 170 | 1.1312 | 0.0074 | -0.0033 | 0.0001 | 080 |
| 180 | 1.1319 | 0.0070 | -0.0036 | 0.0003 | 0.89 |
| 190 | 1.0996 | 0.0126 | -0.0033 | 0.0004 | 0.78 |
| | | Appar | ent Densities | | |
| Temp | $ ho_{{}_0{}_A}$ | | а | | R² |
| (°C) | Estimate | SE | Estimate | SE | |
| 170 | 1.1238 | 0.0028 | 0.0029 | 0.0001 | 0.96 |
| 180 | 1.1386 | 0.0075 | 0.0028 | 0.0003 | 0.82 |
| 190 | 1.1354 | 0.0042 | 0.0017 | 0.0001 | 0.89 |

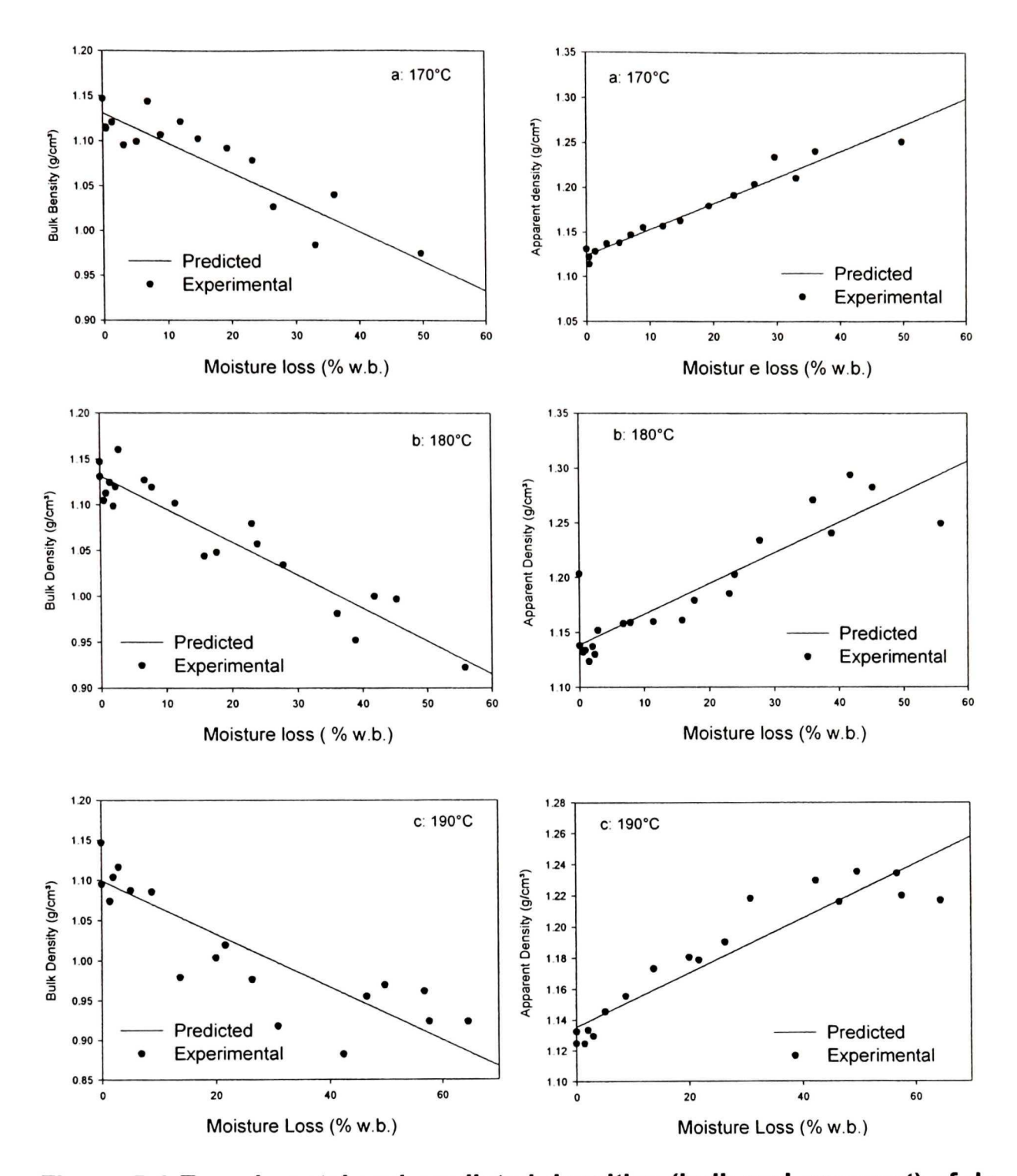


Figure 5.4 Experimental and predicted densities (bulk and apparent) of deboned chicken meat as a function of water loss fraction during deep-fat frying.

5.4.2 Shrinkage

Shrinkage is a change in volume induced by moisture loss and probably formation of pores. Shrinkage in meat products is usually anisotropic. Rahman and Perera (1999) reported that shrinkage in a direction parallel to the muscle fibers is significantly different from that perpendicular to the fiber direction. Madamba et al. (1994) reported shrinkage of biological materials to be based on their fiber-orientation and anisotropic structure. Since this leads to shape irregularity as shrinkage proceeds, shrinkage was therefore determined by the volume displacement method rather than by dimensional measurement. The ANOVA for volumetric shrinkage is given in Appendix Table 10. This parameter changes significantly in time and is temperature-dependent. The trend in time is not affected by temperature as indicated by the non-significant interaction. Shrinkage increases logarithmically with time as seen by the shape of the curve in Figure 5.5. The mean comparison by DMCT of the effect of FOT and time are compiled in Appendix Table 11 and 12. The rate of shrinkage (0.013, 0.001, and 0.008) was rapid during the first 90 s of deep-fat frying for temperatures 170, 180, and 190° C, respectively and decreased as frying time increased.

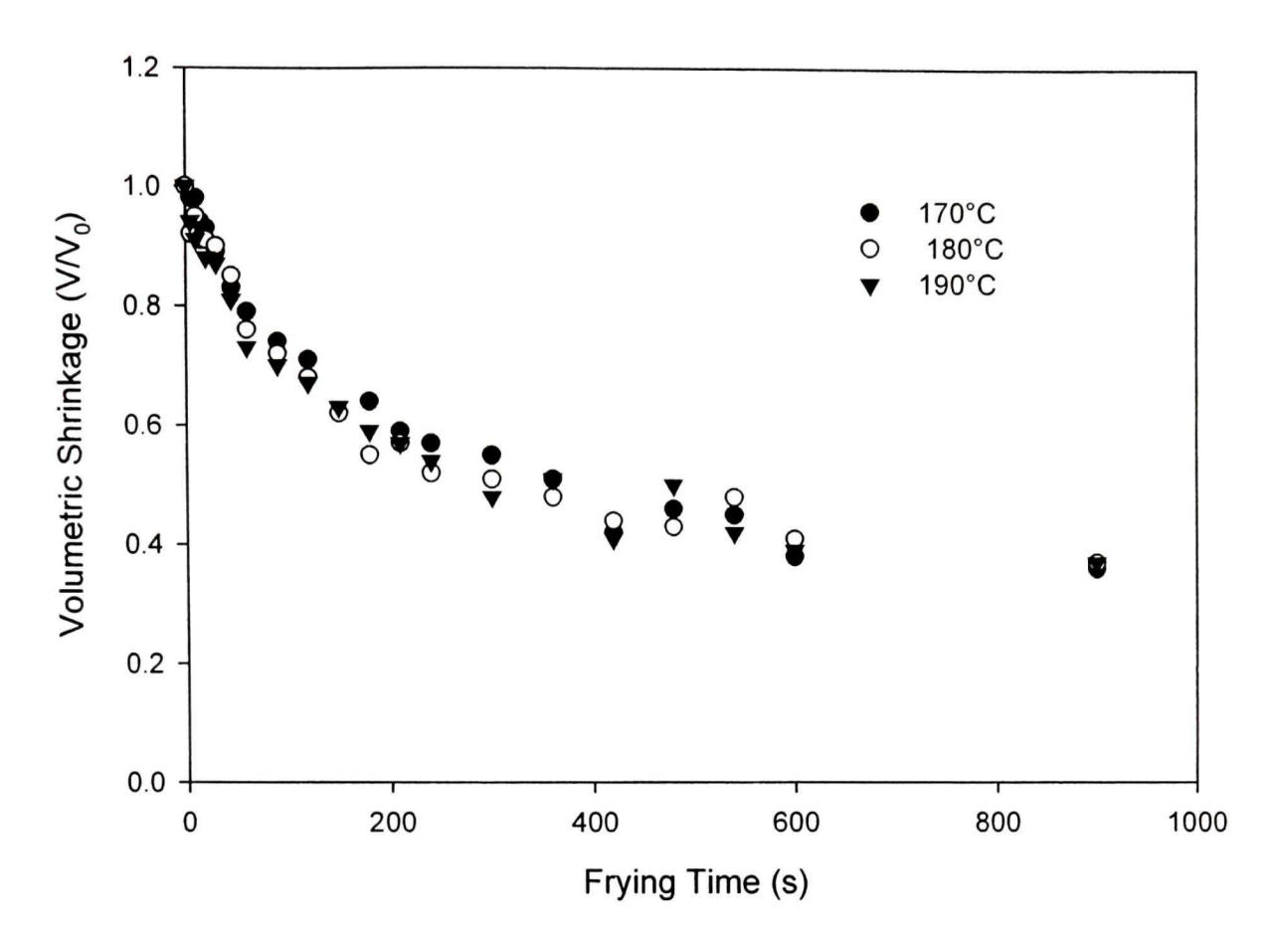


Figure 5. 5 Volumetric shrinkage as a function frying time.

Volumetric shrinkage curves (Figure 5.5) exhibited similar pattern as that of time function moisture loss in our previous studies (Chapter IV). The relationship between shrinkage and moisture loss was found to be linear as shown in Figure 5.6. However, the rate of volumetric shrinkage slows down after 300 s of frying probably due to the oil uptake at low moisture regions. A linear relationship was observed at all levels of FOT, similar correlations were reported by others researchers on drying of foods (Moreira and Sereno, 2003; Krokida et al., 2000; Sjoholm and Gekas, 1994; Karathanos et al., 1993; Lozano et al., 1983). The regression equations for each temperature are given in Table 5.3. The correlation coefficients indicate a close fit to the experimental data.

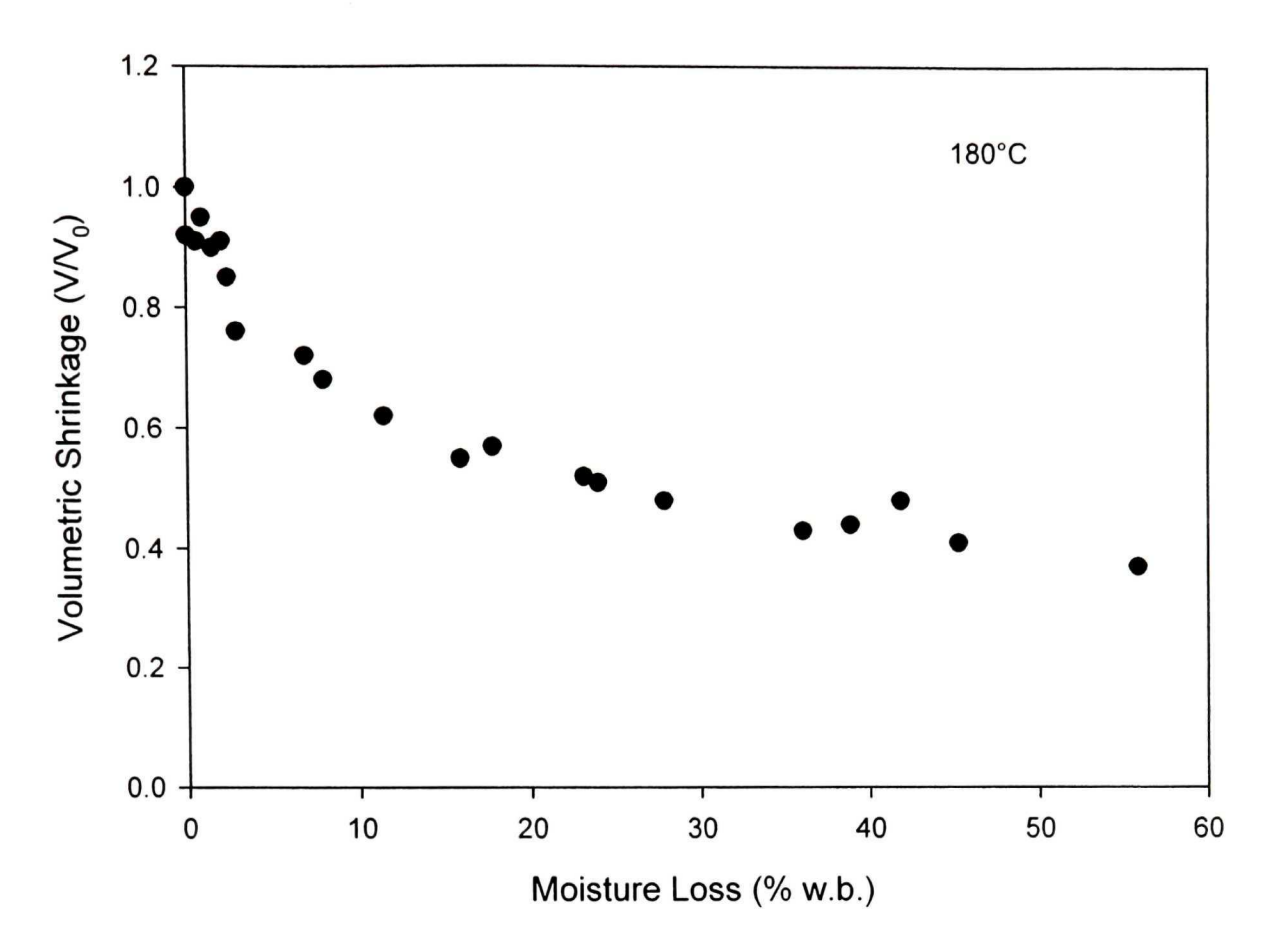


Figure 5.6 A typical apparent volumetric shrinkage of as a function of moisture loss for FOT 180°C.

Table 5.3 Regression equations describing volumetric shrinkage as a function of moisture fraction for de-boned chicken meat during deep-fat frying.

| Temperature | Regression Equation | R² |
|-------------|----------------------------|------|
| 170° C | $S_{\nu} = 0.85 - 0.0131x$ | 0.82 |
| 180° C | $S_{\nu} = 0.83 - 0.0011x$ | 0.83 |
| 190° C | $S_{v} = 0.84 - 00082x$ | 0.83 |

 S_v = volumetric shrinkage; x = moisture loss; R^2 = coefficient of determination; (P < 0.01)

5.5 Conclusions

Process variables such as frying temperature and time have a significant (P < 0.01) influence on the physical properties of food materials during the deep-fat frying process. Bulk density decreases with an increase in frying time, while apparent density increases. Strong correlations existed between the densities (bulk and apparent) and moisture loss. A linear equation was used to predict the densities. The relationship between volumetric shrinkage and moisture loss was linear. Finally, the data and analysis from this experiment would give a good foundation for the analysis of pore development during the deep-fat frying of food products. The results of volumetric shrinkage may be utilized to adequately predict apparent moisture diffusivity during frying.

5.6 References

- Balaban, M., and G. M. Pigott. 1986. Shrinkage in fish muscle during drying. Journal of Food Science. 51(2): 510-511.
- Brusewitz, G. H. 1975. Density of rewetted high moisture grain. Transaction of ASAE 18(5):935-938.
- Hough, G., J. Chirife, J., and C. Marini. 1993. A simple model for osmotic dehydration of apple. Lebensmittel-Wissenschaft und. Technologie 26: 151-166.
- Karathanos, V. T., S. Anglea and M. Karel. 1993. Collapse of structure during drying of celery. Drying Technology, 11(5): 1005-1023.
- Karathanos, V. T., N. K. Kanellopoulos, and V. G. Belessiotis. 1996.

 Development of porous structure during air drying of agricultural plant products. Journal of Food Engineering 29:167-183.
- Kassama, L. S. and M. O. Ngadi. 2001. Development of Pores and Pore Size Distribution in Chicken Meat During Deep-fat Frying. Canadian Society of Agricultural Engineering, Mansonville, QC, Paper No. 01-322.
- Kilpatrick, P.W., E. Lowe and W. B. van Arsdel. 1955. Tunnel dehydrators for fruits and vegetables. Advances in Food Research 6:360.
- Krokida, M. K., and Z. B. Maroulis. 1997. Effect of drying method on shrinkage and porosity. Drying Technology 15 (10): 951-966.
- Krokida, M. K., V. Oreopoulou and Z. B. Maroulis. 2000. Effect of frying condition on shrinkage and porosity of fried potatoes. Journal of Food Engineering, 43: 147-154.

- Krokida, M. K., V. Oreopoulou, Z. B. Maroulis and D. Marinos-Kouris. 2001. Deep-fat frying of potato strips quality issues. Drying Technoloy, 19(5): 879-935.
- Lozano, J. E., E. Rotstein, and M. J. Urbicain. 1983. Shrinkage, porosity and bulk density of foodstuffs at changing moisture content. Journal of Food Science 48:1497-1553.
- Mattea, M., M. J. Urbicain, and E. Rotstein. 1990. Prediction of thermal conductivity of cellular tissues during dehydration by a computer model. Chemical Engineering Science 45(11):3227-3232.
- Madamba, P. S., R. H. Driscoll and K. A. Buckle. 1994. Shrinkage, density and porosity of garlic during drying. Journal of Food Engineering 23: 309-319.
- Moreira, R., and A. M. Sereno. 2003. Evaluation of mass transfer coefficients and volumetric shrinkage during osmotic dehydration of apple using sucrose solutions in static and non-static conditions. Journal of Food Engineering. 57: 25-31.
- Marousis, S. N., and G. D. Saravaco. 1990. Density and Porosity in drying starch materials. Journal of Food Science. 55(5):1367-1372.
- McMinn, W. A. M. and T. R. A. Magee. 1996. Quality and physical structure of dehydrated starch-based systems. Drying Technology 15(6&8):1961-1971.
- Micromeritics. 1992. *Multivolume Pycnometer 1305 Operator's Manual.*Norcross, GA: Micromeritics Instrument Corporation.

- Misra, R. N., and J. H. Young. 1980. Numerical solution of simultaneous diffusion and shrinkage during soybean drying. Transactions of ASAE, 23:1277.
- Moreira, R., A. M. Figueiredo and A. M. Sereno. 2000. Shrinkage of apple disks during drying by warm air convection and freeze drying. Drying Technology 18 (1&2):279-294.
- Moreira, R., and A. M. Sereno. 2003. Evaluation of mass transfer coefficient and volumetric shrinkage during osmotic dehydration of apple using sucrose solutions in static and non-static conditions. Journal of Food Engineering 57:25-31.
- Mulet, A., J. Garcia-Reverter, J., Bon and A. Berna. 2000. Effect of shape on potato and cauliflower shrinkage during drying, Drying Technology 18 (6):1201-1219.
- Nelson, S. O. 1980. Moisture dependent kernel and bulk density relationships for wheat and corn. Transaction of ASAE, 23:139-143.
- Ngadi, M.O., L. S. Kassama, and G. S. V. Raghavan. 2001. Porosity and pore size distribution in cooked meat patties containing soy protein. Canadian Biosystems Engineering, 43 (3): 17-24
- Perez, M. G. R and A. Calvelo. 1984. Modeling thermal conductivity of cooked meat. Journal of Food Science 49:152-156.
- Rahman, S. M., C. O. Perera, X. D. Chen, R. H. Driscoll and P. L. Potliri. 1996. Density shrinkage, and porosity of calamari mantle meat during air drying in a cabinet dryer as a function of water content. Journal of Food Enginering. 30: 135-145.

- Rahman, M. S., and Potluri, P. L. 1990. Shrinkage density of squid flesh during air drying. Journal of Food Engineering, 12(2):133-143.
- Rahman, M. S. and C. O. Perera. 1999. Drying and food preservation. In: Handbook in Food Processing. Edited by M. Shafiur Rahman. Marcel and Dekker Inc. NY. Pp 173-216.
- Rahman, M. S. 2001. Towards prediction of porosity in foods during drying: A Brief Review. Drying Technology 19(1): 1 13.
- Roman, G. N., M. J. Urbicain, and E. Rotstein. 1982. Moisture equilibrium in apples at several temperatures: experimental data and theoretical considerations. Journal of Food Science 47:1484-1489.
- Rapusas, R. S. and R. H. Driscoll. 1995. Thermophysical properties of fresh and dried white onion slices. Journal of Food Engineering 24: 149 164.
- Sereno, A. M. and G. L. Medeiros. 1990. Simplified model for the prediction of drying rates of food. Journal of Food Engineering 12(1):1-11.
- Sjoholm, I., and V. Gekas. 1995. Apple shrinkage upon drying. Journal of Food Engineering 25(1):123-130.
- Shepherd, H, and R. K. Bhardwaj. 1986. Moisture dependent physical properties of pigeon pea. Journal of Agricultural Engineering Research 35(4)227-234.
- Suzuki, K., K. Kubota, T. Hasegawa and H. Hosaka. 1976. Shrinkage in dehydration of root vegetables. Journal of Food Sciences 41:1189-1193.

Wang, N. and J. G. Brennan. 1995. Changes in structure, density and porosity of potato during dehydration. Journal of Food Engineering, 24: 61-76.

CONNECTING TEXT

The results in Chapter V confirmed that frying oil temperature and frying time significantly influenced the bulk and apparent densities. The bulk density decreases with frying time while the apparent density behaves in the contrary. Linear relations existed between the densities and moisture loss within the 540 s frying time region, after which they tend to equilibrate, a behavior observed in Chapter III for oil uptake. Volumetric shrinkage was also found to be significantly affected by frying oil temperature and time. The changes in density and volumetric shrinkages implicitly affect oil uptake, therefore it is important to study the effect of this properties on moisture loss and oil uptake.

VI. PORE DEVELOPMENT IN CHICKEN MEAT DURING DEEP-FAT FRYING

6.1 Abstract

In this study, the effect frying oil temperature (FOT) and frying time pore development was investigated during deep-fat frying (DFF) of chicken breast meat. The samples were sized to the following dimension: length (20 mm), width 15 mm and thickness (10 mm). The chicken meat slabs were fried at different frying oil temperatures (170, 180, and 190°C) in an industrial fryer for periods varying from (5 to 900 s). Oil uptake analyses were conducted by soxhlet extraction method with petroleum ether being the base extraction solvent. The pore development calculations were based on the measured densities (bulk and apparent) after the end of each frying time, and were measured by fluid displacement pycnometry. The process variables significantly (P < 0.01)influenced pore development in chicken meat during DFF. An exponential model gave the best fit for pore development in chicken meat. A porosity of 0.28, 0.24 and 0.22 were found after 900 s of frying at the FOT (170, 180, and 190°C). Pore development and moisture loss are interdependent, while oil uptake determines the final porosity.

6.2 Introduction

The absorption of frying oil during deep-fat frying (DFF) of many popular foods is of concern to the health-conscious due to changes in the degree of saturation of the fatty acids, and to the possible absorption of contaminants (Pinthus et al., 1995). Absorption of oil also influences the quality attributes of the finished product. During the DFF process, the rapid evacuation of moisture creates pores in the product, these providing a venue for entry of oil into the product (Moreira et al., 1995, 1997; Farkas and Singh, 1991; King et al., 1968). Rahman, (2001) described pore formation to be the result of the transport mechanisms of free water, bound water and water vapor. At high initial water content, liquid mass flow within the porous medium is due to the capillary forces. The formation of these capillary pathways is a phenomenon that controls oil uptake as suggested by Perkins and Erikson (1996).

The amount of water lost could be correlated to porosity as a function of time. There have been various attempts to correlate moisture the loss to porosity (Hussain et al., 2002; McDonald and Sun, 2001; Rahman et al., 1996; Rahman and Potluli, 1990). The authors concluded that porosity increases in time as water content diminishes. However, Pinthus et al. (1995) determined the net porosity of French fries by recalculating the sample bulk and particle densities after subtracting the mass of absorbed oil and assuming that the pores are filled with air. They concluded that intrusion of oil after the evacuation of moisture tends to decrease final pore sizes.

Process variables such as frying oil temperature (FOT) and frying time significantly influence porosity (Pinthus et al., 1995; Pinthus and Saguy, 1994; DuPont et al., 1992; Gamble and Rice, 1987; Pravasani and Calvelo, 1986). Pore development due to moisture loss during cooking of meat products is usually accompanied by shrinkage and a change in density, as reported by Perez and Calvelo (1984) and by Rahman (1995, 2001).

Information concerning pore formation in foods during DFF is not readily available; however such information is important to process design, to the prediction of the physical properties of the final product, as well as to the characterization of the quality of deep-fried foods. The objective of this study was to investigate the relationships between the operating conditions (frying oil temperature and frying time), moisture loss and porosity of de-boned chicken breast meat.

6.3 Materials and Methods

Fresh de-boned chicken breast meat was purchased from a local supplier.

The sample stock was stored in a freezer at –20°C until used, and was thawed in a refrigerator at 4°C for 24 to 36 h prior to use.

6.3.1 Sample preparation

Thawed samples were cut into rectangular slabs with length, width and thickness of 20, 15 and 10 mm, respectively. The samples were deep-fat fried individually according to the procedure described in Chapter V.

6.3.2 Moisture analysis

Moisture loss was determined by weighing the sample in a TR-4102D (Denver Instrument Co., Denver, CO), before and after frying and subtracting the mass of oil absorbed. Details see Chapter V.

6.3.3 Fat analysis

Samples were freeze-dried in a ModulyOD-115 freeze-dryer (Thermo Savant, Holbrook, NY), according to the procedure described in chapter V. They were then ground using a blender (Proctor-Silex, model E160B, Picton, ON), and placed in a thimble. Fats were analyzed according the procedure described in Chapter III.

6.3.4 Density analysis

The bulk and apparent densities were determined by the fluid displacement technique. The measuring fluids were water and helium for measuring bulk and particle density, respectively. Details are given in Chapter V.

6.3.5 Porosity analysis

Porosity is volume fraction of void space or air in a material matrix and is defined as the air or void volume per total volume of material. Porosity was computed based on the bulk and apparent density data (measured and reported in the previous Chapter V) using the following empirical relationship (Eq. 6.1).

$$\varepsilon = 1 - \frac{\rho_b}{\rho_s} \tag{6.1}$$

Where ε is the porosity, ρ_{b} is the bulk density, and ρ_{s} is the apparent density of the fried chicken sample.

6.3.6 Experimental design

Three samples were fried for each of the following times (5, 10, 15, 20, 30, 45, 60, 90, 120, 150, 180, 210, 240, 300, 360, 420, 480, 540, 600, and 900 s), and three raw samples were used as controls. The frying times were randomized within the frying oil temperatures (170, 180, and 190°C) and the replicates were run in sequence at a given frying times. A Generalized Linear Model (GLM) was used for pore development estimation as a function of moisture loss while a non-linear regression was used for the estimate of oil uptake and correlations analysis was conducted using SAS software. All mean comparisons were by the Duncan's multiple range test (DMRT) and the levels of significance were tested at the 5% level.

6.4 Results and Discussion

The changes in porosity in time are plotted for the three FOT's in Figure 6.1. In the initial stages of frying, some porosity values are negative. The porosity of the product is shown to increase more or less linearly with frying time to about 420 s, after which the porosity tends to level off.

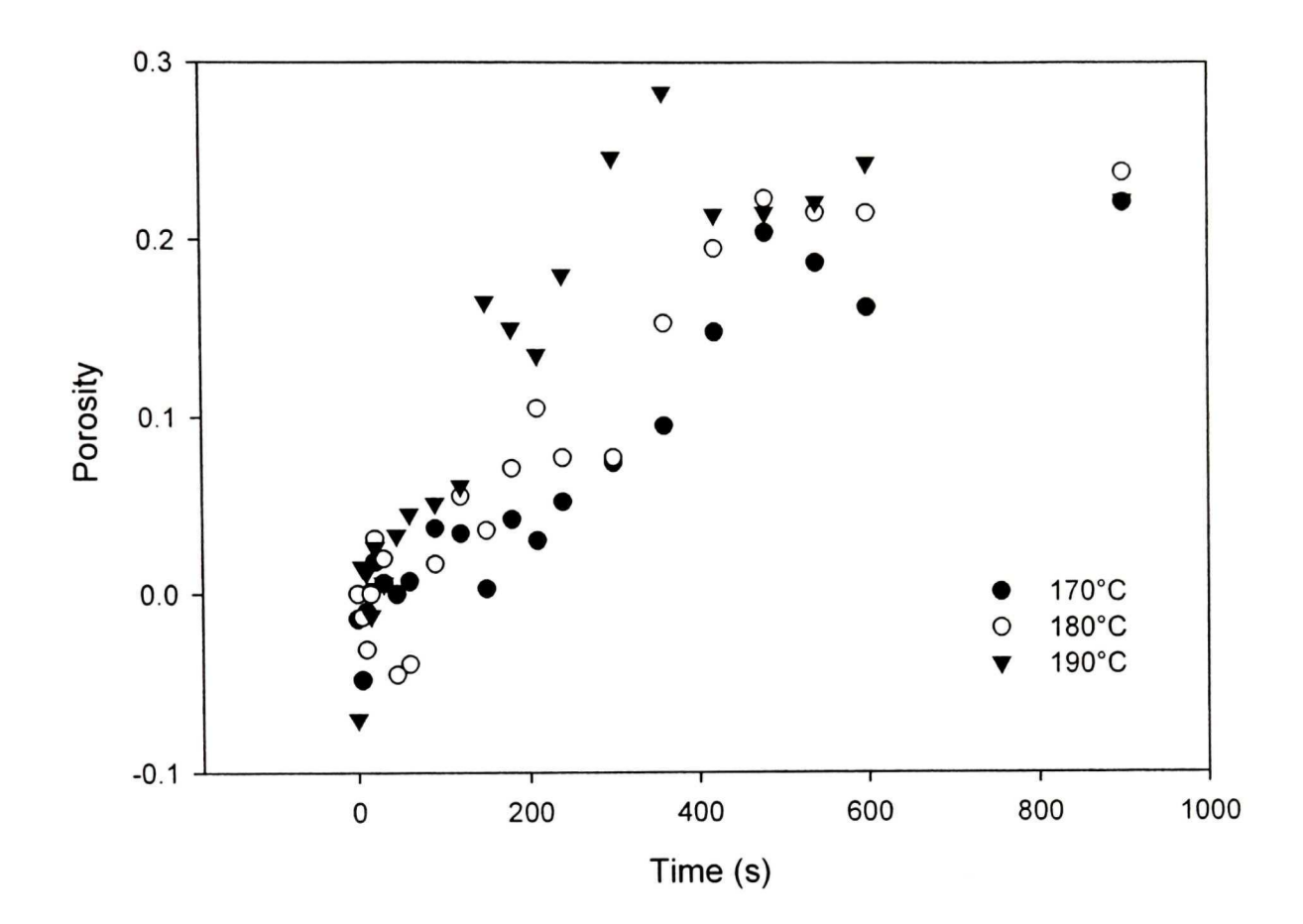


Figure 6.1 Change in porosity with frying time at different temperatures in de-boned chicken meat slabs.

This tendency was similar to that exhibited by oil uptake (Chapter III), apparent density and volumetric shrinkage (Chapter V). The leveling off could be attributed to shrinkage and oil uptake. Pinthus and Saguy (1994) suggested that the intrusion of oil in voids left by evacuated moisture hinders pore development. The absorbed oil may also minimize structural collapse.

During the initial unstable phase of frying (<45 s) excess volumes exists within the 45 s frying time regions, a region labeled as a zone of instability in Chapter III. The excess volumes contribute to the creation of negative pores. Rahman (1995) describes the existence of excess volume as a result of the interaction of phases during processes. In our case, swelling and shrinkage of myofibrils, which are the contractile elements of tissues, may have contributed to such erratic behavior. The reaction of the collageneous connective tissues to initial heating corresponding to the constant-rate period of moisture loss could induce erratic volume change thus effect porosity.

The analysis of variance (ANOVA) was conducted and results tabulated in Appendix Table 13. Pore formation changes significantly in time as modulated by frying oil temperature (P < 0.01). Frying time and temperature had a highly significant (P < 0.01) combined effect on pore formation. The interaction of time and FOT was also significant. Maroulis and Saravacos (1990) and Rahman et al. (1996) also found that pore formation was dependent on drying air temperature of various food products. Differences between the mean porosities at each time-temperature combination were tested for significance by Duncan's Mean Comparison Test in Appendix Table 14.

The relationship between pore development and moisture loss is plotted in Figure 6.2. The increase in pore development is associated with increased moisture loss ratio, as observed by others (Hussain et al., 2002; Rahman, 2001; Moreira et al., 1999; Pinthus and Saguy, 1994; Gamble and Rice, 1987; King et al., 1968; King, 1968). Pearson correlation coefficients were computed and are

shown in Table 6.1. A strong correlation (r = 0.81; P < 0.01) existed between porosity and time. The correlation between porosity and moisture loss was about the same as that between porosity and time (r = 0.77; P < 0.01), as one would expect given the linearity found between moisture loss and time (Chapter III).

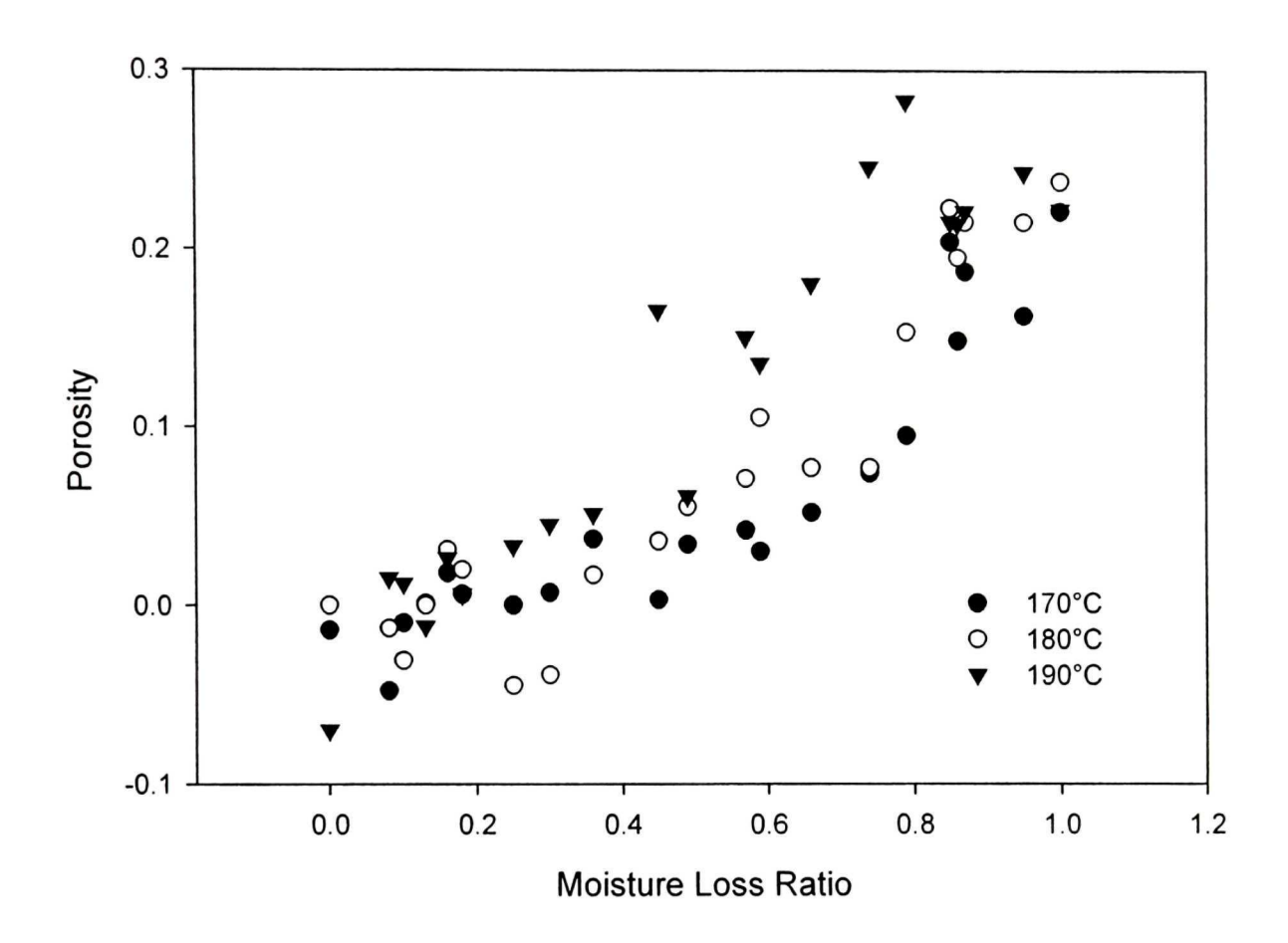


Figure 6.2 Porosity as a function of moisture loss at different frying temperatures in de-boned chicken meat samples during deep-fat frying.

Table 6.1 The Pearson correlation coefficient matrix between dependent and independent variables of de-boned chicken meat during deep-fat frying. (probabilities are in parentheses).

| | Time | Tomporaturo | Moisture | Porosity | Oil |
|-------------|--------|-------------|----------|----------|--------|
| | TITLE | Temperature | loss | Porosity | Uptake |
| Time | 1.00 | 0.00 | 0.94 | 0.81 | 0.71 |
| | | (0.01) | (0.01) | (0.01) | (0.01) |
| Tomporatura | | 1.00 | 0.14 | 0.23 | 0.26 |
| Temperature | 0.00 | | (0.07) | (0.01) | (0.01) |
| Moisture | 0.94 | 0.14 | | 0.77 | -0.74 |
| Loss | (0.01) | (0.07) | 1.00 | (0.01) | (0.01) |
| Danaite | 0.81 | 0.23 | 0.77 | 1.00 | 0.79 |
| Porosity | (0.01) | (0.01) | (0.01) | | (0.01) |
| Oil Hatalia | 0.71 | 0.26 | -0.74 | 0.79 | 1.00 |
| Oil Uptake | (0.01) | (0.01) | (0.01) | (0.01) | |

The porosity was then modeled as a linear function of moisture loss (Eq. 6.2):

$$\varepsilon = \varepsilon_0 + a * x \tag{6.2}$$

where ε equals porosity, ε_0 is initial porosity (intercept) x is moisture loss and a is a constants (slope). Parameters and their standard errors were estimated by GLM regression for each frying temperature, and the results are shown in Table 6.2. The models were all significant (P < 0.05). This is an indication that the linear model (Eq. 6.2) can adequately be used to predict pore development in deboned chicken meat during deep-fat frying as shown in Figure 6.3. Rahman et al. (1996) used a quadratic model to predict porosity as a function of moisture content in calamari mantle meat. There appears to be excess porosity in the moisture loss region $x \le 1.48$. This may have affected the degree of accuracy of the model. This being in the early stages of frying may be due to instability caused by evaporative cooling as observed in the previous studies (Chapter III and IV) and the reaction of the muscle fiber tissues to heat. Some authors describe this phase as a warm-up period analogous to the constant-rate period in drying (Singh, 1995; Rizvi, 1994).

Table 6.2 Pore development model parameters as a function of moisture loss in de-boned chicken meat during deep-fat frying and ANOVA statistics for the regression coefficients.

| | Model Parameters | | | | |
|--------------|--------------------------|--------|----------|--------|------|
| Temp (°C) | $oldsymbol{arepsilon}_0$ | | а | | R² |
| | Estimate | SE | Estimate | SE | |
| 170 | -0.0052 | 0.0031 | 0.0050 | 0.0004 | 0.91 |
| 180 | -0.01225 | 0.0085 | 0.00051 | 0.0003 | 0.92 |
| 190 | 0.0278 | 0.0148 | 0.0041 | 0.0005 | 0.80 |

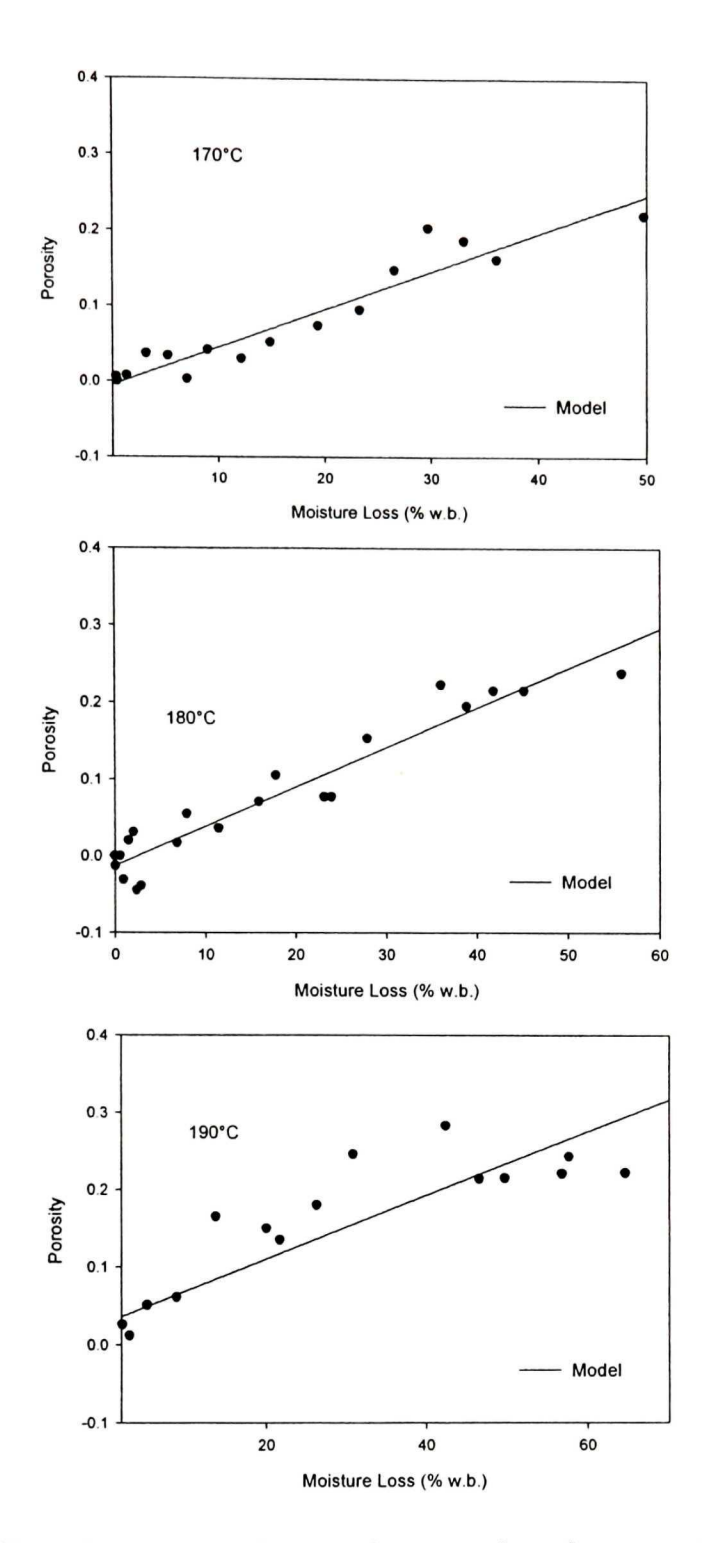


Figure 6.3 Predicted vs experimental pore development as a function of moisture loss at different frying temperatures in de-boned chicken meat samples during deep-fat frying.

An exponential model was used to describe porosity in terms of oil uptake for each frying temperature, Eq. 6.3:

$$\varepsilon = a * [\exp(b * C)] \tag{6.3}$$

where, ε is porosity, C is the oil uptake per frying time and a and b are constants. The estimated regression parameters their standard errors are presented in Table 6.3. The results show that porosity and oil uptake are interdependent, the relationship being depicted in Figure 6.4. Pore formation due to moisture evacuation and protein denaturation facilitates transport of oil into the porous medium. McDonald and Sun (2001) associated pore development in cooked beef with denaturation of protein as a result of moisture loss and shrinkage. The rate of pore development decreases significantly at higher FOT. This may be explained by increases in oil uptake at higher temperatures, which may eventually fill the pores to hinder any further uptake. The final porosity may be reduced as a result of increase oil uptake, fact that was corroborated by Pinthus and Saguy (1994). Deep-fat frying may reduce the cohesiveness of fried products as a result of pore development and hence improve the texture and mechanical properties (Hussain et al., 2002).

Table 6.3 Pore development model parameters as a function of oil uptake in de-boned chicken meat during deep-fat frying and ANOVA statistics for the regression coefficients.

| Temperature | Pore Model Parameters | | | |
|-------------|-----------------------|----------|--------|----------|
| | а | | b | |
| 170°C | 0.0036 | (0.0015) | 0.5045 | (0.0347) |
| 180°C | 0.0067 | (0.0015) | 0.3446 | (0.0227) |
| 190°C | 0.0129 | (0.0037) | 0.2941 | (0.0308) |

SE in Parenthesis.

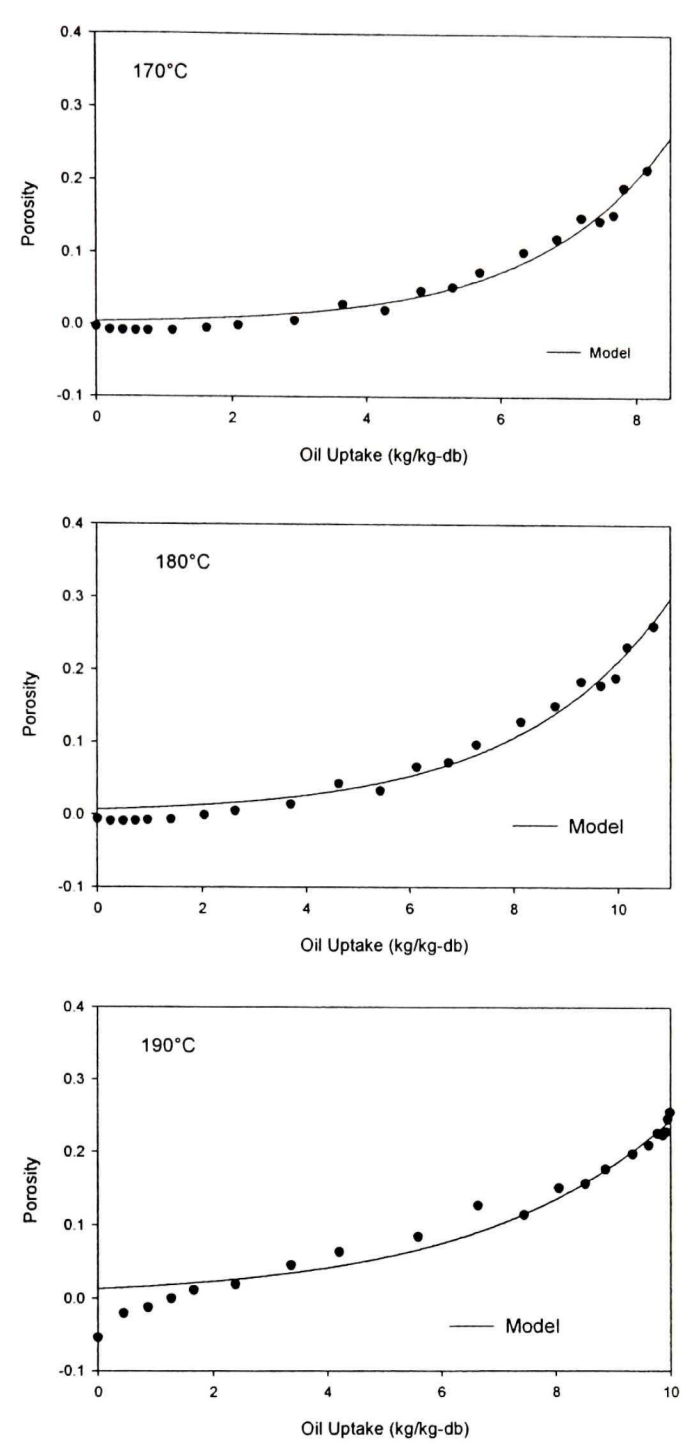


Figure 6.4 Predicted vs experimental pore development as a function of oil uptake at different frying temperatures in de-boned chicken meat samples during deep-fat frying.

6.5 Conclusions

Pore development in de-boned chicken meat during deep-fat frying were investigated. The results indicated that porosity increased as frying time and temperature increased. Frying temperature and time have significant (P < 0.01) influences on pore development. A peak pore fraction of 0.283, 0.238 and 0.220 at frying temperatures 190, 180 and 170° C respectively was observed. A linear model was developed to fit porosity in de-boned chicken meat as a function of moisture loss while and exponential model fitted best in the case of oil uptake. Pore development is dependent on moisture loss and oil uptake influences the final porosity.

6.6 References

- DuPont, M. S., A. B. Kirby and A. C. Smith. 1992. Instrumental and sensory tests of cooked frozen French fries. International Journal of Food Science and technology, 27: 285-295.
- Farkas B. E. and R. P. Singh. 1991. Physical properties of Air-dried and freeze-dried chicken white meat. *Journal of Food Science* 56(3): 611-615.
- Gamble, M.H., and P. Rice. 1987. Effect of pre-fry on oil uptake and distribution in potato chip manufacture. International Journal of Food Science and Technology. 22: 535-548.
- Gomez, A. K., and A. A. Gomez. 1984. Statistical Procedures for Agricultural Research, 2nd Edition, NY: John Willey and Sons Inc.
- Hussain, M. A., M. S. Rahman and C. W. Ng. 2002. Prediction of pores formation (porosity) in foods during drying: generic models by the use of hybrid neural network. Journal of Food Engineering 51: 239-248.
- King, J. C., W.K. Lam and O.C. Sandal. 1968. Physical properties important for freeze-drying poultry meat. Food Technology. 22: 1302.
- King, J. C. 1968. Rate of moisture sorption and desorption in porous, dried foodstuffs. Food Technology 22: 165-171
- McDonald, K., and D-W. Sun. 2001. The formation of pores and their effects in a cooked beef product on the efficiency of vacuum cooling. Journal of food Engineering 47: 175-183.
- Maroulis, S. N. and D. D. Saravacos. 1990. Density and porosity in granular starch drying. Journal of Food Science 55.

- Moreira, R.G., J.E. Palau, V.E. Sweat and X. Sun. 1995. Thermal and physical properties of tortilla chips as a function of frying time. Journal of Food Preservation, 19:175-189.
- Moreira, R.G., X. Sun and Y. Chen. 1997. Factors affecting oil uptake in tortilla chips in deep-fat frying. Journal of Food Engineering. 31:485-498.
- Moreira, R.G., Castell-Perrez, M.E. and Barrufet, M.A. 1999. Deep-fat frying: Fundamentals and applications. Maryland: Aspen Publishers, Inc.
- Perez, M. G. R. and A. Calvelo. 1984. Modeling the thermal conductivity of cooked meat. Journal of Food Science, 49: 152-156.
- Pinthus E.J., and I. S. Saguy. 1994. Initial Interfacial tension and oil uptake by deep-fat fried foods. Journal of food science. 59 (4): 804-807.
- Pinthus E. J., P. Weinberg, and I. S. Saguy. 1995. Oil uptake in deep fat frying as affected by porosity, Journal of Food Science, 60(4):767-769.
- Pravisani, C. I., and A. Calvelo. 1986. Minimum cooking time for potato strip frying. Journal of Food Science. 51: 614-617.
- Rahman, M. S., and P. L. Potluri. 1990. Shrinkage and density of squid flesh during air drying. Journal of Food Engineering 12: 133 143.
- Rahman, M. S. 1995. Food Properties Hand Book. NY: CRC Press Inc.

- Rahman, M. S., C. O. Perera, X. D. Chen, R. H. Driscoll and P. L. Potluri. 1996. Density, shrinkage and porosity of calamari mantle meat during air drying in a cabinet dryer as a function of water content. Journal of Food Engineering, 30: 135-145.
- Rahman, M. S. 2001. Towards prediction of porosity in food foods during drying: a brief review. Drying Technology, 19(1): 3-15.
- Rizvi, S. S. H. 1994. Thermodynamic properties of foods in dehydration. In Engineering Properties of Food 2nd edition. Edited by M. A. Rao and S. S. H. Rizvi.New York, Marcel Dekker Inc. page, 223-309.
- Singh, P. R. 1995. Heat and mass transfer in foods during deep-fat frying: Mathematical modeling provides new tools to study the effect of processing conditions in deep-fat frying of foods. Food Technology, Presented at a symposium sponsored by the IFT Food Engineering Division. 134-137.

CONNECTING TEXT

The effect of frying oil temperatures and frying times on pore development was investigated in Chapter VI. Process variables were found to influence pore development during deep-fat frying. Pore development was dependent on moisture loss. Oil uptake tends to inhibit pore development and hence tend to affect the final porosity during the deep-fat frying process. It is therefore, important to characterize pore structures to understand the effect of oil uptake on pore structure. To accomplish this task, pore structure characterization studies was conducted on pan-fried restructured meat blended with soy-protein extender. This study was performed to explore the possibilities of using mercury porosimetry on fried products.

The materials presented in this chapter was peer reviewed and published in a scientific journal (International Journal of Foof Properties). See detailed in page viii on publications.

VII. STRUCTURAL AND INSTRUMENTAL TEXTURAL PROPERTIES OF MEAT PATTIES CONTAINING SOY PROTEIN

7.1 Abstract

The effect of 2 different types of soy protein namely soy protein flour (SPF) and texturized soy protein (TSP); soy protein extender concentration; cooking times; and cooking temperatures on structural and textural properties of pan-fried patties were studied. Beef patties were formulated using extra lean (10 kg fat/100 kg) ground beef samples, with different concentrations of soy protein (0, 2, 3,5) and 5 % kg/kg total mass). They were formed into patties, and cooked on a griddle at different temperatures (177 and 187°C) and cooking times (10, 15 and 20 min). Water holding capacity (WHC) and total cooking loss (TCL) were determined. Instrumental textural profiles of the cooked samples were obtained using a Universal Testing Machine Instron. Porosity and pore size distributions were determined by a mercury intrusion porosimeter. The results indicated that increasing soy protein concentration increased WHC and reduced TCL. Beef patties extended with TSP were harder and more cohesive than those extended with SPF. Total mean porosities at the 5% soy protein extender concentration were 0.42 and 0.40 for the SPF and TSP extended samples, respectively. Samples extended with SPF had up to 84% capillary pores.

7.2 Introduction

Plant base proteins are extensively used as fillers, binders and extenders in meat systems (Huang et al., 1997). Different plant based proteins such as soy protein, corn germ protein, wheat germ protein, and rapeseed concentrate have been used as meat extenders (Troutt et al., 1992; Rocha-Garza and Zayas, 1995; Ngadi et al., 2001). Soy proteins contain about 50% protein including the eight essential amino acids and considerable quantities of vitamins and minerals (Lockmiller, 1972). They are excellent additives in low fat meat systems. They are available in different forms such as coarse grit (texturized soy protein) to very fine flour (200 mesh) (soy protein flour). The use of soy protein as an extender enhanced water binding capacity and textural properties (Drake et al., 1975); it minimized total cooking loss (Lecomte et al., 1993; Ray et al., 1981) and minimized shrinkage (Smith et al., 1976). Thus, soy protein extension improves the functional characteristics and stability of meat products.

Extension of meat systems with soy protein develops a complex composite heterogeneous and anisotropic structure. It alters the physical and textural characteristics of extended beef patties. This change may upset the microscopic structure of the native material and ultimately the physical properties. Thus meat extension with soy proteins may have a significant influence on textural attributes.

Texture in food is closely associated with the structural makeup of the material. The structural matrix is mostly a network of protein strands surrounded by individual muscle pieces and fibbers (Ma et al., 1991). The ease of

mechanical destruction by mastication is a fundamental textural phenomenon of interest in food industries. Food texture is one of the most important quality attributes, which influences consumer preferences of food products. An objective instrumental textural profile analysis (ITPA) attempts to quantify textural parameters the Universal **Testing** Machine using Instron. The objective method of measurement of meat texture are capable of explaining about 60% of variation in panel scores and the remaining 40% is the inescapable consequence of human error in making judgments (Rhodes et al., 1972). Troutt et al. (1992) also reported a strong correlation between objective Instron method and sensory panel texture traits. Many researchers (Rocha-Garza and Zayas, 1996; Brennan et al., 1974; Lin and Keeton, 1998; Cross et al., 1980; Berry et al., 1999; Ju and Mittal, 2000) reported ITPA on beef patties using Instron.

Mechanical and textural properties such as porosity and pore size distribution can significantly influence the mechanical and textural characteristics of cooked and dried foods (Ngadi et al., 2001; Karathanos et al., 1996; Rahman et al., 2002), these parameters could also be correlated to the mechanical and textural properties (Gogoi et al., 2000; Pietsch, 1999). Mercury porosimetry is one of the most commonly used methods to study physical properties of porous materials. The method provides data on densities, porosity and pore size distributions of materials, although the values of porosity measured by porosimetry are usually lower than values measured with a pycnometer (Rahman et al., 2002), due to the phenomenon of interconnectedness and dead-end or

blind pores (Hicsasmaz and Clayton, 1992). Ngadi et al. (2001) used porosimetry data to characterize porosity and pore size distributions in beef patties extended with soy protein. Other authors (Rahman et al., 2002; Farkas and Singh, 1991; Karathanos and Saravacos, 1993) also used the technique to characterized pore size distribution in food products. The knowledge of physical and textural properties is vital to the design of better quality foods and as well as mathematical model of food systems (Datta and Zhang, 1999).

The objective of this research study was to investigate the effect of temperature, cooking time, types of soy protein, and soy protein extender concentration on physical properties of pan-fried beef patties, while exploring the use of mercury porosimetry on fried products.

7.3 Materials and Methods

Extra lean (10 kg fat/100 kg) ground beef samples were used throughout this study. Samples were purchased from a local grocery chain. Two types of soy protein were used namely: low fat soy-protein flour (SPF) with particle size (100 mesh) and medium grade texturized soy-protein (3 − 6.4 mm) particle size (TSP) (IOWA SOYTM, Vinton, IO). Experimental samples were formulated by adding various levels of soy protein concentrations (0, 2, 3.5, and 5 % kg/kg total mass) and other ingredients as shown in Table 7.1, and details as described by (Ngadi et al., 2001). The same formulation was use for both the SPF and TSP. The formed patties were frozen at −18°C ± 1°C until required for use.

Table 7.1 Formulation of ground beef patties extended with soy-protein (soy protein flour and textured soy-protein) at different concentrations.

| Ingredient | Treatment [composition (g)] | | | |
|-----------------|-----------------------------|------|------|------|
| Extender | 0 | 2 | 3.5 | 5 |
| Ground Beef | 82.5 | 80.5 | 79.0 | 77.5 |
| Salt | 2.5 | 2.5 | 2.5 | 2.5 |
| Distilled water | 15 | 15 | 15 | 15 |
| Total | 100 | 100 | 100 | 100 |

The water holding capacity (WHC) for the uncooked beef patty samples that had been extended with SPF and TSP were determined by centrifugation method. Ten grams of samples were mixed with 40 mL distilled water in centrifuge tubes and were allowed set for 30 min in a water bath (Isotemp 1028S, Fisher Scientific, Pittsburgh, PA) at 22°C prior to the test run. The centrifuge tubes were inserted in the centrifuge (Model HN-S, International Equipment Company, Needham Heights, MA) holding chambers, and spun at 1200g for 30 min. At the end of the centrifugation the extra water was removed. The new mass of the sample was recorded and hence the WHC was determined (Ngadi et al., 2001).

Frozen patty samples were thawed overnight in a refrigerator at 4°C. Cooking was accomplished at 177 and 187°C using a pan fryer (Moffat,

Specialites De Cuisine Inc., Montreal). All the patty samples were turned over after the first 5 min of each time variable used. Internal center temperatures of patties were monitored using T-Type thermocouples that were attached to a data logger (Hotmux, DCC Corporation, Pennsauken, NJ). Cooking loss after each cooking treatment was determined after the samples had equilibrated at room temperature (23°C \pm 1°C) as the ratio of the total mass loss after pan-frying and the original mass of the raw patty.

Instron Universal Testing Apparatus, (model 4502, Canton, MA) was used to obtain textural profile of cooked samples. Patty samples were cut with a cylindrical die (36 mm diameter) into 12 mm thick sizes. A 50 KN load cell and a flat-headed plunger attachment (19.1 mm diameter) were used. Samples were individually compressed at a crosshead traveling speed of 20 mm/min. The equipment was interface to a microcomputer for the data acquisition, and all the data of the measured ITPA parameters were acquired through the microcomputer for further analysis. Instrumental textural profile parameters obtained by twice compressing the samples to 75% of their original thickness. Hardness is the maximum applied force (N) which was indicated by the height of the first peak in the ITPA curve. Cohesiveness, a measure of the internal strength of the bonds that make up the product, was obtained as the ratio of the area under the second peak and the area under the first peak. Toughness, which is the ability of the product to withstand repeated stress before fracture, was measured as the area under the first curve of ITPA.

Porosity and pore size distributions were determined using a porosimeter (Autopore III series 9400, Micromeritics Instrument Corporation, Norcross, GA) following the methods of (Ngadi et al., 2001). The equipment was designed with the capacity to measure micropores up to 5 nm pore diameter at a maximum pressure of 228 MPa. Samples measured with the porosimeter were vacuum dried prior to the test, using the method described by (Ngadi et al., 2001). Data on porosity and cumulative volume of intrusion were acquired through a microcomputer interfaced to the porosimeter. Mercury intrusion and extrusion volumes are plotted as a function of pore diameter or pressure. Pore sizes are calculated based on the Washburn equation (Eq. 7.1) (Webb and Orr, 1997) on the assumption that the pores are cylindrical in shape.

$$D = -\left(\frac{1}{P}\right) 4\gamma \cos \varphi \tag{7.1}$$

where D is the pore diameter, P is the applied pressure at which the mercury is forced into the sample, γ is the surface tension of mercury given as 0.485 N/m, and φ is the solid-liquid contact angle (130°). Although the assumption may not represent the actual nature of pores, it is generally accepted in the practical sense of estimation, or else may be too complicated. The pore size distribution are usually computed based on the relationship between pore radius and pore volume as defined (Eq. 7.2)

$$D(v) = \frac{P}{r} \frac{d(v_t - v)}{dP} \tag{7.2}$$

where D_v is the pore size volume distribution function, P is the applied pressure at which the mercury is forced into the sample and r pore radii measure to every corresponding P, v_r is the total pore volume and v is the pore volume.

A factorial experimental design was used for this study. The experimental factors involved and their levels were as follows: type of soy protein extender (control, SPF, TSP); soy protein concentration (0, 2, 3.5 and 5%); cooking time (0, 10, 15, 20 min) and temperature (177 and 187°C) with 3 replicates. Analysis of variance (ANOVA) and the mean comparison using the Duncan's multiple range test (DMRT) was accomplished by statistical analysis system (SAS v.8).

7.4 Results and Discussion

7.4.1 Water holding capacity and cooking losses

Water holding capacity (WHC) and total cooking losses (TCL) were determined on beef patties extended with soy protein flour (SPF) and texturized soy protein (TSP). The analysis of variance (ANOVA) of data indicated that the type of soy protein (SPF or TSP) and concentration used have significant effect (P < 0.01) on WHC of beef patties. The Duncan's mean comparison test (DMRT)

results for WHC is presented in Table 7.2. The results show that increasing soy protein extension concentrations improved the water holding capacity.

Table 7.2 Mean comparison of types of soy-protein used on WHC and TCL on pan-fried beef patties extended with soy protein.

| Concentration | WHC | | TCL | |
|---------------|---------|---------|---------|---------|
| (%) | SPF (%) | TSP (%) | SPF (%) | TSP (%) |
| 0 | 9.0a | 9.0a | 29.5a | 29.5a |
| 2 | 13.9ab | 17.1b | 26.6ab | 20.7b |
| 3.5 | 20.9c | 20.6b | 24.0bc | 15.6c |
| 5 | 18.9bc | 24.0b | 21.6c | 13.8c |

Means with the same letter and in the column are not significantly different at 5% level.

Similar results were reported by other authors (Mansour and Khalil, 1997; Trius et al., 1994; Karathanos and Saravacos, 1993; Ngadi et al., 2001). No significant difference (P > 0.05) was observed between the control samples and the samples with 2% SPF extension, whereas there was significant difference (P < 0.01) between control samples and 2% TSP extended samples. The mean value of WHC obtained at 5% extender concentration using TSP was higher than the value obtained for SPF. This may be due to differences in the physical characteristics of the extenders. Soy protein flour has a fine powdery texture whereas TSP has a coarse texture that apparently provided pockets for moisture

absorption. Water holding capacity correlates to juiciness in meat patties systems (Smith et al., 1976). Extension of meat patties with soy protein should improve moisture retention and final product quality.

Analysis of variance (ANOVA) showed that there was significant effect (P < 0.01) of the type of soy protein on TCL. The DMRT showed that the total cooking loss decreased as the extender concentration increased and as WHC also as shown in Table 7.2. Other authors (Troutt et al., 1992; Ray et al., 1981; Cross et al., 1980; Mansour and Khalil, 1997; Trius et al., 1994) have reported similar observations. This could be attributed to the rehydration effect of the soy protein during patty formulation. Cooking time, temperatures also have significant effect (P < 0.01) on TCL. There were increased cooking losses with cooking time and temperature increments. Beef patties extended with TSP incurred less cooking loss as compared to SPF (Table 7.2). The use of soy protein in beef patty systems has favorable implications because of its moisture retention ability associated with textural attributes.

7.4.2 Textural analysis

Textural parameters such as compressive force (hardness), cohesiveness, and toughness were determined from the instrumental textural profile analysis (ITPA) using an objective instrumental measurement method. The effects of the temperature, cooking time, soy protein types and concentration were evaluated for the pan-fried beef patties. Types of soy proteins used had significant influence (P < 0.01) on the hardness, cohesiveness and toughness of

pan-fried beef patties. The mean comparisons of measured ITPA for samples extended with SPF and TSP are shown in Tables 7.3 and 7.4 respectively. It was apparent that increased concentration of SPF significantly decreased (P < 0.05) hardness of the beef patty samples.

Table 7.3 Mean comparison of extender concentration on textural properties of pan-fried beef patties extended with SPF.

| Concentration | SPF | | | |
|---------------|--------------|--------------------|--------------|----------|
| (%) | Hardness (N) | Toughness (MPa) | Cohesiveness | Porosity |
| 0 | 105.9a | 0.036a | 0.31a | 0.44a |
| 2 | 69.6b | 0.026b | 0.35a | 0.37b |
| 3.5 | 68.6b | 0.027b | 0.31a | 0.39b |
| 5 | 58.8c | 0.028b | 0.35a | 0.42a |

Means with the same letter and in the column are not significantly different at 5% level.

Table 7.4 Mean comparison of extender concentration on textural properties of pan-fried beef patties extended with TSP.

| Concentration (%) | TSP | | | |
|-------------------|--------------|--------------------|--------------|----------|
| | Hardness (N) | Toughness (MPa) | Cohesiveness | Porosity |
| 0 | 105.9a | 0.036a | 0.31c | 0.44a |
| 2 | 71.6c | 0.025c | 0.50a | 0.40b |
| 3.5 | 85.3b | 0.030b | 0.42b | 0.40b |
| 5 | 103.9a | 0.038a | 0.36bc | 0.41b |

Means with the same letter and in the column are not significantly different at 5% level.

Montejano et al. (1985) reported a hardness value of 41 N for comminuted beef whereas (Huang and Clayton, 1997) reported maximum compressive force values of 68, 49, 43, and 33 N for ground beef samples extended with 0, 2, 4 and 6% sorghum flour, respectively. Other researchers (Rocha-Garza and Zayas, 1996; Andersson and Lundgren, 1981) have also made similar observations using different extenders. Hardness values obtained in this study are higher than reported values probably due to difference in the extenders. Addition of meat extenders apparently modifies the structure of ground meat patties resulting in decreased hardness. The result may be linked to extender influence on water

holding capacity of the products. The effect of SPF on meat patties may be attributed to its physical characteristics namely: fine particle texture, uniform size distribution, disparsibility and water binding capacity. Extension of meat patties with SPF also significantly (P < 0.01) changed the toughness of samples. However, there was no significant difference (P > 0.05) between the 2, 3.5 and 5% concentrations of SPF used in this study. Cohesiveness of the samples was not changed (P > 0.05) as a result of SPF extension concentration. Samples extended with TSP appeared to be more cohesive and harder than those extended with SPF. Montejano et al. (1985) reported cohesiveness for comminuted beef as 0.31. Brown and Zayas (1990) reported a value of 0.70 as cohesiveness for beef patties extended with corn germ protein. The results obtained in this study were close to the value reported by Montejano et al. (1985). The integrity of pan-fried samples extended with SPF was not compromised by the heat treatment as compared to the TSP extended samples. Large particle chunks of TSP grits were visible on the surface of the patties after extension formulation, which could have contributed to their toughness and cohesiveness. Control samples apparently will require greater force to chew than the samples that were extended with soy protein. As a result, samples with soy protein extensions will be more desirable than control samples. The cooking temperatures had no significant effect (P > 0.05) on cohesiveness at different levels of concentrations of patties extended with SPF. Toughness was influenced (P < 0.05) by cooking temperature and time for samples extended with TSP as indicated by the ANOVA. Cooking time affected cohesiveness of samples extended with SPF. Proteins as extender improve the water retention ability while enhancing textural attributes such as juiciness and binding characteristics. Therefore, the addition of soy protein slurries as extenders had a dilution effect on patties and thus enhanced their functional properties (Lecomte et al., 1993).

7.4.3 Porosity and pore size distribution

The effects of the independent parameters (type of soy protein, soy protein concentration, cooking time and temperature) on porosity were determined using a mercury porosimeter. Total porosities of 0.33 to 0.45 and 0.35 to 0.42 for samples extended with SPF and TSP, respectively were obtained. These values are close to the values reported by (Farkas and Singh, 1991) for air-dried chicken meat, and reported by (Rahman et al., 2002) for vacuum dried tuna meat. However, values are greater than those reported by (Ngadi et al., 2001) for oven cooked meat patties containing soy protein. The ANOVA showed that type of soy protein significantly (P < 0.01) influenced pore development in pan-fried beef patties. Mean comparison of porosity data shown in Tables 7.3 and 7.4, indicated that control samples exhibited higher porosity (P < 0.05). Formulating beef patties with soy protein decreased porosity of samples. Cooking at high temperature could enhance shrinkage as a result of protein denaturation and thus reduce pore sizes (Rahman, 2001). Pan and Singh (2001) attributed shrinkage to structural collapse as a result of severity of heating. There was a significant decrease in porosity when beef patties were extended with 2% TSP. However, increasing the TSP concentration from 2 to 5% did not significantly (P > 0.05) influence porosity of the beef patties. Similar to TSP, extending beef patties with 2% SPF significantly decreased sample porosity. Mean value of porosity obtained with 5% SPF was higher than values obtained using 2 and 3.5% concentrations and was not different from the mean value obtained for control samples. At the 5% soy protein concentration, mean porosity values of 0.42 and 0.40 were observed for samples extended with SPF and TSP, respectively. The initial decrease in porosity in the patties extended with SPF could be attributed to increased solubility and the filling of pores in the patties matrix by fine particles of SPF.

Cumulative pore volumes of pan-fried beef patty extended with 5% soy protein concentration are shown in Figure 7.1.

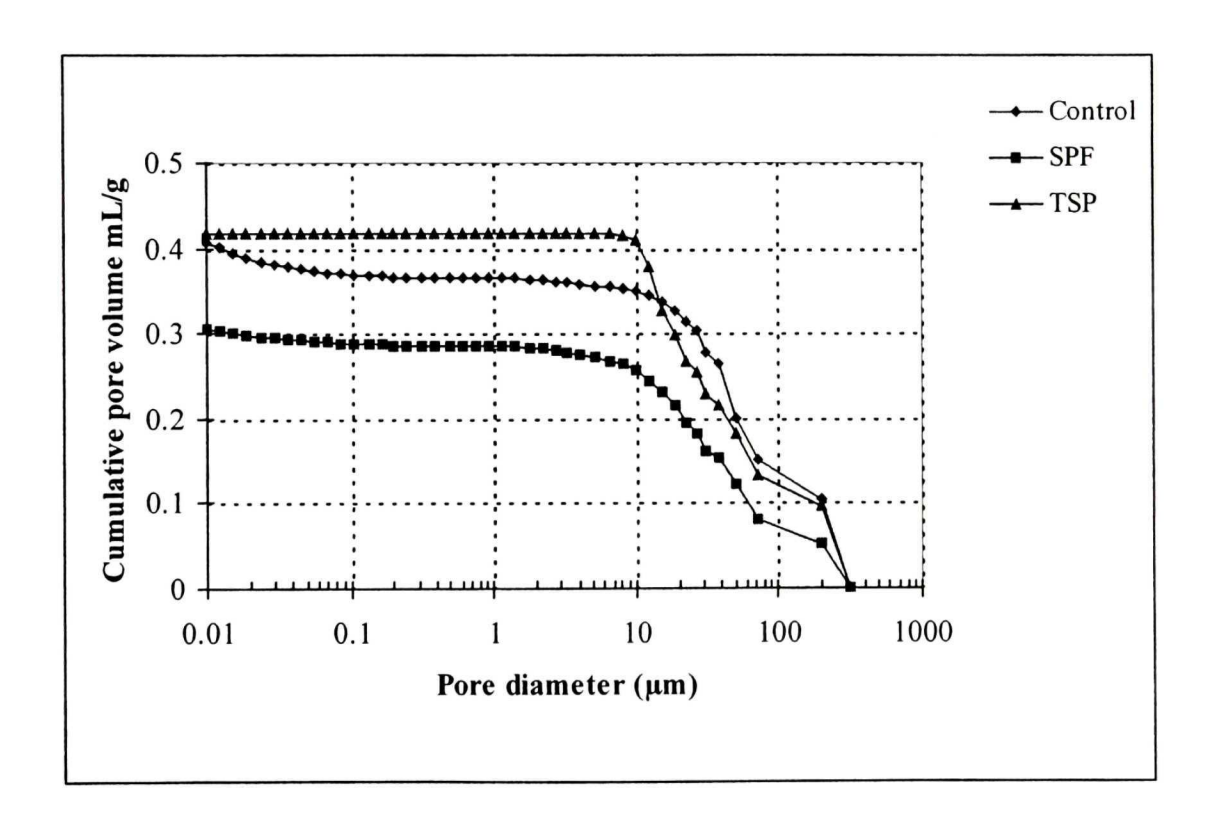


Figure 7.1 Cumulative pore volume (mL/g) of pan-fried beef patties extended with 5% different soy protein concentrations.

The total cumulative pore volume in control samples was 0.416 mL/g. The total cumulative pore volumes in patties extended with SPF and TSP were 0.313 and 0.416 mL/g, respectively. Karathanos et al. (1996) reported a cumulative intrusion volume of 0.623 mL/g for Amioca starch. Ngadi et al. (2001) reported cumulative pore volumes of 0.33 and 0.20 mL/g for oven cooked beef patties extended with SPF and TSP, respectively. The TSP curves showed coarseness within structural matrix, thus exhibiting distinct characteristic large voids due to its gritty texture, while it plateau after a cumulative pore volume of 0.416 mL/g when mercury saturation breakthrough at low pressure (207 KPa) was achieved. No pore volume increment was observed as pressure increased further. It was evident that solubility of TSP in ground beef mixture was difficult to achieve because of the structural makeup with large particle sizes (3 to 6.4 mm). The existence of large planar pore sizes (10 to 70 µm) and interior matrix pores ranging between 0.01 to 10 µm was observed on control and samples extended with SPF.

Cumulative pore volume percentages were also used to characterize pore size distribution on control samples and samples extended with SPF and TSP for pan-fried beef patties. Pore sizes of about 40 µm and smaller were used in this analysis. The effect of type of soy proteins used in patty formulation beef patties is shown in Figure 7.2. Up to 84 and 70% of the pores are capillary pores that exist within the samples extended with SPF and the control, respectively. Nearly all pores in the samples extended with TSP are greater than 10 µm in diameter.

Farkas and Singh (1991) reported that for slowly frozen freeze-dried chicken white meat have 80% pore volume as micropores. Soy protein flour exhibit better quality attributes due to its smaller particle size (100 mesh) of about 0.149 mm, uniformity and solubility. This characteristic trait contributes to its textural enhancement. Control samples exhibited lower percentage of pore volumes, and the effect of soy protein extension appeared to enhance pore development.

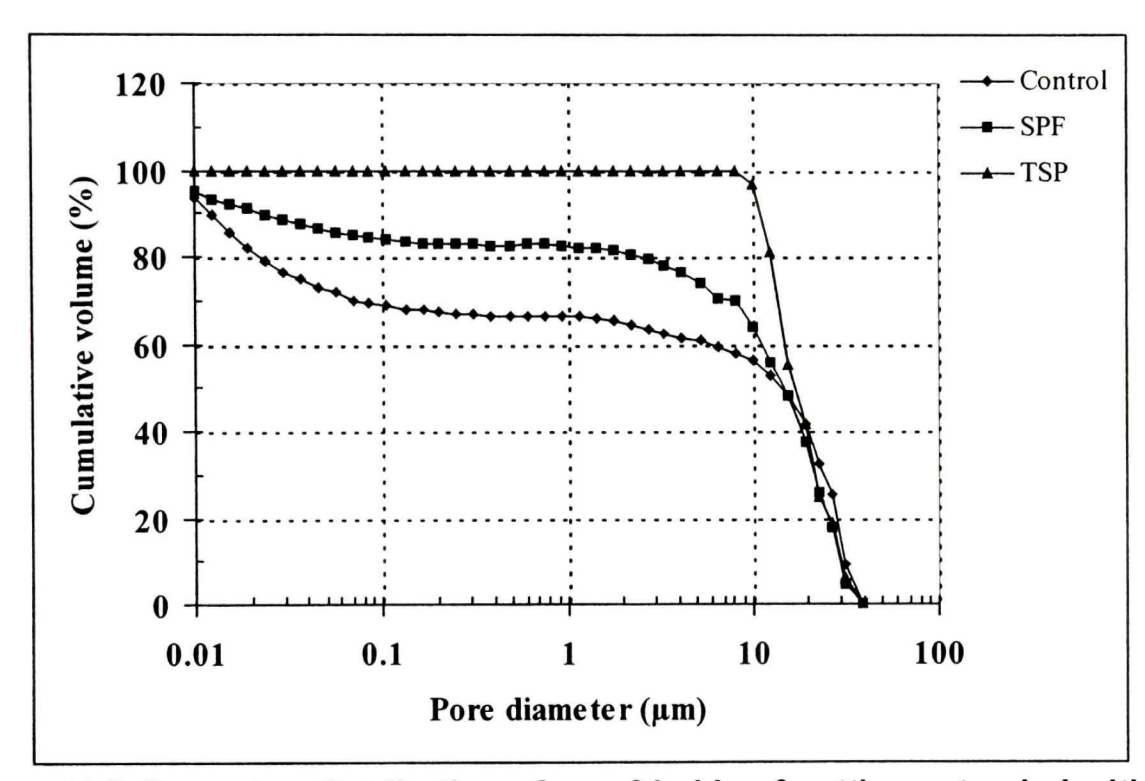


Figure 7.2 Pore size distribution of pan-fried beef patties extended with 5% of different soy protein concentration

7.5 Conclusions

The type of soy protein extender used in the formulation of pan-fried beef patties significantly influences (P < 0.05) the water holding capacity (WHC) and total cooking losses (TCL). Extending beef patties with soy protein increase WHC by 42% thus decreases the TCL by 69% at the highest level of concentration level of 5%. The cooking time and temperature negatively influences (P < 0.01) on TCL. The type of soy protein (TSP and SPF) used in the beef patty system significantly influenced (P < 0.05) textural attributes such as cohesiveness, toughness, and hardness. Pan fried beef Patties extended with SPF appeared to be less hard than those extended with TSP. The use of soy protein had a decreasing effect on porosity. Samples extended with SPF contain over sixty percent of capillary pores within their structural matrix.

ACKNOWLEDGEMENT

This study was supported in part by funding from the Natural Science and Engineering Research Council (NSERC) of Canada.

7.6 References

- Andersson, Y.; Lundgren, B. 1981. Sensory Texture/Consistency Descriptors of Beef Patties Containing protein Products. Journal of Textural Studies, 12, 217-241.
- Berry, B.W.; Bigner-George, M.E.; Eastridge, J.S. **1999.** Hot Processing and Grind Size Affect Properties of Cooked Patties. Meat Science, 53, 37-43.
- Brennan, J.G.; Jowwit, R.; Williams, A. **1974.** Sensory and Instrumental Measurement of 'Brittleness' and 'Crispness' in Biscuits. Forth-international congress of food science and technology, Madrid, Spain, Sept 22-27.
- Brown, L.M.; Zayas, J.F. **1990.** Effect of Corn Germ Protein on the Quality Characteristics of Beef Patties Heated by Microwave. Journal of Food Processing and Preservation, 13, 155-168.
- Cross, H.R.; Berry, B.W.; Wells, L.H. 1980. Effect of Fat Level and Source On the Chemical, Sensory and Cooking Properties of Ground Beef Patties. Journal of Food Science **1980**, 45, 791-793.
- Datta, A. K.; Zhang, J. **1999.** Porous media approach to heat and mass transfer in solid foods. Paper No: 99-3068. St. Joseph, MI: ASAE.
- Drake, S.R.; Hinnergardt, L.C.; Kluter, R.A.; Prell, P.A. **1975.** Beef Patties: The Effect of Textured Soy Protein and Fat Levels On Quality and Acceptability. Journal of Food Science, 40, 1065-1067.
- Farkas, B.E.; Singh, R.P. **1991.** Physical Properties of Air-Dried and Freeze-Dried Chicken While Meat. Journal of Food Science, 56 (3), 611-615.

- Gogoi, B.K.; Alavi, S.H.; Rizvi, S.S.H. **2000.** Mechanical Properties of Proteinstabilized Starch-based Supercritical Fluid Extrudates. International Journal of Food Properties, 3 (1), 37-58.
- Hicsasmaz, Z.; Clayton, J.T. **1992.** Characterization of the Pore Structure of Starch Based Food Materials. Food Structure, 11, 115-132.
- Huang J.; Zayas, J.F.; Bowers, J.A. **1997.** Functional Properties of Sorghum Flour As An Extender In Ground Beef Patties. Journal of Food Quality, 22, 51-61.
- Ju, J.; Mittal, G.S. **2000.** Relationships of Physical Properties of Fat-Substitute, Cooking Methods and Fat Levels With Quality of Ground Beef Patties. Journal of Food Processing and Preservation, 24, 125-142.
- Karathanos, V.T.; Kanellopulos, N.K.; **1996.** Belessiotis, V.G. Development of Porous Structure During Air Drying of Agricultural Plant Products. Journal of Food engineering, 29, 167-183.
- Karathanos, V.T.; Saravacos, G.D. **1993.** Porosity and Pore Size Distribution of Starch Materials. Journal of Food Engineering, 18, 259-280.
- Lecomte, N.B.; Zaya, J.F; Kastner, C.L. **1993** Soya Protein Functional Characteristics Improved in Comminuted Meats. Journal of Food Science, 58 (3), 464-466.
- Lin K.W.; Keeton, J.T. **1998.** Textural and Physicochemical Properties of Low-Fat, Precooked Ground Beef Patties Containing Carrageenan and Sodium Alginate. Journal of Food Science, 63 (4), 571-574.

- Lockmiller, N. R. **1972.** What Are Textured Protein Products? Food Technology, 56-58.
- Ma, C.-Y.; Yiu, S.H.; Khanzada, G. **1991.** Rheological and Structural Properties of Wiener-Type Product Substituted With Vital Wheat Gluten. Journal of Food Science, 56 (1), 228-233.
- Mansour, E. H.; Khalil, A. H. **1997.** Characteristics of Low-Fat Beefburger as Influence by Various Types of wheat Fibers. Food Research International, 30 (3/4), 199-205.
- Montejano, J.G.; Hamann, D.D.; Lanier, T.C. **1985.** Comparison of Two Instrumental Methods With Sensory Texture of Protein Gels. Journal of Textural Studies, 16: 403-424.
- Ngadi, M.O.; Kassama, L.S.; Raghavan, G.S.V. **2001.** Porosity and Pore Size Distribution In Cooked Meat Patties Containing Soy Protein. Canadian Biosystems Engineering, 43 (3), 17-24.
- Pan, Z.; Singh, R. P. **2001.** Physical and Thermal Properties of Ground Beef During Cooking. Lebensmittel.-Wissenschaft und-Technologie, 34, 437-444.
- Pietsch, W. **1999.** Readily Engineering Agglomerates With Special Properties From Micro- and nanosized Particles. Chemical Engineering Progress, 95 (8), 67-81.
- Rahman, M.S. **2001.** Towards Prediction of Porosity in Foods During Drying: A Brief Review. Drying Technology, 19 (1), 3-15.

- Rahman, M.S; Al-Amri, O.S.; Al-Balushi, I.M. **2002.** Pore and Physico-chemical Characteristics of Dried Tuna Produced by Different Methods of Drying. Journal of Food Engineering, 53, 301-313.
- Ray, F.K.; Parrett, N.N.; van Stavern, B.D.; Ockerman, H.W. 1981. Effect of Soy Level and Storage Time on the Quality Characteristics of Ground Beef Patties. Journal of Food Science, 46, 1661-1664.
- Rhodes, D.N.; Jones, R.C.D.; Chrystall, B.B.; Harries, J.M. 1972. Meat Texture II: The Relationship Between Subjective Assessment and Compressive Test On Roast Beef. Journal of Textural Studies, 3, 298-309.
- Rocha-Garza A.E.; Zayas, J.F. **1995.** Effect of Wheat Germ Protein Flour on the Quality Characteristics of Beef Patties Cooked on a Griddle. Journal of Food Processing and Preservation, 19, 341-360.
- Rocha-Garza A.E.; Zayas, J.F. 1996. Quality of Broiled Beef Patties Supplemented With Wheat Germ Protein Flour. Journal of Food Science, 61 (2), 418-421.
- Smith, G.C.; Marshall, W.H.; Carpenter, Z.L. 1976. Textured Soy Proteins for Use In Blended Ground Beef Patties. Journal of Food Science, 41, 1148-1152.
- Trius, A.; Sebranek, J. G.; Rust, R. E.; Car, J. M. 1994. Low-Fat Bologna and Beaker Sausage: Effect of Carrageenans and Chloride Salts. Journal of Food Science, 59, 941-945.
- Troutt E.S.; Hunt, M.C.; Johnson, D.E.; Claus, J.R.; Kastner, C.L.; Kropf, D.H. 1992. Characteristics of Low-Fat Ground Beef Containing Textured-Modifying Ingredients. Journal of Food Science, 57 (1), 19.

Webb P. A.; C. Orr. **1997.** Analytical Methods in Fine Particle Technology. Norcross, GA: Micromeritics Instrument Corporation.

CONNECTING TEXT

Soy protein extenders influenced the water holding capacity and textural characteristics of the restructured meat patties as demonstrated in Chapter VII. Porosity was also affected influenced by extender concentration. Methods of characterization of pore structure were used in the Chapter VII. It was decided to pursue further step in characterizing porosity and pore size distributions on oven-fried restructured with various combinations of type of soy extender and concentration, using response surface methodology to find possible maxima and minima.

The materials presented in this chapter was peer reviewed and published in a scientific journal (see detailed in pages viii on publications).

VIII. POROSITY AND PORE SIZE DISTRIBUTION IN COOKED MEAT PATTIES CONTAINING SOY PROTEIN

8.1 Abstract

The effect of soy-protein flour (SPF) and textured soy-protein (TSP) at concentrations of 0 to 6%; temperatures 167 and 187°C and cooking times 10 and 18 min on porosity and pore size distribution in cooked beef patties were investigated. Ground beef samples were extended with either SPF or TSP, formed into patties and cooked in a convection oven. Water holding capacity (WHC), water activity (aw) and total cooking loss (TCL) of samples were Porosity and pore size distribution measurements were determined. accomplished using a mercury intrusion porosimeter. Increasing either SPF or TSP concentrations marginally increased WHC and decreased total cooking losses (TCL) of samples. Water activity was not affected by various treatments used in this study. Beef patties extended with SPF developed larger pore volumes with porosity ranging from 21 to 34% whereas for the TSP extended patties, porosity was from 4 to 20%. The cumulative intrusion volume for patties extended with SPF and TSP was 0.33 and 0.20 mL/g, respectively. contribution of pores with sizes larger than 10 µm in diameter in the beef patty extended either with SPF or TSP was up to 80%.

8.2 Introduction

Different extenders in the form of soy protein, corn germ protein, wheat germ protein and rapeseed concentrate have been used as binders to modify textural and quality characteristics of meat patties (Rocha-Garza and Zayas, 1996; Lacomte et al., 1993; Troutt et al., 1992). Soy-protein is known for its high nutritive qualities. It has positive influence on health by lowering blood cholesterol and reducing the risk of heart disease (FDA, 1998). Frankfurters extended with soy-protein as pre-emulsified fat increased water holding capacity (WHC) and decreased cooking losses (Lecomte et al., 1993). Soy protein has the capacity to bind water in meat systems thereby increasing cooking yield and prolonging product shelf life substantially (Ray et al., 1981; Yasumatsu et al., Meat extenders alter a product's structural makeup by forming a 1972). heterogeneous product resulting in different physical characteristics during cooking. Heat transfer during cooking also affects physical characteristics and quality of meat patties. Knowledge of the changes in physical properties of extended beef patties is essential for optimizing product quality during heat and mass transfer processes.

The porous structure of meat patties is an important factor that influences heat and mass transfer within the materials (Al-Rqobah et al., 1988; Vagenas and Karathanos, 1991; Farkas and Singh, 1991 and Datta and Zhang, 1999). A porous material can be conceptualized as a network array of capillary vessels separated by random empty spaces of various sizes and shapes. Porosity is the ratio of open (empty) space within a porous solid to the total volume of the solid.

Porosity and pore size distribution affected mechanical and textural characteristics of starch extrudates (Huang and Clayton, 1990). Karathanos et al. (1996) reported that bulk porosity increased during freeze drying of plant products such as apples, potatoes, cabbage, and carrots whereas gradual air drying resulted in decreased porosity. The authors determined that pore sizes of dried plant products varied according to type of product and drying method due to pore structural collapse in air dried samples during dehydration.

Porosity and pore size distributions are important indicators of microstructure and physical characteristics of products. Available data on porosity and pore size distribution in meat patties during cooking is very limited. The data may be important in developing accurate mathematical models of heat and mass transfer during cooking, process design, quality control and development of new extenders. Mercury porosimeter has been used to measure and quantify microstructure of dehydrated food products (Karathanos et al., 1996; Farkas and Singh, 1991). The objective of this study was to investigate the effect of temperature, cooking time and concentration of extenders on physical characteristics such as porosity and pore size distributions of beef patties extended with soy-protein flour and textured soy-protein.

8.3 Materials and Methods

8.3.1 Materials

Extra lean (90/10) ground beef samples with 10% fat was used throughout this study. Samples were purchased from a local grocery chain. Two types of soy protein were used namely: low fat soy-protein flour (SPF) and textured soy-protein (TSP) (IOWA SOYTM, Vinton, IO).

8.3.2 Sample preparation

Samples were formulated by mixing ground beef with soy-protein ingredients and other additives, as shown in Table 8.1. Soy-protein extender was hydrated with distilled water in a glass jar, held for 3 min at room temperature (22°C) before the slurry was thoroughly and manually mixed with the ground beef. The mixture was left for 15 min at room temperature. Beef patty was then formed using a manual patty former. Extended meat sample size of 90 g was pressed to form a beef patty. Dimensions of the formed patty were 90 mm (diameter) x 12 mm (thickness). The formed patties were sandwiched in waxed papers and frozen at –18°C for 24 hr before they were used in experiments.

Table 8. 1 Formulation of ground beef patties extended with soy-protein at different concentrations from 0 to 6%, for both the soy protein flour and textured soy-protein.

| Ingredients | Treatment (composition (g)) | | | | | |
|-------------|-----------------------------|-------|------|------|------|------|
| Extender | 0 | 1 | 2 | 3.5 | 5 | 6 |
| Ground | 20.5 | 0.4.5 | | | | |
| beef | 82.5 | 81.5 | 80.5 | 79.0 | 77.5 | 76.5 |
| Salt | 2.5 | 2.5 | 2.5 | 2.5 | 2.5 | 2.5 |
| Distilled | | | | | | |
| water | 15 | 15 | 15 | 15 | 15 | 15 |
| Total | 100 | 100 | 100 | 100 | 100 | 100 |

8.3.3 Water holding capacity

The water holding capacity (WHC) for raw ground beef samples extended with SPF and TSP was determined using the centrifuging technique. Ten grams of extended meat sample was mixed with 40 mL distilled water, placed in centrifuge tubes and allowed to set at room temperature for about 45 min prior to the test run. The tubes were then inserted in a centrifuge (Model HN-S, International Equipment Company, Needham Heights, MA), set at 1200 g (3000 rpm) for 30 min. After the test run was completed, the extra water from the centrifuged sample was dispensed with a micropipette and the new weight of the

sample was determined. The WHC was computed using the following relationship:

$$WHC(\%) = \frac{Hydrated\ Wt\ of\ sample-Wt.\ of\ sample\ before\ Hydration}{Wt\ .of\ Sample\ before\ Hydration} x100 \tag{8.1}$$

3.3.4 Heat treatment

Frozen patty samples were thawed overnight in a refrigerator at 4°C. Cooking was accomplished at 167 and 187°C using a convective oven (Isotemp 700, Fisher Scientific, Pittsburgh, PA). Internal center temperatures of patties were monitored using T-Type thermocouples that were attached to a data logger (Hotmux, DCC Corporation, Pennsauken, NJ).

8.3.5 Water activity

Water activity (a_w) of the cooked samples were measured with a water activity meter (Aqua Lab Model 3-TE, Decagon Devices, Pullman, WA). The equipment was turned on for 30 min prior to testing in order to allow for equilibration at the preset temperature of 23°C.

8.3.6 Cooking loss

Initial weights of samples were recorded prior to cooking. Cooked patties were allowed to equilibrate at room temperature before the measurement of cooked weight. Total cooking loss (TCL) was computed (Eq. 8.2) as follows:

$$TCL(\%) = \frac{Raw\ Pattty\ wt - Cooked\ Patty\ Wt}{Raw\ Patty\ Wt} \times 100$$
 (8.2)

8.3.7 Porosity and pore size distribution

Cooked beef patty samples were dried at 35°C for 48 hr in a vacuum oven (VWR Scientific, Shel Lab, Cornelius, OR) before pore size measurements. This was performed in order to minimize major changes in their microstructure as a result of further shrinkage due to the protein denaturation during drying. Porosity and pore size distribution in cooked samples were measured using a mercury porosimeter (AutoPore III series 9400, Micromeritics Instrument Corporation, Norcross, GA). The instrument was capable of measuring micropore of up to 0.005 µm pore diameter at a maximum pressure of 228 MPa. To measure porosity and pore size distribution, patty samples were weighed, placed in the penetrometer and loaded in the low-pressure port of the porosimeter. After running the sample at the low-pressure port, the penetrometer assembly was transferred to the high-pressure port according to the standard protocol (Micromeritics, 1999). It was assumed that pores were cylindrical in shape. Pore sizes were calculated using the Washburn equation (Eq. 8.3) (Webb and Orr 1997):

$$D = -\left(\frac{1}{P}\right) 4\gamma \cos \varphi \tag{8.3}$$

where D is the pore diameter, P is the applied pressure at which the mercury is forced into the sample, γ is the surface tension of mercury given as 0.485 N/m,

and φ is the solid-liquid contact angle (130°). This assumption may not accurately represent pores in actual meat samples. However, it is generally accepted as a practical means of estimation of what otherwise would be a very complicated term. The pore surface area of the samples were computed by the following relationship (Eq. 8.4):

$$A = -\frac{\int PdV}{\gamma \cos \varphi} \tag{8.4}$$

where V is pore volume corresponding to the amount of mercury intruded into the sample. The terms γ and φ were assumed not to vary with pressure. Using the pressure - volume mercury penetration data, the cumulative pore surface areas is calculated (Eq. 8.5) thus:

$$\sum \Delta A = -\frac{\sum P \ dV}{\gamma \cos \varphi} \tag{8.5}$$

Data on total intrusion volume, total pore surface area, medium pore diameters, average pore diameter, bulk densities, skeletal density and percent porosity were acquired through a microcomputer data acquisition system interfaced with the porosimeter. The porosity data acquired from the porosimeter was verified by values obtained by independent calculation as shown in Eq. 8.6.

$$\varepsilon = 1 - \frac{\rho_b}{\rho_s} \tag{8.6}$$

where ε is porosity and ρ_b is bulk density. Solid density, ρ_s was measured using a helium pycnometer (Model 1305 Multivolume, Micromeritics Instrument Corporation, Norcross, GA).

8.3.8 Experimental design

The randomized complete block design (RCBD) (Gomez and Gomez, 1984) and the central composite rotatable design (CCRD) (Box and Draper, 1987) were used in this study. The RCBD used was a two-factored factorial design in three blocks (3 x 2) factorial design. Factors involved and their levels were as follows: extender concentration (0, 2, and 5%); cooking temperature (167 and 187°C). Cooking time was held constant at 10 min. The results were analyzed using the Statistical Analysis System (SAS v.8) software.

The CCRD consisted of a three-factored factorial with two levels. The factors were extender concentration (2 and 5%), cooking temperature (167 and 187°C), and cooking time (10 and 18 min.). The matrix for the CCRD optimization experiment is summarized in Table 8.2. The CCRD design has eight experimental points in a cube (run No. 1-8), six star points with an axial distance of 1.682 (run No. 9-14), 5 replications at the central point of the design (run No. 15-19) for experimental error determination, and control (run No. 20). A full second-order polynomial model of the type shown in Eq. 8.7 was used to evaluate the yield (response variable, y) as a function of dependent variables (x)

Table 8.2 Selected factors and their levels for the first factorial design with the CCRD design.

| Standardized (coded) levels | | | | Actual level | | | |
|-----------------------------|-------------|-------------|--------|------------------------|------------------|---------------|--|
| Run | Soy-protein | Temperature | Time | Soy- protein (%) | Temperature (°C) | Time (Min) | |
| 1 | -1 | -1 | -1 | 2 | 167 | 10 | |
| 2 | 1 | -1 | -1 | 5 | 167 | 10 | |
| 3 | -1 | 1 | -1 | 2 | 187 | 10 | |
| 4 | 1 | 1 | -1 | 5 | 187 | 10 | |
| 5 | -1 | -1 | 1 | 2 | 167 | 18 | |
| 6 | 1 | -1 | 1 | 5 | 167 | 18 | |
| 7 | -1 | 1 | 1 | 2 | 187 | 18 | |
| 8 | 1 | 1 | 1 | 5 | 187 | 18 | |
| 9 | -1.682 | 0 | 0 | 1 | 177 | 14 | |
| 10 | 1.682 | 0 | 0 | 6 | 177 | 14 | |
| 11 | 0 | -1.682 | 0 | 3.5 | 160 | 14 | |
| 12 | 0 | 1.682 | 0 | 3.5 | 194 | 14 | |
| 13 | 0 | 0 | -1.682 | 3.5 | 177 | 8 | |
| 14 | 0 | 0 | 1.682 | 3.5 | 177 | 21 | |
| 15 | 0 | 0 | 0 | 3.5 | 177 | 14 | |
| 16 | 0 | 0 | 0 | 3.5 | 177 | 14 | |
| 17 | 0 | 0 | 0 | 3.5 | 177 | 14 | |
| 18 | 0 | 0 | 0 | 3.5 | 177 | 14 | |
| 19 | 0 | 0 | 0 | 3.5 | 177 | 14 | |
| 20 | 0 | 0 | 0 | 0 | 177 | 14 | |

namely extender concentration (denoted by subscript 1), temperature (denoted by subscript 2), cooking time (denoted by subscript 3) and their interactions.

$$y = b_0 + b_1 x_1 + b_2 x_2 + b_3 x_3 + b_{12} x_{12} + b_{13} x_{13} + b_{23} x_{23} + b_1 x_1^2 + b_{22} x_2^2 + b_{33} x_3^2 + b_{123} x_{123}^2 + b_{123} x_{123}^2$$

$$(8.7)$$

Analysis of variance (ANOVA) for treatment main effects was conducted using the SAS software. Multiple comparison of means were by the Duncan's multiple range test (DMRT). All statistical significance was determined at the 5% significance level (P < 0.05).

8.4 Results and Discussion

8.4.1 Water holding capacity and water activity

Analysis of variance (ANOVA) of data indicated significant effect (P < 0.05) of soy-protein on the WHC of beef patties. Mean comparison using the (DMRT) indicated that the mean WHC obtained with patties extended at 5% SPF concentration was significantly higher than the mean WHC obtained at the 0 and 2% SPF concentrations as shown in Table 8.3. A similar trend was obtained with the samples extended with TSP. The mean WHC obtained at the 5% extender concentration was lower with SPF than the corresponding value obtained with the TSP. This could be attributed to the difference in size distributions of the two ingredients. The SPF is fine and of powdery texture whereas the TSP is coarse with grits that apparently provided more pockets for moisture adsorption. The

result shows that increase in soy-protein extension concentration correspondingly increased the WHC of meat samples. Lecomte et al. (1993) reported similar observation on comminuted meat extended with soy-protein. Similarly Yasumatsu et al. (1972) reported a directly proportionality of soy-protein concentration to WHC in bread flour samples. The ability of soy-protein to hold moisture in meat samples has favorable implications in the final product quality by preventing excessive moisture loss in products thus avoiding undesirable crunchy and flaky texture.

Table 8.3 Water holding capacity (WHC) of beef patties extended with soyprotein flour and textured soy-protein.

| Patties | Patties extended with soy-protein WHC (%)* | | | | | |
|-------------------|--------------------------------------------|------|--|--|--|--|
| Concentration (%) | SPF | TSP | | | | |
| 0 | 17a | 19a | | | | |
| 2 | 21.6a | 22ab | | | | |
| 5 | 27.5b | 39b | | | | |

^{*} Means within a column for a given soy-protein that are followed by the same letter are not significantly different (P < 0.05).

8.4.2 Total cooking losses and water activity

Total cooking losses (TCL) were computed using Eq. 8.2 and the results are tabulated in Table 8.4. The ANOVA showed no significant effect (P > 0.05) of the extender concentration and temperature on TCL in patties extended with

Table 8.4 Total cooking losses and water activity data of the different treatments soy-protein flour and texture soy-protein.

| Concentration (%) | Cooking | SPF* | | TSP* | |
|-------------------|-------------|---------|--------------------|---------|--------------------|
| | temperature | TCL (%) | a _w (%) | TCL (%) | a _w (%) |
| 0 | 167 | 12.9a | 0.975a | 10.2ab | 0.963a |
| | 187 | 14.2a | 0.971a | 13.6c | 0.965a |
| 0 | 167 | 12.8a | 0.969a | 9.4a | 0.960a |
| 2 | 187 | 12.6a | 0.973a | 12.9c | 0.969a |
| 5 | 167 | 12.7a | 0.973a | 9.4a | 0.960a |
| | 187 | 13.4a | 0.976a | 11.7bc | 0.966a |

^{*} Means within a column for a given soy-protein that are followed by the same letter are not significantly different (P < 0.05).

SPF within the levels of parameters used in this study. However, the effect of concentration and temperature on TCL was found to be significant in patties extended with TSP. It was observed that as the cooking temperature increased from 167 to 187°C, TCL increased significantly (P < 0.05) for all patties extended with TSP. In general, increasing extension concentration tended to decrease TCL in meat patties. The high cooking temperature apparently increased the rate of moisture migration resulting in shrinkage and cooking loss (Shafer and Zabik, 1975). The lower TCL (higher yield) obtained with TSP could be explained as due to increased capacity of the ingredients to bind water (Mansour and Khalil, 1997). There was no significant difference between the a_w obtained for the different treatments used in this study. The average a_w for all the samples were 0.97.

8.4.3 Porosity

The experimental results of porosity measured using mercury porosimeter, for three response variables for each of the SPF and TSP extenders are shown in Table 8.5. Average porosities of SPF and TSP extended samples were from 21 to 34% and from 4 to 22%, respectively. The porosity values obtained using mercury porosimeter were within the range obtained using helium pycnometer (Eq. 8.6) namely 18 to 40% for SPF extended samples and 10 to 24% for TSP extended samples. Thus mercury intrusion into samples did not appreciably change porosity of samples. The results of this study are also close to reported porosity values for air-dried chicken meat (Farkas and Singh, 1991). Beef patties extended with SPF were more porous than those extended with TSP due to the difference in particle size of the ingredients. The smaller particle size ingredient were apparently more stable and experienced less structural collapse during cooking as in the case of SPF, compared to the larger particle size TSP.

The main effects of extension concentration, cooking temperature and time on porosity were investigated using response surface analysis. Regression models were generated and the parameters that were not significant were dropped from the regression equation. Regression analysis showed no significant effect of experimental variables on porosity for samples extended with TSP. However, for samples extended with SPF, the effect of experimental variables on porosity was significant. Equations 8.8 to 8.10 were used to predict the maximum porosity in cooked SPF extended beef patties for the various

Table 8.5 Structure of the experimental design and data of the dependent variables of the porosity of the samples extended with soyprotein flour and textured soy-protein.

| Expt. | Coded levels | | | Soy-F | Protein |
|--------|--------------|---------|---------|----------|----------|
| # # | Ext | Temp | Time | SPF | TSP |
| π | (coded) | (coded) | (coded) | Porosity | Porosity |
| 1 | -1 | -1 | -1 | 31.7 | 12.5 |
| 2 | 1 | -1 | -1 | 34.1 | 20.8 |
| 3 | -1 | 1 | -1 | 21.8 | 15.4 |
| 4 | 1 | 1 | -1 | 25.0 | 20.2 |
| 5 | -1 | -1 | 1 | 21.3 | 20.4 |
| 6 | 1 | -1 | 1 | 22.1 | 19.0 |
| 7 | -1 | 1 | 1 | 28.1 | 21.7 |
| 8 | 1 | 1 | 1 | 24.0 | 5.2 |
| 9 | -1.682 | 0 | 0 | 27.2 | 5.0 |
| 10 | 1.682 | 0 | 0 | 31.3 | 21.6 |
| 11 | 0 | -1.682 | 0 | 29.8 | 21.6 |
| 12 | 0 | 1.682 | 0 | 29.5 | 5.9 |
| 13 | 0 | 0 | -1.682 | 27.9 | 20.3 |
| 14 | 0 | 0 | 1.682 | 24.6 | 21.4 |
| 15 | 0 | 0 | 0 | 23.4 | 19.9 |
| 16 | 0 | 0 | 0 | 22.9 | 17.3 |
| 17 | 0 | 0 | 0 | 30.0 | 4.9 |
| 18 | 0 | 0 | 0 | 22.1 | 16.8 |
| 19 | 0 | 0 | 0 | 31.0 | 15.6 |
| 20 | 0 | 0 | 0 | 27.0 | 18.1 |

independent variables used in this study. The second-order surface models derived from the regression analysis are as follows:

$$y_1 = 28.8 - 5.7x_1^2 x_2^2 \tag{8.8}$$

where y_1 represent porosity at different extender concentrations (x_1) and cooking temperatures (x_2) at a constant cooking time (10 min.).

$$y_2 = 23.8 + 4.6x_2x_3 + 2.9x_2^2 (8.9)$$

where y_2 represent porosity at different cooking temperatures (x_2), cooking times (x_3) and at a constant extender concentration (2%).

$$y_3 = 23.8 + 2.9x_2^2 \tag{8.10}$$

where y_3 represent porosity at different cooking temperatures (x_2) at the constant extender concentration (5%).

Figure 8.1 shows the response surface diagram for porosity of samples extended with SPF at different extender concentrations and cooking temperatures at constant cooking time of 10 min (Eq. 8.8). A maximum porosity of 24% was obtained at the SPF extender concentration of 3.5% and cooking temperature of 182°C after 10 min cooking time. The response surface analysis of porosity of samples extended with 2% SPF concentration is shown in Figure 8.2. Porosity of patties decreased with increasing cooking temperatures at lower cooking times. However, at higher cooking times, porosity was observed to increase with increasing cooking temperature. Maximum porosity of 39% was

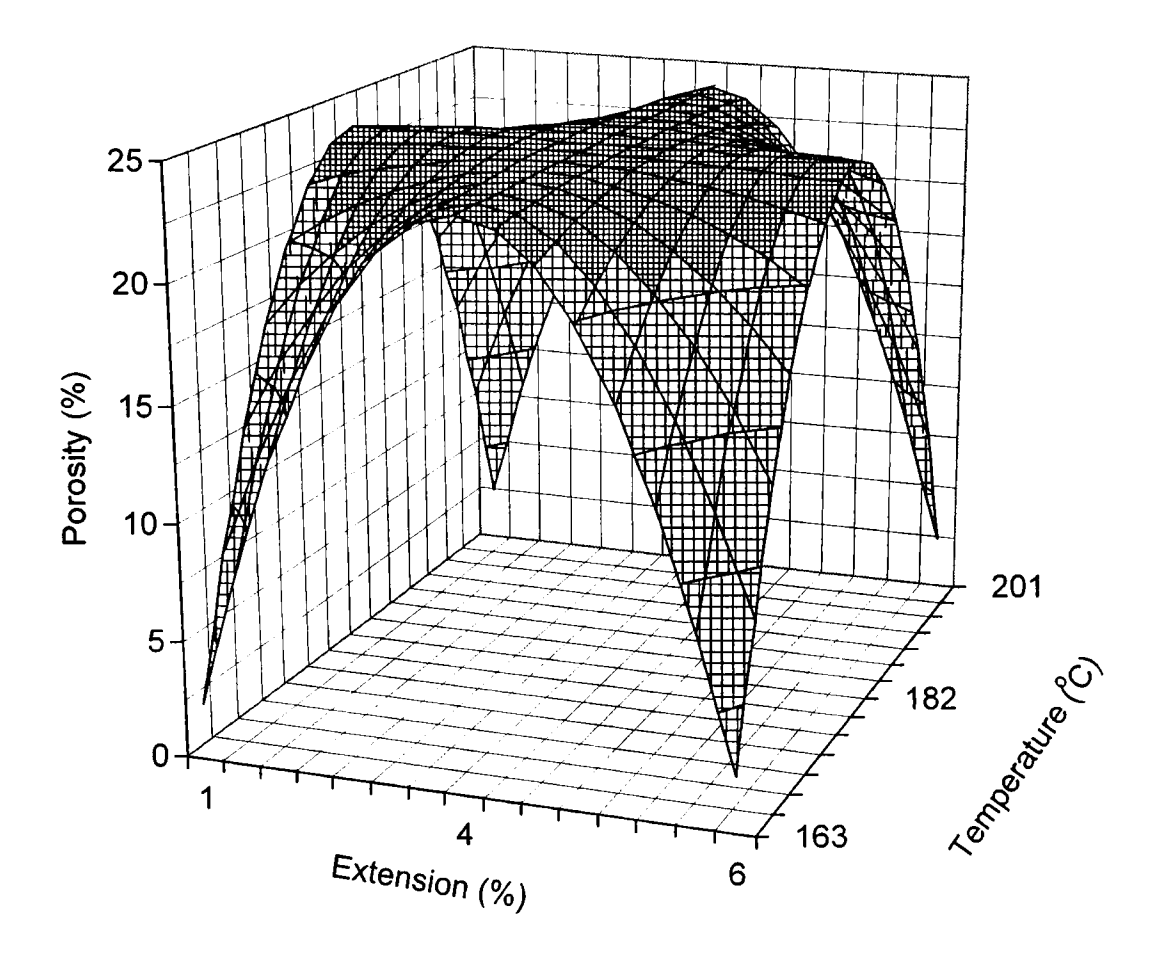


Figure 8.1 Response surface graph of the effect extender concentration and cooking temperature at constant cooking time (10 min.) on porosity of beef patty samples extended with soy-protein flour.

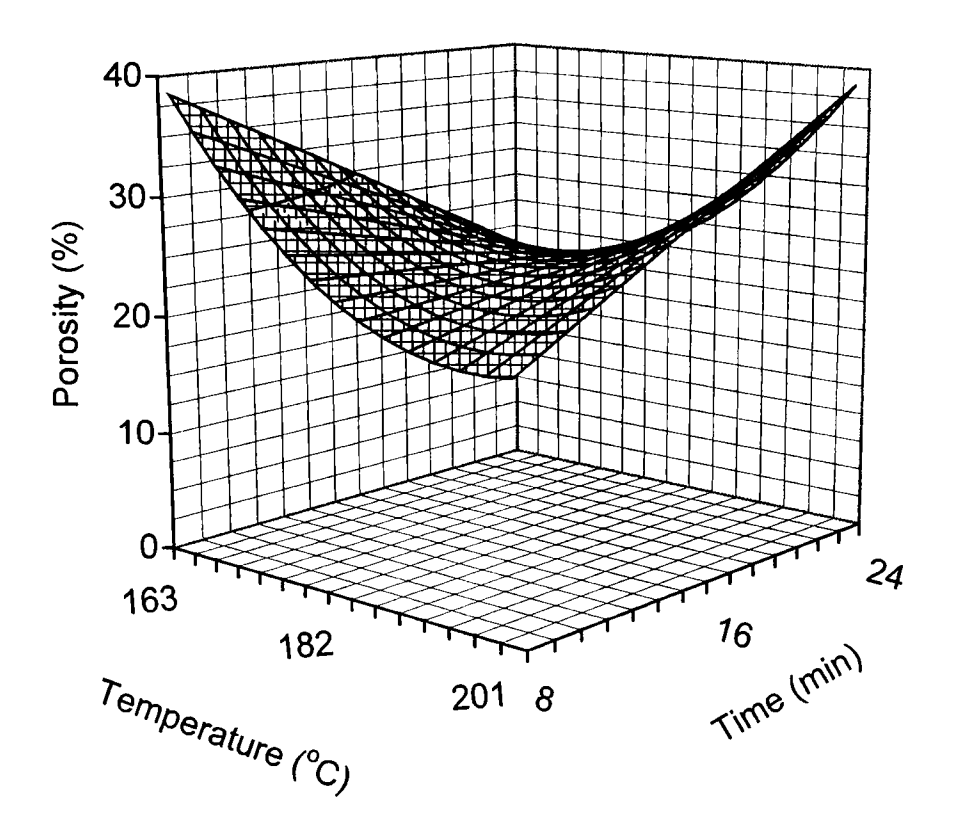


Figure 8.2 Response surface graph of the effect cooking temperature and cooking time at constant extender concentration (2%) on porosity of beef patty samples extended with soy- protein flour.

obtained at both the temperatures and times of 201°C and 22 min, and 163°C and 8 min, respectively. This can be attributed to the pattern of moisture vaporization and transfer in the products during cooking. Denaturation and pore collapse apparently occurred with increasing cooking temperatures and at lower cooking times resulting in the decreasing porosity. However, at higher cooking times, internal moisture vaporization occurred resulting in rapid evacuation of moisture from the internal regions of the products resulting to the increase in

- --

porosity. Figure 8.3 shows a response surface analysis of porosity of meat patty samples with 5% SPF extension. Porosity decreased as cooking temperature increased from 163 to 182°C. Further increase in temperature from 182 to 201°C resulted in an increase in porosity. Minimum porosity of 24% was obtained at 182°C whereas maximum porosity of 30% was obtained at the cooking temperatures of 163 and 201°C. This variation in porosity is again attributed to moisture vaporization and transfer in the patties during cooking.

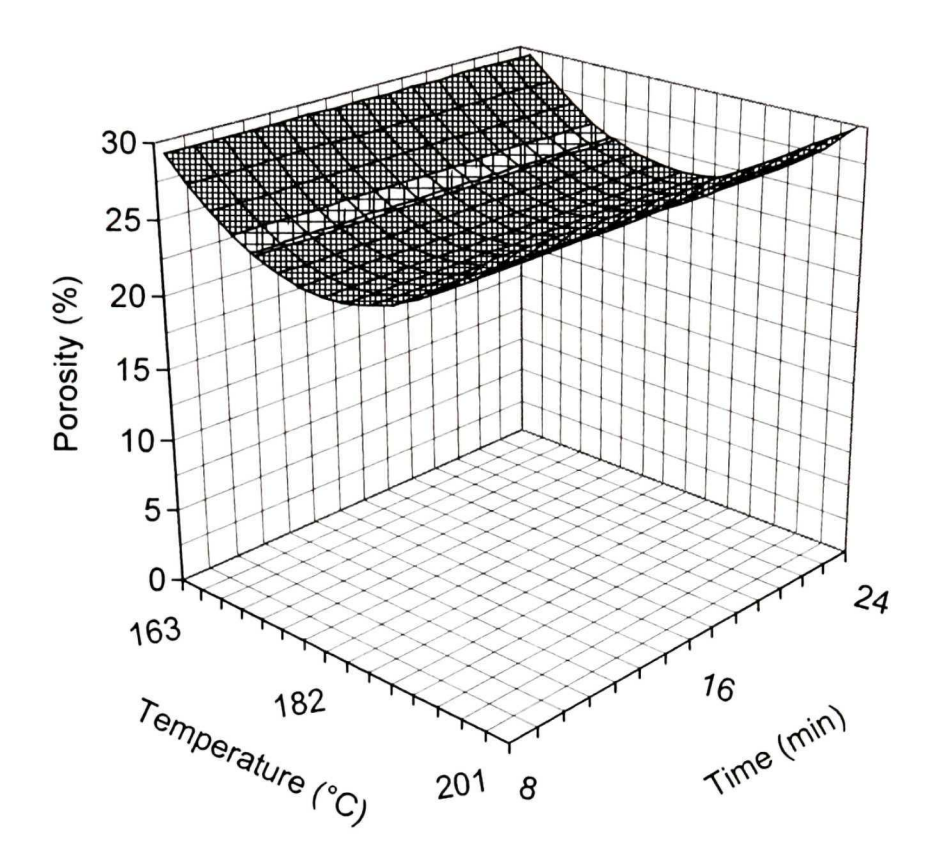


Figure 8.3 Response surface graph of the effect cooking temperature and cooking time at constant extender concentration (5%) on porosity of beef patty samples extended with soy-protein flour.

8.4.3.1 Pore size distribution

Pore size distribution was used to characterize void volumes and surface area in cooked beef patties. Figure 8.4 shows pore size distribution in cooked patty extended with SPF. Cumulative pore volume in the SPF extended samples varied from 0.19 to 0.37 mL/g depending on SPF extender concentrations and cooking temperatures. At each extender concentration, increasing cooking temperature from 167 to 187°C decreased cumulative pore volume for the same pore diameter in the sample. This is attributed to collapse of structure due to protein denaturation and other factors such as the rate of moisture vaporization in the products. Other authors have observed food structure collapse during drying or heating (Bellows and King, 1972; Karathanos et al., 1996). phenomena of structure collapse may have some implication on the development of textural attributes of meat patties. Increasing SPF extender concentration from 2 to 5% increased the cumulative pore volume in cooked samples. Extended meat samples apparently formed a composite structure consisting of a matrix of muscle and extension fibers providing more void spaces with increasing soy protein extension concentration.

The pattern of pore size distribution obtained in cooked meat patties extended with TSP was similar to the result obtained using SPF extension as shown in Figure 8.5. However, cumulative pore volumes in TSP extended patties were lower than the cumulative pore volumes obtained using SPF extensions. Majority of the pores in meat patties extended with either TSP or SPF was greater than $10~\mu m$. The contribution of pores with sizes larger than

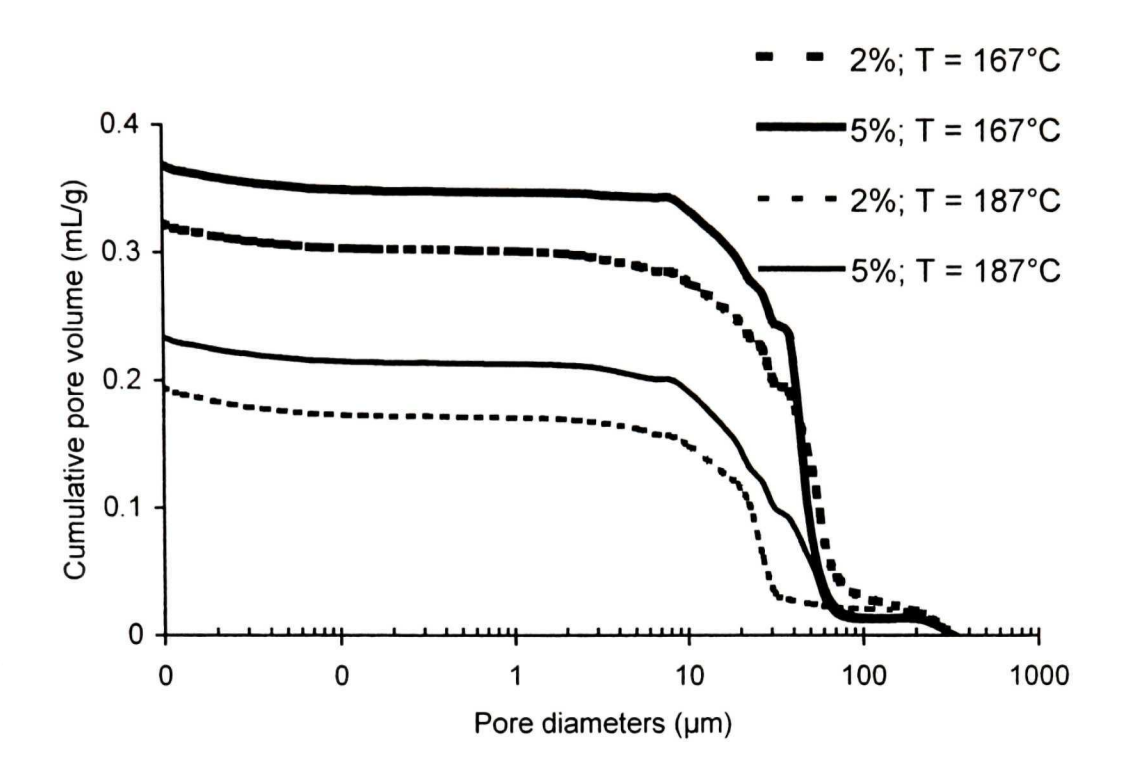


Figure 8.4 Pore size distribution (total open volume mL/g) of beef patty extended with different concentration of soy-protein flour at different cooking temperature.

- --

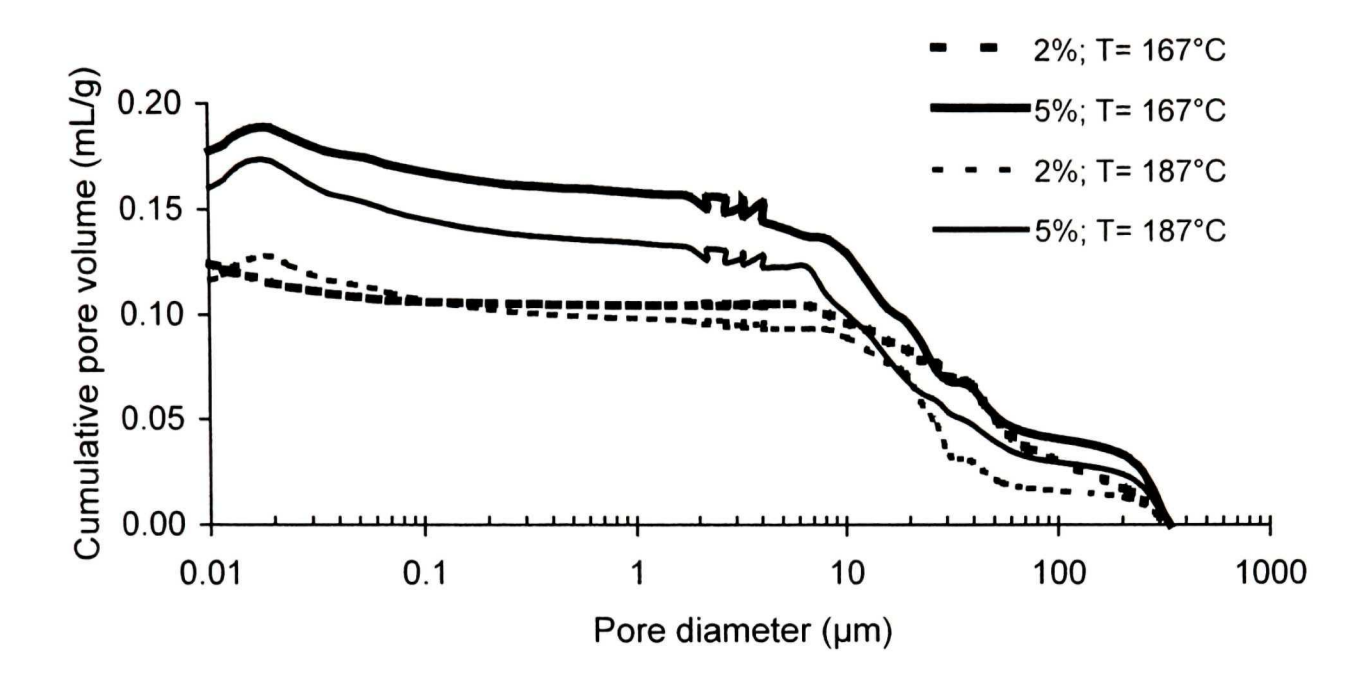


Figure 8.5 Pore size distribution (total open volume mL/g) of beef patty extended with different concentration of textured soy-protein at different cooking temperatures.

100 μm in TSP extended samples was approximately 20 to 25% (depending on extension concentration and cooking temperature) of the cumulative pore volume whereas similar contribution in SPF extended samples was less than 5%. Whereas SPF extension resulted in greater pore volumes in cooked meat patties, larger pore surface areas were obtained using TSP extensions.

Pore surface area was computed (Eq. 8.4) for SPF extended meat patties, maximum pore surface area was about 4 m²/g, irrespective of extension concentration and cooking temperature as shown in Figure 8.6. The effect of extension concentration and cooking temperature on pore surface area was more evident in TSP extended meat patties as shown in Figure 8.7. Cumulative pore surface area in TSP extended samples varied from about 4 to 9 m²/g. Values were higher than results reported for dried chicken samples (Farkas and Singh, 1991). Increasing cooking temperature and TSP extension concentration, increased total pore surface area in cooked meat patty samples. TSP extended samples had larger pore surface areas than SPF extended samples. Combined with cumulative pore volume results, there is an indication that pores in TSP extended meat patties were mostly large planar pores whereas in SPF extended meat patties were mostly capillary pores. This might be attributed to variations in the size distribution of the two extenders. Increasing cooking temperature also tended to cause more planar pores particularly in TSP extended samples. The results corroborate well with previous results on WHC and TCL. The larger surface area and planar pores apparently lock moisture more efficiently resulting in the observed high WHC and lower TCL. Capillary pores apparently do not

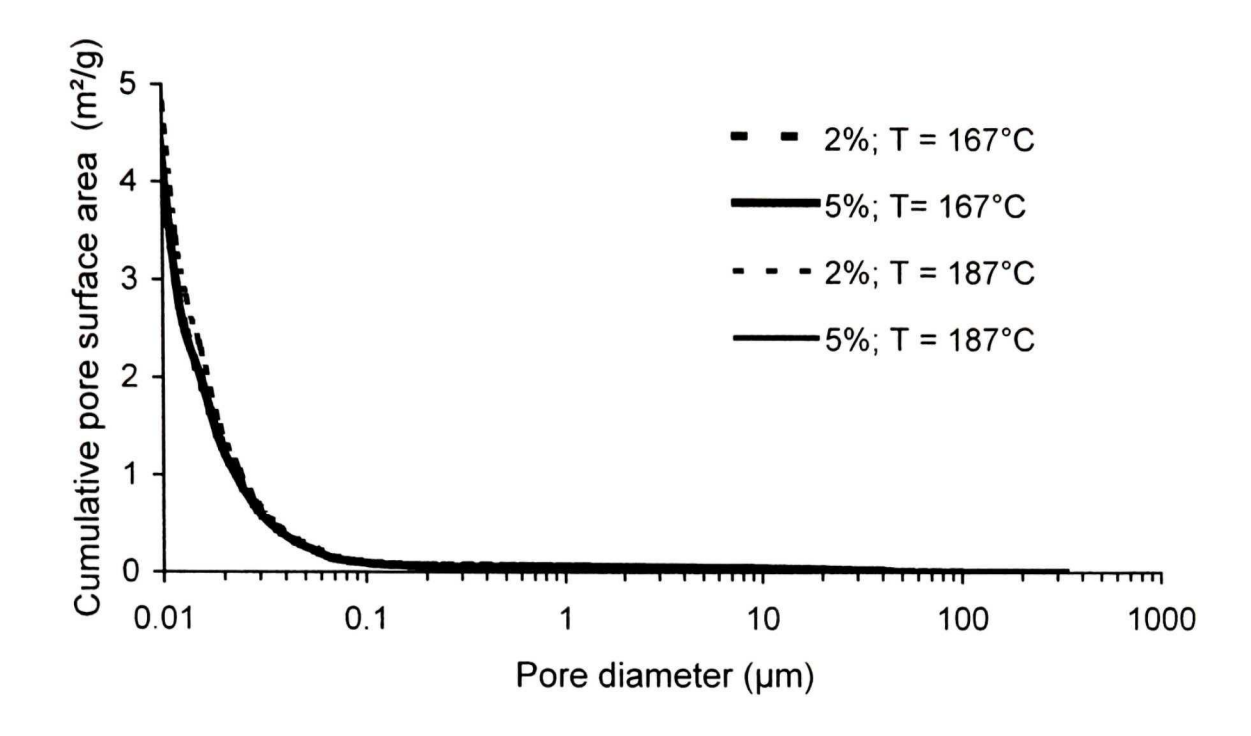


Figure 8.6 Pore size distribution (cumulative pore area m²/g) of beef patty extended with different concentration of soy-protein flour at different cooking temperatures. Pore size distributions obtained at 2%, 167°C; 5%, 167°C and 5%, 187°C were very close to each other.

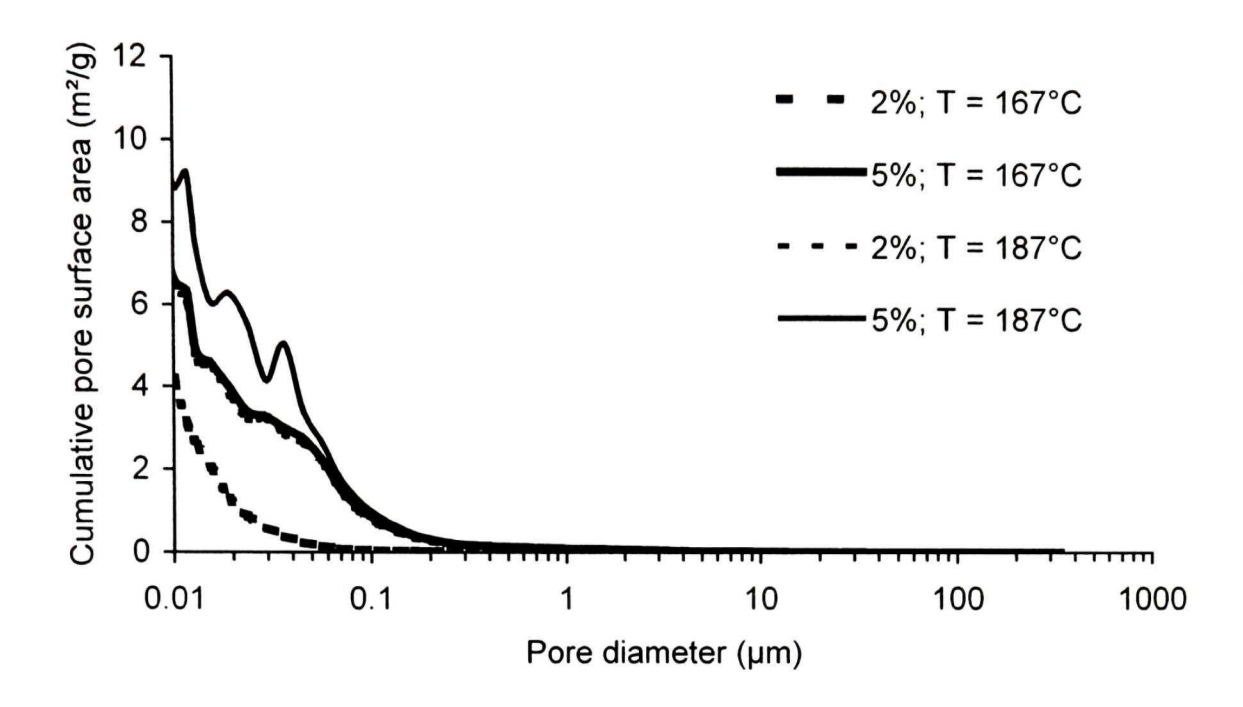


Figure 8.7 Pore size distribution (cumulative pore area m²/g) of beef patty extended with different concentration of textured soy-protein at different temperatures. Pore size distributions obtained at 2%, 187°C and 5%, 167°C were very close to each other.

seem to retain moisture as much as planar pores. This phenomenon should be investigated further. These results present an interesting perspective on microstructure of the cooked samples, however, it is evident that a complete picture of pore size distribution in soy-protein extended beef patties will be enhanced by combination of image analysis approach.

8.5 Conclusions

Soy-protein flour (SPF) and textured soy-protein (TSP) used as extenders increased water holding capacity (WHC) in beef patties due to their ability to retain moisture within the product matrix. WHC increased from 17 to 28% for SPF extended samples and from 19 to 39% for TSP extended samples. Extender concentration and cooking temperature had significant effect (P < 0.05) on pore formation and pore size distribution in the products. Samples extended with SPF showed porosity ranging from 21 to 34% compared to 4 to 22% for TSP extended samples. Extending meat patties with smaller particle size SPF resulted in higher porosity and cumulative intrusion volume of 0.33 mL/g whereas using the larger particle size TSP resulted in lower porosity and cumulative intrusion volume of 0.20 mL/g. The contribution of pores with sizes larger than 10 μ m in diameter was up to 80%. These results maybe used as reasonable indicators in optimizing quality and mass transfer during cooking of meat patties extended with soy protein.

ACKNOWLEDGEMENT

This study was supported in part by funding from the Natural Science and Engineering Research Council of Canada.

8.6 References

- Al-Rqobah, H. A., E. K. T. Kam and R. Hughes. 1988. Dynamic determination of diffusion in porous particles. *Chemical Engineering* 9: 275-283.
- Bellows, R. J., and C. J. King. 1972. Freeze-drying of aqueous solutions: maximum allowable operating temperature. *Cryobiology* 9: 559-561.
- Box, G. E. P. and N. R. Draper. 1987. Empirical Model-building and Response Surfaces. NY: John Willey and Sons Inc.
- Datta, A. K., and J. Zhang. 1999. Porous media approach to heat and mass transfer in solid foods. Paper No: 99-3068. St. Joseph, MI: ASAE.
- Farkas, B. E., and R. P. Singh. 1991. Physical properties of Air-dried and freeze-dried chicken white meat. *Journal of Food Science* 56(3): 611-615.
- FDA. 1998. *Talk Paper*. US department of Health and Human Service. Rockville, MD: Public Health Service.
- Gomez, A. K., and A. A. Gomez. 1984. Statistical Procedures for Agricultural Research, 2nd Edition, NY: John Willey and Sons Inc.
- Huang, C. T. and J. T. Clayton. 1990. Relationships between mechanical properties and microstructure of porous foods: Part I. A Review. In Engineering and Food, Vol.1, PhysicalProperties and Process Control, edited by Spiess, W. E. L. and H. Schubert, 352-360. London: Elsevier Applied Science:

- Karathanos, V. T., N. K. Kanellopoulos and V. G. Belessiotis. 1996.

 Development of porous structure during air drying of agricultural plant products. *Journal of Food Engineering* 29: 167-183.
- Lacomte, N. B., J. F. Zayas, and C. L. Kastner. 1993. Soya protein functional and sensory characteristics improved in comminuted meats. *Journal of Food Science* 58(3): 464-466.
- Mansour, E. H., and A. H. Khalil. 1997. Characteristics of low-fat beef burger as influenced by various types of wheat fibers. *Food Research International* 30(3/4): 199-205.
- Micromeritics 1999. Operator's Manual. Norcross, GA: Micromeritics Instrument Corporation.
- Ray, F. K., N. A. Parret, B. D. van Stavern and H. W. Ockerman. 1981. Effect of soy level and storage time on the quality characteristics of ground beef patties. *Journal of Food Science* 46: 1662-1664.
- Rocha-Garza, A. E. and J. F. Zayas. 1996. Quality of broiled beef patties supplemented with wheat germ protein flour. *Journal of Food Science* 2: 418-421.
- Shafer, M. A. M., and M. E. Zabik. 1975. Dieldrin, fat, and moisture loss during the cooking of beef loaves containing texturized soy protein. *Journal of Food Science* 40: 1068-1071.
- Troutt, E.S., M.C. Hunt, D. E. Johnson, J.R. Claus, C. L. Kastner, and D. H. Kropf. 1992. Characteristics of low-fat ground beef containing textured-modifying ingredients. *Journal of Food Science* 57(1):19-29.

- Vagenas, G. K., and Karathanos, V. T. 1991. Prediction of the moisture diffusivity in granular materials with specific application to foods. *Biotechnology Progress* 7 (5): 419-426.
- Webb P. A., and C. Orr. 1997. Analytical Methods in Fine Particle Technology. Norcross, GA: Micromeritics Instrument Corporation.
- Yasumatsu, K., K. Sawada, S. Moritaka, J. Toda, T. Wada, and K. Ishii. 1972. effects of addition of soybean products on dough properties.

 Agricultural Biology and Chemistry 36(5): 729-735.

CONNECTING TEXT

Response surface analysis was used in Chapter VIII and the effect of the independent variables were investigated and results presented maximas and minimas for various variables used. The effect of soy-protein extenders on restructured meat patties, have created an insight for future studies on deep-fried products using mercury porosimeter. Although, the extender and oil are different properties, The technique developed have helped to overcome the problems encountered during the initial phase of mercury porosimetry analyses of deep-fat fried products.

IX PORE STRUCTURE CHARACTERIZATION OF DEEP-FAT FRIED CHICKEN MEAT

9.1 Abstract

The effect of frying oil temperature and frying times on pore structure was investigated, while the primary focus of this study was directed towards pore structure characterization using a mercury intrusion porosimeter. Samples were cut into rectangular shape and deep-fat fried at different frying oil temperature (170, 180, and 190°C) in an industrial fryer for periods ranging from 5 to 360 s and subsequently freeze-dried. Pore structure characterization was conducted using a mercury porosimeter. Cumulative pore volumes decreased by 24% from 2.13 to 0.51 mL/g and with a corresponding porosity of 0.71 to 0.37 after 360 s of deep-fat frying. Pore structure appeared to be affected by oil absorption, evidently, increased mercury entrappement in pores increased from 0.97 to 10% after 360 s of frying, which implied development of inkbottle shapes. The interfiber (planar) pore diameter was about 10.2 μm while the intra-fiber (internal) pores vary from 0.006 to 10 μm in diameter and over 84% of the pores were capillary pores.

9.2 Introduction

Food systems consist of different complex composite heterogeneous and anisotropic structures (Kassama et al., 2003), are hygroscopic and capillary porous with definite void structures that modulate mass transport during heat processing (Satterfield and Sherwood, 1963; Al-Rqobah et al., 1988; Xiong et al., 1991; Marousis et al., 1991; Saravacos, 1995). In meats, the void structures are primarily the result of the hierarchical arrangement of muscle fibers and connective tissues. A single muscle fiber consists of many myofibrils, the contractile elements, sheathed by the endomysium which is a composite structure of collagen fibers. The muscle itself is composed of bundles of muscle fibers, each fiber (10-100 μ m) (Bailey and Light, 1989) held together by a collagen network, the perimysium, and the whole muscle structure held by a network called the epimysium (Flint, 1994). This type of muscle fiber arrangement is common to most vertebrates, i.e., poultry, beef and vertebrate fish.

Water content of muscles is approximately 70%, the water being held by capillary forces and surface tension within the muscle structure and substructures. The water-holding capacity is highly dependent on pore structure (Ofstad, 1993). When muscle is heated, the fibers begin to shrink in the transverse direction at 40-60°C (Offer et al., 1989). The collagen network shrinks at 60-70°C due to denaturation, significantly increasing the pressure within the bundle and causing aqueous solutions to be evacuated rapidly (Hamm, 1985;

Wilding et al., 1986). Schaller and Powrie (1972) reported that connective tissue between fibers in chicken meat swells before shrinking.

In deep-fat frying (DFF), heating is the result of submersion in hot oil, and the paths of evacuation of aqueous solutions and water vapor can serve as conduits for oil intrusion (Aguilera and Stanley, 1999). In order to understand how the mechanism of oil absorption during DFF may change from the beginning of processing to the cooling stage, the latter having been shown to be crucial to oil absorption of certain deep-fried products (Moreira et al., 1999), it is necessary to understand how the pore structure evolves.

Porous structure can be quantified by porosity, pore size distribution (PSD), specific surface area, specific conductivity and capillary breakthrough pressure (Dullien, 1992; Karathanos et al., 1996; Rahman et al., 2002). Several researchers have quantified food microstructure using mercury porosimetry and helium pycnometry (Kassama et al., 2003; Kassama and Ngadi, 2001; Rahman, 2002; Ngadi et al., 2001; Karathanos et al., 1996; Farkas and Singh, 1991; Huang and Clayton, 1990). Porosity measured by mercury intrusion is usually lower than that obtained by helium pycnometry (Rahman et al., 2002) due to the inability of mercury to fill closed or blind pores (Karathanos et al., 1996; Hicsasmaz and Clayton, 1992). Karathanos and Saravacos (1993) and Karathanos et al. (1996) investigated porosity and characterized PSD by a volume distribution function. They described the PSD of non-meat products by two discrete peaks for freeze-dried potatoes, cabbages and apples and three peaks for carrots. Several authors used cumulative pore volume (CPV),

cumulative surface area and percent pore volume distribution function to characterize PSD for different meat products (Kassama et al., 2003; Rahman et al., 2002; Ngadi et al., 2001; McDonald and Sun, 2001a). Mercury intrusion and extrusion curves (mercury expelled from the pores) were used to characterize pore shape and structure by Orr (1969). Hysteresis of these curves is indicative of the presence of "ink-bottle" pores. These are pores that are wider in the interior than at the throat, such that mercury cannot enter until pressurized to a value corresponding to the radius of the entrance capillary (Webb and Orr, 1997).

The type of product, nature of pretreatment and processing influence the pore size, geometry or shape, and pore size distribution (PSD) of the food matrix. Porosity and PSD within the solid food matrix also influence the mechanical, texture, and sensory properties of food (Kassama et al., 2003; Bhatnagar and Hanna, 1997; Huang and Clayton, 1990; Vincent, 1989; Stanley, 1987; Christensen, 1984; Vickers and Bourne, 1976). Heating during DFF can result in protein denaturation, shrinkage and collapse of pore structures (Hussain et al., 2002; Rahman, 2001). Thermal processing of meat affects the structural and organoleptic properties (Schmidt, 1984) and the degree of intrusion of frying oil can contribute to the structure of the final product. McDonald and Sun (2001a, 2001b) reported change of porosity as a result of quick cooling during vacuum cooling of cooked beef, while Kassama et al. (2003) surmise change in porosity in pan fried comminuted meat as a result of cooking.

The knowledge of the intrinsic pore structure is significant to new product development and hence it can be utilized in modeling and controlling mass

transport and chemical reactions involved in DFF. The object of this study is to use mercury porosimetry to characterize the evolution of pore structure during DFF of chicken meat.

9.3 Materials and Methods

9.3.1 Sample preparation

De-boned chicken meat was purchased from a local supplier. Samples were stored in a freezer till required for further use. Samples were thawed in a refrigerator at 4°C for 24 h prior to use. Samples were diced to the approximately dimensions 5 cm x 3 cm x 1 cm (\pm 0.5 cm).

9.3.2 Frying

Chicken breast slabs were fried in liquid shortening (Can Amera Food, Oakville, ON) at a 1:480 sample to oil ratio (w/w), in a programmable pressure deep-fat fryer (Henny Penny Computron 7000 Pressure Fryer, Model 500C, Henny Penny Corporation, Eaton, OH). The fresh oil was preheated at 170°C for 2 h prior to rising to the study temperature of 180°C. The samples were placed in a wire basket to keep them submerged for the required time, 240, 360 or 480s. The fried samples were cooled at room temperature, weighed on a scale (TR-4102D, Denver Instrument Co., Denver, CO), placed in plastic Zip-Lock sample bags and then frozen at –20°C for 24 prior to freeze drying.

9.3.3 Freeze drying

Samples were freeze-dried in preparation for the mercury porosimeter measurement, which requires dry samples. Freeze-drying is also the method of preserving the structural integrity of the material to be studied (Karathanos et al., 1996). Freeze-drying was conducted in a freeze dryer (ModulyOD-115, Thermo Savant, Holbrook, NY) for 50 h. Settings were –50°C and 1 mbar (0.1 kPa) pressure. Sample mass was determined prior to and after freeze-drying on the TR-4102D scale.

9.3.4 Porosity and pore size distribution

Porosity and PSD were measured with a mercury porosimeter (AutoPore III series 9400, Micromeritics Instrument Corporation, Norcross, GA). The instrument was capable of measuring micropores with diameters as small as 0.005 µm at a maximum pressure of 207 MPa. Samples were weighed, placed in the penetrometer and loaded in the low-pressure port of the porosimeter. The penetrometer was sealed with silicon high vacuum grease. Samples were evacuated of residual air in the low-pressure port where initial mercury intrusion subsequently takes place. The penetrometer assembly was then transferred to the high-pressure port according to standard protocol (Micromeritics, 1999). The penetrometer used for these tests had a bulb volume of 15 cc, a total stem volume of 1.131 cc, and a maximum measurable volume of 1.057 cc. The estimated pore volume was determined between 90 and 25% of the maximum measurable volume (Micromeritics, 1999). It was assumed that pores were

cylindrical in shape such that pore sizes could be calculated using the Washburn equation (Eq. 9.1) (Webb and Orr, 1997):

$$D = -\left(\frac{1}{P}\right) 4\gamma \cos \varphi \tag{9.1}$$

where D is the pore diameter, P is the applied pressure at which the mercury is forced into the sample, γ is the surface tension of mercury given as 0.485 N/m, and φ is the solid-liquid contact angle (130°). Although the cylindrical pore shape assumption may not always be justified, it is generally accepted (Ngadi et al., 2001). The pore surface areas of the samples were computed by the following relationship (Eq. 9.2):

$$A = -\frac{\int PdV}{\gamma \cos \varphi} \tag{9.2}$$

where V is pore volume corresponding to the amount of mercury intruded into the sample. The terms γ and φ were assumed not to vary with pressure. Using the pressure - volume mercury penetration data, the cumulative pore surface areas was calculated (Eq. 9.3) thus:

$$\sum \Delta A = -\frac{\sum P \ dV}{\gamma \cos \varphi} \tag{9.3}$$

Data on total intrusion volume, total pore surface area, medium pore diameters, average pore diameter, bulk densities, skeletal density and percent porosity were acquired through a microcomputer data acquisition system interfaced with the porosimeter. Pore volume distribution function is one of the methods of characterizing PSD and is usually computed based on the relationship (Eq. 9.4)

$$D(v) = \frac{P}{r} \frac{d(v_t - v)}{dP}$$
 (9.4)

where D_v is the pore size volume distribution function, P is the applied pressure at which the mercury is forced into the sample and r pore radii measure to every corresponding P, v_{ℓ} is the total pore volume and v is the pore volume.

The porosity data acquired from the porosimeter was verified by values obtained by independent calculation as shown in Eq. 9.5.

$$\varepsilon = 1 - \frac{\rho_b}{\rho_s} \tag{9.5}$$

where ε is porosity, $\rho_{\rm s}$ is solid density and $\rho_{\rm b}$ is bulk density.

9.4 Results and Discussions

Parameters describing the pore structure are presented in Table 9.1. The porosity of fried samples tended to decrease with frying. This could be attributed to the physical changes that may have prompted conditions such as shrinkage resulting from intense heating. The mean pore diameter decreased from 1.17 μm in the control to 0.25 μm in samples fried for 360 s. Porosity decreased from 0.71 to 0.37. The porosity of the control (0.71) corresponds well with values reported by others for freeze-dried raw chicken meat. Farkas and Singh (1991) reported a value of 0.65, while King et al. (1968) obtained values of 0.7 to 0.8. The decrease in porosity could be attributed to the fact that the absorbed oil within the pore matrix crystallizes thus, formed a composite structure with the muscle fibers, and may caused pores to constrict. Pinthus et al. (1995) elucidated the influence of oil uptake on porosity, suggesting that the final reduction of the pore size was the result of oil uptake. The total pore volume exhibited the same trend as pore diameters.

A normalized pore volume distribution curve, which describes the adsorption characteristics of porous materials under low capillary pressure is shown in Figure 9.1. The values were obtained with the penetrometer in the low-pressure port. Rahman et al. (2002) also show similar sorption behavior for fish muscles.

Table 9.1 Pore structure properties measured by mercury Porosimetry of deep-fat fried chicken meat.

| Treatments (s) | Total Volume (mL/g) | Surface area (m²/g) | Bulk Density (g/mL) | Particle Density (g/mL) | Average Pore Diameter (um) | Porosity |
|----------------|---------------------------|---------------------------|---------------------------|-------------------------------|-------------------------------------|------------------|
| Control | 2.0129 | 6.9220 | 0.3514 | 1.1947 | 1.1669 | 70.5 |
| | (0.1657) | (0.9136) | (0.0195) | (0.0108) | (0.0583) | (1.9092) |
| 5 | 1.8679 (0.0962) | 7.0455 (1.1066) | 0.3733 (0.0178) | 1.2295 (0.0479) | 1.0781 (0.2240) | 69.7 (0.2121) |
| 10 | 1.7625 (0.0341) | 5.861 (1.6617) | 0.3841 | ì.1889 [´] | 1.2497 | 67.7 |
| 15 | 1.5626 | 6.3805 | (0.0052) 0.4162 | (0.0015) 1.1451 | (0.3309) 0.9777 | (0.4243) 63.6 |
| 30 | (0.4143) | (1.5974) | (0.0687) | (0.0156) | (0.0149) | (6.5054) |
| | 1.7211 | 6.7047 | 0.3841 | 1.1307 | 0.9980 | 66 |
| 45 | (0.1022) | (2.2958) | (0.0149) | (0.0003) | (0.1932) | (1.2728) |
| | 1.5356 | 7.1585 | 0.4177 | 1.1638 | 0.8720 | 64.2 |
| | (0.0435) | (1.1858) | (0.0077) | (0.0013) | (0.1687) | (0.63640 |
| | 1.3583 | 7.3665 | 0.4544 | 1.1871 | 0.7530 | 61.7 |
| 60 | (0.0074) | (1.5139) | (0.0003) | (0.0086) | (0.1508) | (0.2828) |
| | 1.0253 | 7.5940 | 0.5311 | 1.1643 | 0.5504 | 54.4 |
| 90 | (0.0631) | (1.7183) | (0.0187) | (0.0043) | (0.0913) | (1.4142) |
| 120 | 1.0982 | 8.1085 | 0.5077 | 1.1459 | 0.5509 | 55.7 |
| | (0.0574) | (1.6964) | (0.0178) | (0.0156) | (0.0869) | (0.9899) |
| 150 | 0.9692 | 7.266 | 0.5501 | 1.1774 | 0.5365 | 53.3 |
| | (0.0480) | (0.9581) | (0.0158) | (0.0061) | (0.0444) | (1.1313) |
| 180 | 1.0469 | 7.7215 | 0.5289 | 1.1849 | 0.5449 | 55.4 |
| | (0.0103) | (0.7771) | (0.0096) | (0.0339) | (0.0496) | (0.4949) |
| 210 | 0.8179 (0.0217) | 8.2055 (1.6256) | 0.6022 (0.0137) | 1.1864 (0.0225) | 0.4056 (0.0697) | 49.3 (0.2121) |
| 240 | 0.6376 | 7.9625 | 0.6601 (0.0065) | 1.1400 | 0.3236 | 42.1 |
| 300 | (0.0357) | (1.3866) | (0.0003) | (0.0271) | (0.0385) | (1.9799) |
| | 0.5400 | 8.2705 | 0.7111 | 1.1487 | 0.2617 | 38.1 |
| | (0.0922) | (0.1619) | (0.0589) | (0.0324) | (0.0498) | (3.3941) |
| 360 | 0.5089 | 8.2390 | 0.7404 | 1.1831 | 0.2465 | 37.4 |
| | (0.0993) | (0.2645) | (0.0568) | (0.0054) | (0.0404) | (4.5255) |

Standard deviation in parenthesis.

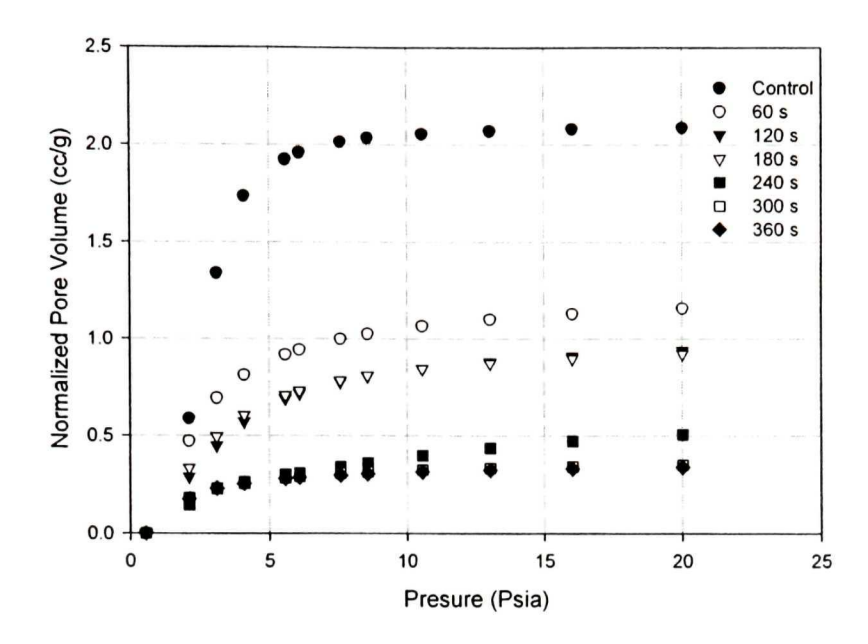


Figure 9.1 Mercury low pressure intrusion curve (normalized intrusion volume versus pressure) deep-fat fried chicken meat samples and the control.

The effect of oil uptake on normalized pore volume is evident, keeping in mind that oil uptake increases with frying time. At 138 kPa (20 psia), a partial breakthrough pressure, and pore size of about 10.2 μ m, the cumulative volume of surface pores was 2.08 mL/g for the raw sample and only 0.34 mL/g for the sample fried for 360 s was achieved. Thus, interfiber muscle penetration between connective tissues (collageneous fiber) is accomplished and pores measured are planer pores. Bailey and Light (1989) had noted that muscle fibers range from 10 to 100 μ m in diameter, while Aguilera and Stanley (1999) recounted 0.1 μ m diameter for collagen fibers of muscle tissues.

The cumulative volume of pore structure as a function of pore size (μm) of freeze-dried chicken meat is given in Figure 9.2 for the different frying times. The

pore size is related to the applied pressure of the mercury porosimeter through the Washburn equation (Eq. 9.1). The total pore volume contained in a unit mass of sample was computed on the basis of accumulation of volumes of pores measured within the porous medium.

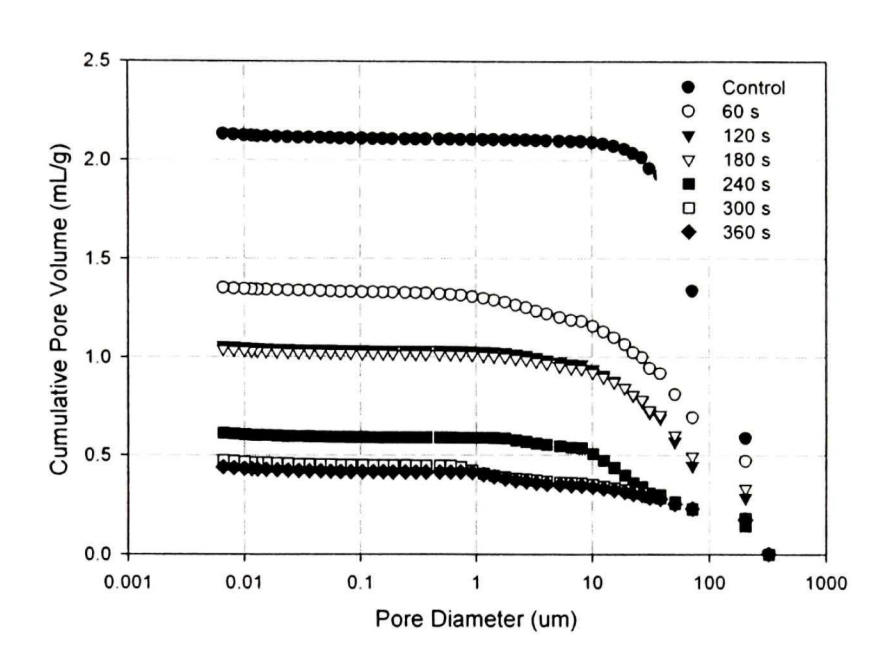


Figure 9.2 Pore volume distribution as a function of pore diameter of deepfat fried chicken samples fried for 0, 4, 6, and 8 min.

Cumulative pore volume (CPV) was used to characterize pore size distribution (PSD) as a function of pore size (μ m) of deep-fat fried chicken meat. Figure 9.2 shows the CPV distribution in deep-fried chicken meat and shows that pore sizes within muscle fibers range from 10 to 0.006 μ m (based on mercury intrusion from 137 kPa to 207 MPa) respectively. The volume distribution is fairly consistent and the majority of pores were smaller than 10 μ m. The cumulative

volume dropped from 2.13 in the raw chicken to 0.51mL/g after frying for 360 s. Ngadi et al. (2001) reported that pore volume of oven-fried soy extended beef patties was in the range 0.19 to 0.37 mL/g. McDonald and Sun (2001a) reported values of 0.63 and 0.71 mL/g for vacuum tumbled and non-vacuum tumbled cooked beef samples, respectively. Farkas and Singh (1991) determined the pore volume of freeze-dried and air-dried chicken meat to be 1.4 and 0.3 mL/g, respectively. Physical changes due to prolonged frying may have caused pore volume to decrease. Deterioration of the connecting tissues due to heat may result in bulk shrinkage, swelling, denaturation of protein and modification of pore structure.

The reduction of pore volumes might also be due to oil uptake. The oil absorbed in the pore matrix crystallizes during the freeze-drying process, forming a composite structure consisting of muscle fiber and solid oil. Thus, pore volume appears to decrease because it is not possible, by mercury porosimetry alone, to distinguish between the muscle fiber and the crystallized oil. Many authors (Kassama et al., 2003; Rahman et al., 2002; Ngadi et al., 2001; Karathanos et al., 1996) have described the pore reduction to be a result of denaturation of protein and starch gelatinization which may lead to structural collapse. However, in frying, one can argue that oil absorbed within the product matrix minimizes the degree of structural collapse. Thus, the limiting factor may be oil absorption.

Mercury intrusion and extrusion data were used to determine the degree of capillary hysteresis of the adsorption and desorption isotherms. The results are reported in Table 9.2 and a typical intrusion- extrusion curve of cumulative

Table 9.2 Comparison of intrusion and extrusion volume and characterization of capillary hysteresis of deep-fat

fried samples.

| + | Intrusion | Intrusion Volume | | | Extrusio | Extrusion Volume | | | Entrapp | Entrapped Volume | e. | |
|---------------|-----------|------------------|--------|--------|----------|------------------|--------|--------|---------|------------------|------|--------|
| reatments (e) | (mL/g) | | | | (mL/g) | | | | (%) | | | |
| <u>(a)</u> | Max | Min | Mean | STDV | Max | Min | Mean | STDV | Max | Min | Mean | STDV |
| Control | 2.1300 | 1.8957 | 2.0129 | 0.1657 | 2.1084 | 1.8780 | 1.9932 | 0.1629 | 1.0141 | 0.9337 | 0.98 | 0.0568 |
| 2 | 1.9360 | 1.7999 | 1.8679 | 0.0962 | 1.9181 | 1.7610 | 1.8396 | 0.1111 | 2.1612 | 0.9246 | 1.54 | 0.8744 |
| 10 | 1.7866 | 1.7284 | 1.7575 | 0.0411 | 1.7646 | 1.7214 | 1.743 | 0.0306 | 1.2314 | 0.4049 | 0.82 | 0.5843 |
| 15 | 1.8555 | 1.2696 | 1.5626 | 0.4143 | 1.8326 | 1.2553 | 1.5439 | 0.4082 | 1.2342 | 1.1263 | 1.18 | 0.0762 |
| 30 | 1.7934 | 1.6488 | 1.7211 | 0.1022 | 1.7561 | 1.5854 | 1.6708 | 0.1207 | 3.8452 | 2.0798 | 2.96 | 1.2483 |
| 45 | 1.5663 | 1.5048 | 1.5356 | 0.0435 | 1.5142 | 1.4688 | 1.4915 | 0.0321 | 3.3263 | 2.3923 | 2.86 | 0.6604 |
| 09 | 1.3635 | 1.3531 | 1.3583 | 0.0074 | 1.3131 | 1.2903 | 1.3017 | 0.0161 | 5.3685 | 3.6964 | 4.16 | 0.6681 |
| 06 | 1.0699 | 0.9807 | 1.0253 | 0.0631 | 1.0437 | 0.9612 | 1.0025 | 0.0583 | 2.4488 | 1.9884 | 2.22 | 0.3256 |
| 120 | 1.1387 | 1.0576 | 1.0982 | 0.0573 | 1.1032 | 1.0299 | 1.0666 | 0.0518 | 3.1176 | 2.6191 | 2.87 | 0.3525 |
| 150 | 1.0031 | 0.9352 | 0.9692 | 0.0480 | 0.9817 | 0.9134 | 0.9476 | 0.0483 | 2.3311 | 2.1334 | 2.23 | 0.1398 |
| 180 | 1.0541 | 1.0396 | 1.0469 | 0.0103 | 1.0277 | 1.0122 | 1.0199 | 0.0109 | 2.6356 | 2.5045 | 2.57 | 0.0927 |
| 210 | 0.8333 | 0.8026 | 0.8179 | 0.0217 | 0.8043 | 0.7824 | 0.7934 | 0.0155 | 3.4801 | 2.5168 | 3.00 | 0.6812 |
| 240 | 0.6628 | 0.6123 | 0.6376 | 0.0357 | 0.6360 | 0.5902 | 0.6131 | 0.0323 | 4.0435 | 3.6093 | 3.83 | 0.3069 |
| 300 | 0.6053 | 0.4748 | 0.5401 | 0.0923 | 0.5823 | 0.4118 | 0.4971 | 0.1206 | 13.268 | 3.7998 | 8.53 | 6.6955 |
| 360 | 0.5792 | 0.4387 | 0.5089 | 0.0994 | 0.5211 | 0.3954 | 0.4583 | 0.0888 | 10.031 | 9.8701 | 9.95 | 0.1139 |
| | | | | | | | | | | | | |

pore volume versus capillary pressure for deep-fried chicken is given in Figure 9.3. The total amount of mercury trapped in the inkbottles was estimated based on the end point of the extrusion point relative to the intrusion point.

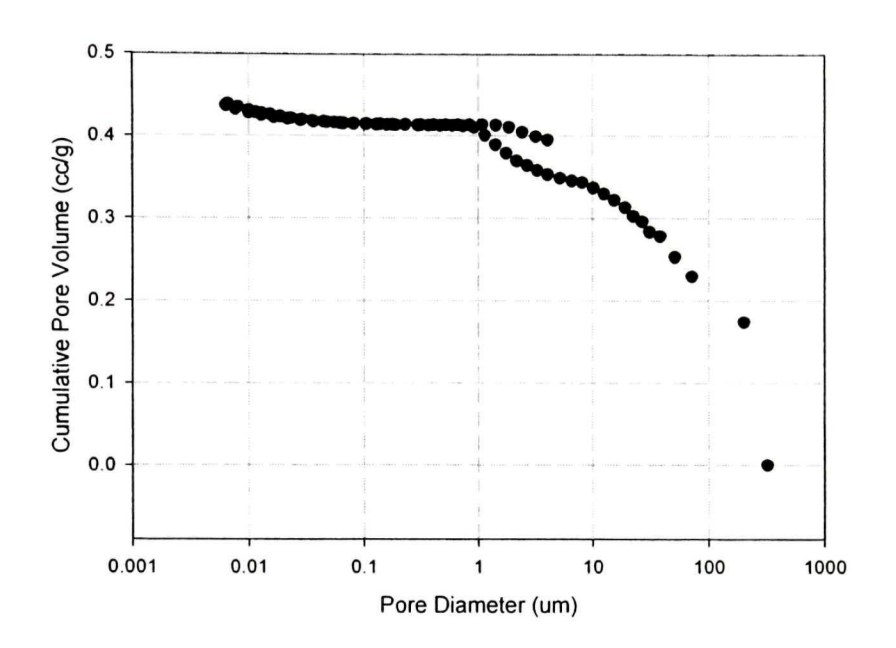


Figure 9.3 Typical intrusion extrusion capillary hysteresis curve for the DFF (6 min) chicken sample.

About 0.97% of the intruded mercury was entrapped in the control (un-fried) sample. This increased to 9.95% after 360 s of DFF. This implies that the pore structure consists of narrow pore segments at the surface and larger pore segment towards the core of the sample, thus exhibiting the inkbottle phenomenon. Hicsasmaz and Clayton (1992) reported over 90 and 81% mercury entrapment in cookies and bread samples, respectively, while Adamson (1990) recorded 80% for activated carbon and a negligible amount for silicalumina. This phenomenon is established based on the end point of the

depressurization (extrusion) point relative to the pressurization (intrusion) from the mercury adsorption/desorption isotherm. The results show that oil absorption due to frying affects the final pore structure. However, in comparison with the results of Hicsasmaz and Clayton (1992) and Adamson (1990) mercury entrapment (hysteresis) was very low in our samples. This implies that the pores are fairly cylindrical in nature, thus justifying the use of the cylindrical capillary model (Eq. 9.1). The fact that mercury entrapment in DFF chicken samples is greater than for the control suggests that oil intrusion into the pore channels contributed to alteration of the pore structure. The absorbed oil may have clogged the open channels, thereby inducing structural distortion of the interconnected pores, and creating dead-end (blind) pores and non-interconnected (closed) pores in the pore network.

Cumulative pore area was determined and the results for the different frying times are shown in Figure 9.4. The highest cumulative surface area was observed at 300 s of frying (8.27 m²/g) increasing from 6.92 m²/g for the raw sample. The variations that occurred between different treatments may be due to the influence of oil uptake on pore geometry.

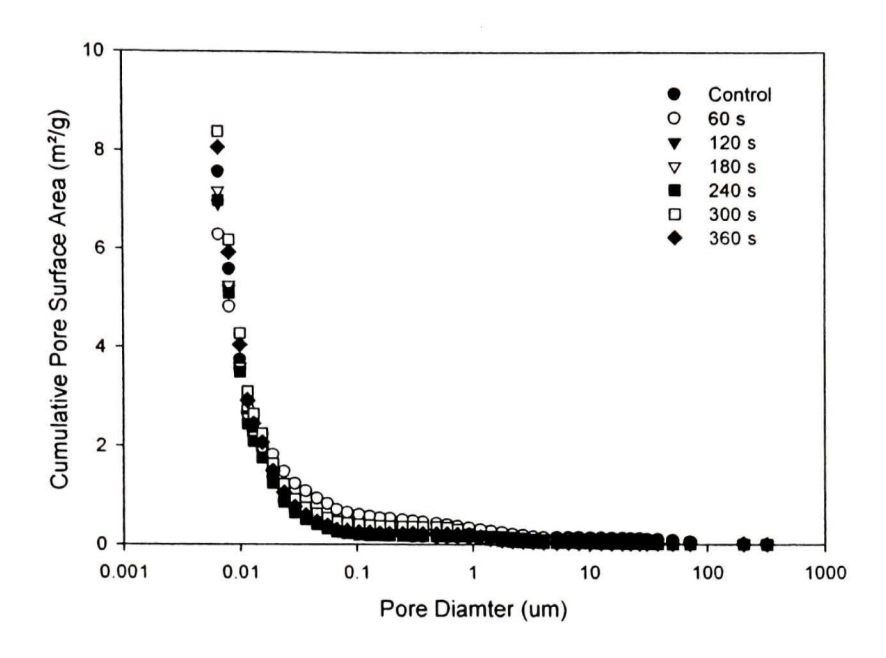


Figure 9.4 Cumulative pore area as a function of pore diameter of deep-fat fried chicken samples fried for 0, 4, 6, and 8 min.

The surface area values of the for the raw sample in our study was higher than that reported by Farkas and Singh (1991) for freeze-dried chicken meat (4.7 m²/g). Ngadi et al, (2001) reported cumulative surface areas of 4 to 9 m²/g for (oven fried) textured soy protein. Our samples exhibited fairly uniform surface areas with pore diameter ranging from 0.1 to 320 μ m.

Another method of quantifying pore size distribution is by the pore volume distribution function (Figure 9.5). The distribution function for DFF chicken meat exhibits a simple peak at around 0.007 μ m, indicating the extent of similar pore sizes within that region. Dullien (1992) also reported a single peak in characterizing sandstone. Rahman et al. (2002) found that freeze-dried tuna meat exhibits several rugged peaks, the major peaks occurring at 5.5, 13, and 30 μ m. Karathanos et al. (1996) found three major peaks at 0.2, 1.1, and 21 μ m for

freeze-dried carrots. The PSD of chicken meat is more uniform than those of tuna meat and beef. This may be attributed to the structural layout of the muscle fibers and their random orientation, and indicates that the majority of pores in DFF chicken meat are capillary pores.

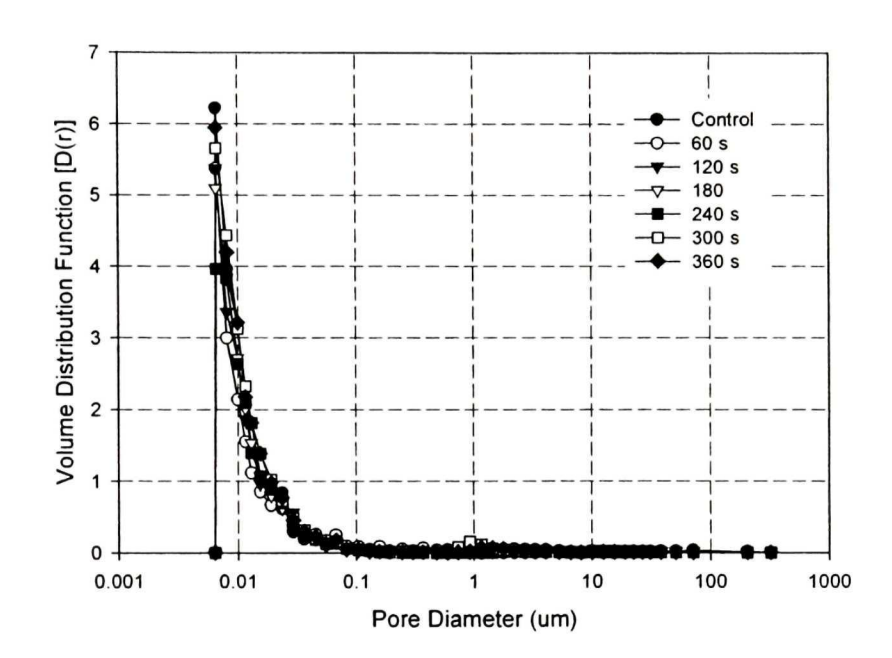


Figure 9.5 Pore size distribution by volume distribution function D(r) as a function of pore diameter for deep-fat fried chicken meat.

Pore structure is characterized in DFF chicken meat using the percent pore volume distribution (PPVD) as shown in Figure 9.6. Pore sizes of 38 μ m and smaller were considered in this analysis. The control samples and the least fried samples exhibit higher PPVD. The effect of fat absorption as a result of extended frying is seen to have affected the PSD (Figure 9.6). The increments in

frying time are associated with shifts of the PSD curve to the left (i.e. to smaller sizes), which is an indication of oil intrusion.

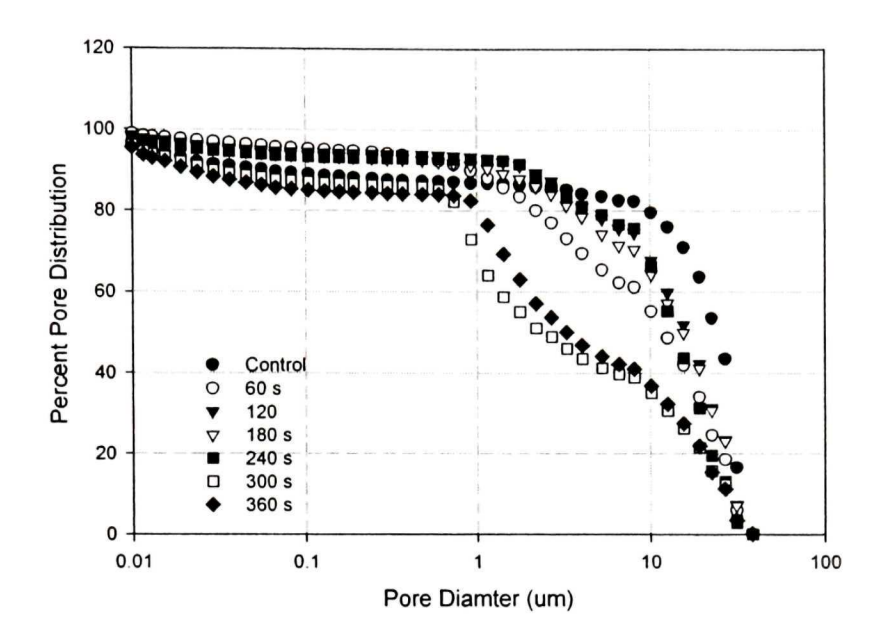


Figure 9.6 Percent volume distribution function as a function of pore diameter for deep-fat fried chicken meat.

Capillary pores account for over 84% of the pore volume in deep-fried samples. Farkas and Singh (1991) reported that 80% of pore volume was accounted for by micropores in freeze-dried raw chicken meat. Kassama et al. (2003) reported that capillary pores accounted for 70 and 84% of pore volume in ground beef samples and in ground beef extended with soy protein, respectively. The intrusion of the frying medium into the porous medium (chicken meat) affected the final pore structure.

9.5 Conclusions

The pore structure of deep-fat fried chicken samples was influenced by oil uptake. The cumulative pore volume varies from 0.51 to 2.13 mL/g as frying time decreases. The mean pore diameter decreased from 1.17 to 0.25 μm and porosity of 0.71 to 0.37 after 360 s of DFF. The cumulative pore surface area of the control was 6.92 m²/g compared to 8.24 m²/g in samples fried for 360 s. Different pore size distribution curves were used to characterize pore structure. The pore size distribution shows a single peak at 0.007 μm , pore volume distribution appeared to be fairly uniform. The assumption of cylindrical pore shape was accurate to some degree and over 84% of the pores were capillary pores. The inter-fiber (planar) pore diameter was about 10.2 μm while the intra-fiber (internal) pores vary from 0.006 to 10 μm in diameter. The interconnectedness of the pore structure was been affected by the amount of oil uptake.

9.6 References

- Adamson, A. W. 1990. Physical Chemistry of Surfaces, 5th edition. John Wiley and Sons, Inc. New York Pages 560-590.
- Aguilera, J. M., and D. W. Stanley. 1999. Microstructure and Principles of Food Processing and Engineering, 2nd Edition. Aspen Publishers, Inc. Gaithersburg, MD.
- Al-Rqobah, H. A., E. K. T. Kam and R. Hughes. 1988. Dynamic determination of diffusion in porous particles. Chemical Engineering Research Des, 66: 275-283.
- Bailey, A. J and N. D. Light. 1989. Connective Tissue in Meat and Meat Products. Elsevier Applied Science, London.
- Bhatnagar, S. and M. A. Hanna. 1997. Modification of microstructure of starch extruded with selected lipids. Starch 49: 12-20.
- Christensen, C. M. 1984. Food texture perception. Advance Food Research 29: 159-199.
- Dullien, F. A. L. 1992. Porous Media: Fluid Transport and Pore Structure.

 Academic Press, INC. New York.
- Farkas B. E. and R. P. Singh. 1991. Physical properties of Air-dried and freeze-dried chicken white meat. Journal of Food Science 56(3): 611-615.
- Flint, O. 1994. Food Microscopy: A Manual of Practical Methods, using Optical Microscopy. Bios Scientific publishers Ltd, Oxford. P: 59-78

- Hamm, R. 1985. The effect of water on the quality of meat and meat products: problems and research needs. In: Proceedings of third International Symposium on Properties of water in relation to food quality and stability. Simatos JL, Multon (eds.). M. Nijhoff Publication, Dordrecht, Netherlands. P: 591-602.
- Hicsasmaz, Z., and J. T. Clayton. 1992. Characterization of the pore structure of starch starched food materials. Food Structure 11: 115-132.
- Huang, C. T. and J. T. Clayton. 1990. Relationships between mechanical properties and microstructure of porous foods: Part I. A Review. "Engineering and Food Vol. 1. Physical Properties and Process Control. W. E. L. Spiess and H. Schubert. Eds. London: Elsevier Applied Science. pp. 352-360.
- Hussain, M. A., M. S. Rahman and C. W, Ng. 2002. Prediction of pore formation (porosity) in foods during drying: generic models by the use of hybrid neural network. Journal of Food Engineering. 51: 239-248.
- Kassama, L. S. and M. O. Ngadi. 2001. Development of pores and pore size distribution in chicken meat during deep-fat frying. Canadian Society of Agricultural Engineering, Mansonville, QC, Paper No. 01-322.
- Kassama, L. S., Ngadi, M.O., and G.S.V. Raghavan. 2003. Structural and instrumental textural properties of meat patties containing soy protein. International Journal of Food Properties. (Accepted for Publication).
- Karathanos, V. T., N. K. Kanellopoulos, and V. G. Belessiotis. 1996.

 Development of porous structure during air drying of agricultural plant products. Journal of Food Engineering 29: 167-183.

- Karathanos, V. T. and G. D. Saravacos. 1993. Porosity and pore size distribution of starch materials. Journal of Food Engineering 18: 259-280.
- King, C.J., W.K. Lam and O.C. Sandal. 1968. Physical properties important for freeze- drying poultry meat. *Food Technology* 22: 1302.
- Marousis, S. N., V. T. Karathanos and G. D. Saravacos. 1991. Effect of physical structure of starch materials on the water diffusivity in hydrated granular starches. Journal of Food Processing and Preservation 15: 183-195.
- McDonald K., and D. Sun. 2001a. Pore size distribution and structure of a cooked beef product as affected by vacuum cooling. Journal of Food process Engineering. 24: 381-403.
- McDonald K., and D. Sun. 2001b. The formation of pores and their effects in cooked beef products on the efficiency of vacuum cooling. Journal of Food Engineering 47: 175-183.
- Micromeritics 1999. Operator's Manual. Norcross, GA: Micromeritics Instrument Corporation.
- Moreira, R.G., Castell-Perrez, M.E. and Barrufet, M.A. 1999. *Deep-fat Frying:Fundamentals and Applications*. Maryland: Aspen Publishers, Inc.
- Ngadi, M.O., L. S. Kassama, and G. S. V. Raghavan. 2001. Porosity and pore size distribution in cooked meat patties containing soy protein. Canadian Biosystems Engineering, 43 (3): 17-24.
- Offer, G., P. Knight, R. Jeacocke, R. Almond, T cousins, J. Elsey, N. Parsons, A, Sharp, R. Starr, P. Purslow. 1989. The structural basis of the water-

- holding, appearance and toughness of meat products. Food Microstructure 8: 151-170.
- Ofstad, R., S. Kidman, R. Myklebust and A. M. Hermansson. 1993. Liquid holding capacity and structural changes during heating of fish muscle: Cod (*Gadus morhua* L.) and salmon (*Salmo Salar*). Food Structure 12: 163-174
- Orr, C. Jr. 1969. Application of mercury penetration to materials analysis: Review paper. Powder Technology 3: 117-123.
- Pinthus E.J., P. Weinberg and I. S. Saguy. 1995. Oil uptake in deep-fat frying as affected by porosity. Journal of Food Science 60 (4): 767-769.
- Rahman, M. S. 2001. Towards prediction of porosity in food foods during drying: a brief review. Drying Technology, 19(1): 3-15.
- Rahman, M. S., O. S. Al-Amri, and I. M, Al-Bulushi. 2002. Pores and physicochemical characteristics of dried tuna produced by different methods of drying. Journal of Food Engineering 53: 301-313.
- Saravacos, G. D. 1995. Mass transfer properties of foods. In Engineering Properties of Foods, eds. M. A. Rao and S. S. H. Rizvi. Marcel Dekker, Inc., New York, pp. 169-221.
- Satterfield, C. N. and Sherwood, T. K. 1963. The Role of Diffusion in Catalysis. Addison Wesley, Reading, Massachusetts.
- Schaller, D. K., and W. D. Powrie. 1972. Scanning electron microscopy of heated beef, chicken and rainbow trout muscle. Journal of International Canadian Science and Technology Aliment 5: 184-190.

- Schmidt, G. R. 1984. Processing effects on meat product microstructure. Food Microstructure 3: 33-39.
- Stanley, D. W. 1987. Food texture and microstructure. In Food Texture: Intrumental and Sensory Measurement, ed. H. R. Moskowitz. Marcel Dekker, New York, pp. 35-64.
- Wilding, P., N. Hedges, and P. Lillford. 1986. Salt-induced swelling of meat: The effect of storage time, pH, ion-type and concentration. Meat Science 18: 55-75
- Vickers, Z. and M. C. Bourne. 1976. Crispiness in food A review. Journal of Food Science 41: 1153-1157.
- Vincent, J. F. V. 1989. Relationship between density and stiffness of apple flesh. Journal of Food Science and Agriculture 47: 443-463.
- Webb P. A., and C. Orr. 1997. Analytical Methods in Fine Particle Technology. Norcross, GA: Micromeritics Instrument Corporation.
- Xiong, X., G. Narsimhan and M. R. Okos. 1991. Effect of composition and pore structure on binding energy and effective diffusivity of moisture in porous food. Journal of Food Engineering 15: 187-208.

X. GENERAL SUMMARY AND CONCLUSIONS

10.1 General Summary and Conclusions

Deep-fat frying is an efficient method of food preparation, leading to much-appreciated and unique quality characteristics. However, concern over the health consequences of excess fat consumption associated with absorption of oil during this process, has caught the attention of researchers. Efforts have been made to understand how the uptake of oil is related to the heat and mass transfers involved in deep-fat frying, and to what extent it is possible to limit oil absorption by controlling processing conditions. Insofar as heating induces structural changes in biological materials, it is essential to explore the relationships between these transport phenomena and such changes.

The literature concerning oil uptake by foods during deep-frying has, until recently, focused primarily on potatoes and flour-based products. The differences in structure and composition between such products and muscle fiber (meat, fish and poultry), whether whole or ground (restructured), have not been fully addressed. In particular, the response of muscle fiber structures to heating can be expected to be different than that of plant cellular structures, on the basis of the natures of their different structural components, proteins in meats versus structural carbohydrates in plants. These considerations, combined with the widespread popularity of deep-fried chicken meats and lack of detailed information on physical properties of deep-fried meats in general, have prompted the research described in this thesis.

The study consisted of five main steps: 1) a preliminary study comparing the time histories of moisture loss and oil uptake at different frying oil temperatures; 2) description of the kinetics of mass transfer diffusivities of water and oil; 3) a study of the relationships between time and temperature of frying on densities and shrinkage and modeling of pore formation; 4) preliminary studies on pore structure characterization of pore structure and texture of restructured meat during oven and pan-frying, with and without extenders and 5) a study on the characterization of pore structure and description of the relationship between parameters describing pore structure and oil uptake.

The study has confirmed that there is a strong relationship between oil uptake and moisture loss during deep-fat frying of chicken breast meat and that the relationship changes with time of frying. During the first 45 seconds, the relationship appears to be erratic, and oil absorption appears to be independent of frying oil temperature. From 45 s to about 360 s, the relationship between the two mass transfers is linear. Thereafter, oil uptake is severely limited, appearing to reach a plateau, whereas the rate of moisture loss drops off gently. Moisture and oil diffusivities were significantly influenced by the change in frying oil temperature.

The changes in bulk and apparent densities of chicken meat were related to frying oil temperature and frying time. The bulk density decreased with time, whereas the solid density increased. However, the apparent increase in apparent density as a result of the mass loss due to thermal deterioration of the muscle fibers. The relationship between bulk density and moisture loss was linear.

Volumetric shrinkage was also affected by temperature, the rate of volumetric shrinkage increasing rapidly during the first 300 s of frying after which it tended to stabilize.

Considering the lack of information on pore development during deep-fat frying, the information acquired on changes in the densities was vital for prediction of oil uptake. A linear model best described pore development as a function of moisture loss, while a exponential model gave the best fit between pore development and oil uptake. This indicates that while pore development is driven by moisture loss, oil uptake is not simply the reverse of moisture loss. While moisture loss is associated primarily with vapor phase transport, oil intrusion is a liquid phase process and is likely limited by the size of pores fatty acids can infiltrate relative to those from which water vapor can escape. During the first 45 s of frying, it appeared that excess volume may have been created, as indicated by negative porosities.

Soy protein extenders were found to have improved the water holding capacity and enhanced the texture of restructured beef (patties). Higher concentrations of extender resulted in a reduction in the cumulative pore volume of the fried patties. The use of soy protein flour resulted in larger pores than did the textured soy protein. Extenders were found to improve the textural quality of restructure beef patties. There were fewer capillary pores in the restructured beef patties than in the deep-fat fried chicken meat.

Decreasing cumulative pore volumes, and porosity were the result of oil uptake into the porous medium. Even though the interconnectedness of the

pore structures was slightly affected, the assumption of cylindrical pores was still valid based on the limited capillary hysteresis of the mercury adsorption-desorption curve observed during the test probably due to oil being absorbed into the porous matrix. Over 80% of pores created by moisture diffusion during deepfat frying were capillary pores. Larger pores existed at the surface whereas smaller pore with a more uniform pore size distribution were detected in the core of the product.

10.2 Claims of Contribution to Knowledge

The main objective of this study was to quantify porosity and pore size distributions of deep-fat fried product by using a mercury porosimeter and a fluid displacement pycnometer.

1. The relationship between moisture loss and oil uptake during deep-fat frying of chicken breast meat was investigated. It was established that a linear relationship existed between the two variables for a restricted time interval during different limitations on oil uptake and moisture loss. Oil uptake was established to be independent of frying oil temperatures during the initial phase (<45 s), during which oil uptake seems to be due to surface adhesion rather than to oil intrusion per se. This seems to be associated with turbulence due to boiling of evacuated moisture at the interface. Effective oil diffusivity was introduced as an analogy to moisture diffusivity, and was found

to increase with temperature, leading to the implication that lower frying temperatures should be investigated in efforts to reduce oil uptake.

- 2. Frying oil temperature and frying time significantly influenced changes in physical properties such as bulk and apparent density and volumetric shrinkage in deep-fat fried chicken meat. A prediction model was developed to predict densities, shrinkages, and pore development as a function of moisture loss during deep-fat frying of chicken meat.
- 3. A methodology was established to measure porosity and pore size distribution of meat products. Porosity and pore sizes were determined based on Wasburn's model and the evolution of pore structure and pore-size distribution haven been characterized for deep-fat fried chicken breast meat and restructure meat.

10.3 Recommendations for Future Research

Further investigation is required to study initial phases (<45 s) of deep-fat frying. The design of a system of frying permitting in situ image analysis to track phase changes during this crucial stage is recommended.

Non-invasive imaging (i.e., scanning electron microscopy) with analysis software should be used to study the structure of deep-fried products. This method would complement the porosimetry technique by differentiating crystallized oil absorbed in the porous matrix from the native cell tissue of the fried product, hence pore the effect of oil uptake would be better understood. Experimental data generated form both can facilitate the development of model to predict moisture loss and oil uptake based on pore networks.

A further study is vital to investigate the swelling and shrinkage behavior of meat during thermal processing using imaging analyses technique. This would provide complementary information on the physical characteristics of muscles responses to deep-fat frying.

GENERAL REFERENCES

- Adamson, A. W. 1990. Physical Chemistry of Surfaces 5th edition New York: John Wiley and Son, Inc.
- Agriculture and Agri-food Canada. 2000. Food export statistics. http://www.agr.gc.ca.
- Aguilera, J. M. and D. W. Stanley. 1999. Microstructural Principles of Food Processing and Engineering, Gaithersburg, Maryland: Aspen Publishers, Inc.
- Atkins, A. G. 1987. The basic principles of mechanical failure in biological systems. *In Food Structure and Behavior*, Ed. J.M.V. Blanshard and P. Lillford, 149-197. London: Academic Press Limited.
- Bailey, A. J and N. D. Light. 1989. Connective Tissue in Meat and Meat Products. Elsevier Applied Science, London.
- Blumental, M. M. 1991. A new look at the chemistry and physics of deep-fat frying. Food Technology: 68-71.
- Blumental, M. M and R.F. Stier. 1991. Optimization of deep-fat frying operations. *Trend in Food Science* 144-148.
- Brooks, D. D. 1991. Some perspectives on deep-far frying. *Inform 2(12): 1091-1095*.
- Burfoot, D. 1987. The nature and significance of heat and mass transfer processes in food stuffs. *In Food Structure and Behavior*, Ed. J.M.V. Blanshard and P. Lillford, 219-243. London: Academic Press Limited.
- Chang, C. S. 1988. Measuring density and porosity of grain kernels using a gas pycnometer. *Cereal Chemistry* 65(1): 13-15.
- Clayton, J. T. and C. T. Huang. 1984. Porosity of extruded foods. In Engineering and Food Volume 2, edited by B. M. Mckenna. Elsevier Applied Science Publishers. London.
- Costa, R.M., F.A.R. Oliveira. 1999. Modeling the kinetics of water loss during potato frying with a compartmental dynamic model. *Journal of Food Engineering 41: 177-185.*

- Crank, J. 1975. The mathematics of diffusion, 2nd edition, Oxford, UK: Oxford University Press.
- Datta, A.K. and J. Zhang. 1999. Porous media approach to heat and mass transfer in solid foods. ASAE Paper No. 99-3068. St. Joseph, MI: ASAE.
- Dullien, F. A. L. 1992. Porous Media: Fluid Transport and Pore Structure, 2nd edition San Diego, California: Academic Press.
- Farkas B. E. and R. P. Singh. 1991. Physical properties of Air-dried and freeze-dried chicken white meat. *Journal of Food Science* 56(3): 611-615.
- Farkas B. E., R. P. Singh, and T. R. Rumsey. 1996. Modelling heat and mass transfer in immersion frying. Part II: Model solution and verification. *Journal of Food Engineering* 29: 227-248.
- Farkas, B. E. 1994. Modeling immersion frying as moving boundary problem. Ph.D. Dissertation. University of California, Davis.
- FDA. 1998. *Talk Paper*. US department of Health and Human Service. Rockville, MD: Public Health Service.
- Flint, O. 1994. Food Microscopy: A Manual of Practical Methods, using Optical Microscopy. Bios Scientific publishers Ltd, Oxford. P: 59-78
- Fritsch, C.W. 1981. Measurements of frying fat deterioration: A brief review. Journal of The American Oil Chemists' Society 58:272.
- Gamble, M.H. and P. Rice. 1988. The effect of strip thickness on potato crisp yield and composition. *Journal of Food Engineering 8:31-46.*
- Gamble, M. H., P. Rice. 1987. Effect of pre-frying drying of oil uptake and distribution in potato crisp manufacture. *International Journal of Food Science and Technology 22: 535-548*.
- Gamble, M. H., P. Rice, J.D. Selman. 1987. Distribution and morphology of oil deposit in some deep-fried products. *Journal of Food Science* 52(6): 1742-1745.
- Gupta, P., U.S. Shivhare and .S. Bawa. 2000. Studies of frying kinetics and quality of French fries. *Drying Technology* 18(1&2): 311-321.
- Hicsasmaz, Z., and J. T. Clayton. 1992. Characterization of the pore structure of starch starched food materials. Food Structure 11: 115-132.

- Huse, H.L., P. Mallikarjunan, M.S. Chinnan, Y.C. Hung and .D. Phillips. 1998. Edible coatings for reducing oil uptake in production of akara (Deep-fat frying of cowpea paste). *Journal of Food Processing and Preservation* 22(2): 155-165.
- Huang, C. T. and J. T. Clayton. 1990. Relationship between mechanical properties and microstructure of porous foods: Part I. A review. In W. E. L. Spiess and H. Schubert (Eds.), Engineering and Food, Vol 1. The physical properties and process control (pp. 352-360). London: Elsevier.
- Hussain, M. A., M. S. Rahman and C. W, Ng. 2002. Prediction of pore formation (porosity) in foods during drying: generic models by the use of hybrid neural network. Journal of Food Engineering. 51: 239-248.
- laonnidis, M. A. and I. Chatzis. 1993. A mixed-percolation model of capillary hysteresis and entrapment in mercury porosimetry. Journal of Colloid and Interface Science. 161: 278-291.
- Kalapathy, U. and A. Proctor. 2000. A new method for free fatty acid reduction in frying oil using silicate films produces from rice hull ash. *Journal of American The Chemists' society 77(6):* 593-597.
- Karathanos, V. T., N. K. Kanellopoulos and V. G. Belessiotis. 1996. Development of porous structure during air drying of agricultural plant products. *Journal of Food Engineering* 29: 167-183.
- Karathanos, V.T. and G.D. Saravacos. 1993. Porosity and pore size distribution of starch materials. *Journal of Food Engineering* 18: 259-279.
- Kassama, L. S. and M. O. Ngadi. 2001. Development of pores and pore size distribution in chicken meat during deep-fat frying. Canadian Society of Agricultural Engineering, Mansonville, QC, Paper No. 01-322.
- Kassama, L.S. and M.O. Ngadi. 2000. Development of pores and pore size distribution in chicken meat during deep-fat frying. Mansonville, QC: Canadian Society of Agricultural Engineers, Paper No. 01-322.
- Kassama, L. S., Ngadi, M.O., and G.S.V. Raghavan. 2003. Structural and instrumental textural properties of meat patties containing soy protein. International Journal of Food Properties 6 (3): 1-11
- Keller and Eseher 1989. Heat and mass transfer during deep-fat frying of potato products. Poster presentation, International Congress on Engineering and Food. Cologne, May 5 to June 1.

- King, C.J., W.K. Lam and O.C. Sandal. 1968. Physical properties important for freeze-drying poultry meat. *Food Technology* 22: 1302.
- Krokida, M.K., V. Oreopoulou and Z.B. Maroulis. 2000. Water loss and oil uptake as a function of frying time. *Journal of Food Engineering 44: 39-46.*
- Lamberg, I., Halstrom, B., and Olsson, H. 1990. Fat uptake in a potato drying/frying process. *Lebensm-Wiss U-Technol* 19:346-348.
- Lee, J. K. 1991. The effects of processing conditions and maize varieties on physicochemical characteristics of tortilla chips. Unpublished Ph.D. Thesis. Department of animal Science. Texas A & M University. College Station, TX.
- Mamur, A. 1989. Capillary rise and hysteresis in periodic porous media. Journal of Colloid and Interface Science 129(1): 278-85.
- Marousis, S. N. and D. D. Saravacos. 1990. Density and porosity in granular starch drying. Journal of Food Science 55.
- McDonough, C., M. H. Gomez, J. K. Lee, R. D. Waniska, and L. W. Rooney. 1993. Environmental scanning electron microscopy evaluation of tortilla chip microstructure during deep-fat frying. Journal of Food Science 58(1): 199-203.
- Mittelman, N., S. Mizrahi, and Z. Berk. 1984. Heat and mass transfer in frying. In Engineering of Food, Vol.1: Engineering Science in the Food Industry, Ed. B. McKenna, 109-116. New York, NY: Elsevier Applied Science Publishers.
- Mohamed, S., N.A. Hamid, and M.A. Hamid. 1998. Food Components affecting the oil absorption and crispness of fried batter. *Journal of Food Science and Agriculture* 78 (1): 39-45.
- Moreira R.G. and M. A. Barrufet. 1998. A new approach to describe oil absorption in fried foods: a simulation study. *Journal of food engineering* 35: 1-22.
- Moreira, R.G., X. Sun and Y. Chen. 1997. Factors affecting oil uptake in tortilla chips in deep-fat frying. *Journal of Food Engineering* 31:485-498.
- Moreira, R.G., Castell-Perrez, M.E. and Barrufet, M.A. 1999. *Deep-fat Frying: Fundamentals and Applications*. Maryland: Aspen Publishers, Inc.

- Moreira, R.G., J.E. Palau, V.E. Sweat and X. Sun. 1995. Thermal and physical properties of tortilla chips as a function of frying time. *Journal of Food Preservation* 19: 175-189.
- Nagai, N. and Y. Toshimasa. 1990. Transformation of fractal structure of starch materials to improve their physical properties. *In Engineering and Food, Vol. 1, Physical Properties and Process Control*, eds. W.E.L. Spiess and H. Schubert, 297-304. London: Elsevier Applied Science.
- Ngadi, M. O. 1995. Finite element modeling of heat and mass transfer during deep-fat frying of chicken drums. Ph.D Dissertation. Technical University of Nova Scotia. Halifax, Nova Scotia.
- Ngadi, M.O., L.S. Kassama and G.S.V. Raghavan. 2001. Porosity and pore size distribution in cooked meat patties containing soy protein. *Canadian Biosystems Engineering* 43 (3): 17-24.
- O'Brien, R. 1993. Foodservice use of fat and oil. INFO 4 (8):913-921.
- Orr, C. 1969/70. Application of mercury penetration to material analysis. Review paper. *Powder technology 3: 117-123*.
- Ofstad, R., S. Kidman, R. Myklebust and A. M. Hermansson. 1993. Liquid holding capacity and structural changes during heating of fish muscle: Cod (*Gadus morhua* L.) and salmon (*Salmo Salar*). Food Structure 12: 163-174
- Perkins E. G. and M. D. Erikson. 1996. *Deep Fryng: Chemistry, Nutrition, and Practical Applications*. Champaign, II: AOCS press.
- Pinthus E. J., P. Weinberg and I. S. Saguy. 1995. Oil uptake in deep fat frying asaffected by porosity, *Journal of Food Science* 60(4): 767-769.
- Pinthus E.J., and I. S. Saguy. 1994. Initial interfacial tension and oil uptake by deep-fat fried foods. *Journal of food science* 59 (4): 804-807.
- Rahman, M. S., O. S. Al-Amri, and I. M, Al-Bulushi. 2002. Pores and physico-chemical characteristics of dried tuna produced by different methods of drying. Journal of Food Engineering 53: 301-313.
- Reeves, P.C. and M.A. Celia. 1996. A functional relationship between capillary pressure, saturation and interfacial area as revealed by a pore-scale network model. *Water Resources Research* 32(8): 2345-2358.
- Rice, P. and M. H. Gamble. 1989. Technical Note: Modeling moisture loss during potato slice frying. International Journal of Food Science and technology 24: 183-187.

- Romero, A., C. Cuesta, and F.J. Sanchez-Muniz. 2000. Cyclic fatty acid monomers and thermoxidative alteration compounds formed during frying of frozen foods in extra virgin olive oil, *Journal of The American Oil Chemists' Society* 77(11): 1169-1175.
- Shaw, R. and A.C. Lukes. 1968. Reducing the oil content of potato chips by controlling their temperature after frying. USDA, ARS-73-58. U.S. Department of Agriculture, Washington, D.C.
- Singh, R. P. 1995. Heat and mass transfer in foods during deep-fat frying: Mathematical modeling provides new tool to study the effect of processing conditions in deep-fat frying of foods, *Food Technology* 49:134-137.
- Stockwell, A.C. 1988. Oil choice. Baking and Snack, 20(2): 74-80.
- Subramanian, R., K.E. Nandini, P.M. Sheila, A.G. Gopallakrishna, K.S.M.S. Raghavarao, M. Nakajima, T. Kimura and T. Maekawa. 2000. Membrane processing of used frying oils. *Journal of The American Oil Chemists' Society* 77(3): 323-328.
- Sun, X. and R.G. Moreira. 1994. Oil distribution in tortilla chips during deep-fat frying. St Joseph, MI: American Society of Agricultural Engineers, Paper No. 94-6506.
- Ufheil G., and Escher, F. 1996. Dynamics of oil uptake during deep-fat frying of potato slices. Food Science and Technology_Lebensmittel-Wissenshaft and Technologie 29(7):640-644.
- Varela, G. 1988. Current facts about the frying of food. *In Frying of Food: Principle, Changes, New approaches*, eds. G. Varela, A.E. Bender, and I.D.Morton, 9 –25. Chichester, UK: Ellis Horwood.
- Walter, L.C. and G.W. Serbia. 1991. Safety aspects of frying fats and oils. *Food Technology: 84-89.*
- Webb P. A., and C. Orr. 1997. Analytical Methods in Fine Particle Technology. Norcross, GA: Micromeritics Instrument Corporation.
- White, P. 1991. Methods for measuring changes in deep-fat frying oils. *Food Technology: 75-80.*
- William, R., and G.S. Mittal. 1999. Water transfer properties of polysaccharide film on fried pastry mix. Food Science and Technology-Lebensmittel-Wissenschaft and Technologie 32(7): 440-445.

- Xiong, X., G. Narsimhan, and M.R. Okos. 1991. Effect of composition and pore structure on binding energy and effective diffusivity of moisture in porous food. *Journal of Food Engineering* 15: 187-208.
- Yamsaengsung, R. and R. G. Moreira. 2002. Modeling the transport phenomena and structural changes during deep-fat frying. Part 1. Model development. Journal of Food Engineering 53: 1-10.

APPENDICES

Appendix Table 1 Analysis of variance for the effects of time and frying oil temperature on moisture loss.

| Source of | | Dť | Summer of Courses | M 0 | | |
|-------------|---|----|-------------------|-------------|-------------|-----------|
| Variation | | Df | Sum of Square | Mean Square | F_{Value} | $P_r > F$ |
| Time | | 14 | 9297.94 | 664.14 | 259.92 | 0.0001 |
| Temperature | | 2 | 408.78 | 204.39 | 79.99 | 0.0001 |
| Time | X | 28 | 500.42 | 17.87 | 6.99 | 0.0001 |
| Temperature | | 20 | 300.42 | 17.07 | 0.99 | 0.0001 |
| Error | | 90 | 229.96 | 2.56 | | |

Appendix Table 2 Analysis of variance of oil uptake as a function of time and temperature.

| Source of | | Df | Sum of Square | Mean Square | F_{Value} | P _r > F |
|-------------|---|----|---------------|--------------|-------------|--------------------|
| Variation | | וט | Sum of Square | Wearr Square | ▼ Value | 1151 |
| Time | - | 14 | 1118.18 | 79.87 | 28.21 | 0.0001 |
| Temperature | | 2 | 144.85 | 72.42 | 25.58 | 0.0001 |
| Time | X | 28 | 168.04 | 6.00 | 2.12 | 0.0041 |
| Temperature | | | | | | |
| Error | | 90 | 254.85 | 2.83 | | |

Appendix Table 3 Analysis of variance of moisture diffusivity during deepfat frying of chicken meat at different temperatures.

| Df | Sum of Square | Mean Square | F_{Value} | $P_r > F$ |
|----|---------------|--------------------------|--------------------------------------------|--------------------------------------------------|
| 2 | 2.15E-17 | 1.07E-17 | 66.09 | 0.0001 |
| 6 | 9.76E-19 | 1.63E-19 | | |
| 8 | 2.25E-17 | | | |
| | 2 | 2 2.15E-17 6 9.76E-19 | 2 2.15E-17 1.07E-17 6 9.76E-19 1.63E-19 | 2 2.15E-17 1.07E-17 66.09 6 9.76E-19 1.63E-19 |

Appendix Table 4 Analysis of variance of bulk density data for de-boned chicken breast meat deep-fat fried at 170, 180 and 190°C and at different times.

| Source of | | | | | |
|-------------|-----|---------------|-------------|-------------|-----------|
| Variation | Df | Sum of Square | Mean Square | F_{Value} | $P_r > F$ |
| Time | 20 | 0.7682 | 0.0384 | 21.04 | 0.0001 |
| Temperature | 2 | 0.1402 | 0.0701 | 38.41 | 0.0001 |
| Time* Temp | 40 | 0.1961 | 0.0049 | 2.68 | 0.0001 |
| Error | 126 | 0.2300 | 0.0018 | | |
| Total | 188 | 1.3356 | | | |

^{**} Highly significant; ns, not significant; R²=0.83, CV = 3.99

Appendix Table 5 Analysis of variance of apparent density data for deboned chicken breast meat deep-fat fried at 170, 180 and 190°C and at different times.

| Source of | | | | | |
|-------------|-----|---------------|-------------|-------------|-----------|
| Variation | Df | Sum of Square | Mean Square | F_{Value} | $P_r > F$ |
| Time | 20 | 0.3733 | 0.0187 | 53.88 | 0.0001 |
| Temperature | 2 | 0.0209 | 0.0104 | 30.11 | 0.0001 |
| Time* Temp | 40 | 0.0299 | 0.0007 | 2.16 | 0.0001 |
| Error | 126 | 0.0436 | 0.0003 | | |
| Total | 188 | 0.4677 | | | |

^{**} Highly significant; ns, not significant; R² = 0.91, CV = 1.59

Appendix Table 6 Mean comparison of bulk density values by DMRT of deboned chicken meat during deep-fat frying at different levels of frying temperatures.

| Temperature (°C) | Bulk density Mean Value | | N | Std Deviation |
|---------------------|----------------------------|---|----|---------------|
| 170 | 1.0889 | а | 63 | 0.0685 |
| 180 | 1.0915 | а | 63 | 0.0789 |
| 190 | 1.0324 | b | 63 | 0.0913 |

Appendix Table 7 Mean comparison of bulk density values by DMRT of deboned chicken meat during deep-fat frying at different levels of frying times.

| Time (s) | Bulk density Mean Value | | N | Std Deviation |
|----------|----------------------------|----------|---|---------------|
| 0 | 1.1845 | а | 9 | 0.0505 |
| 5 | 1.1431 | b | 9 | 0.0579 |
| 10 | 1.1365 | bc | 9 | 0.0512 |
| 15 | 1.1363 | bc | 9 | 0.0265 |
| 20 | 1.1301 | bcd e | 9 | 0.0173 |
| 30 | 1.1296 | bcd | 9 | 0.0267 |
| 45 | 1.1108 | bc | 9 | 0.0642 |
| 60 | 1.1069 | bc | 9 | 0.0627 |
| 90 | 1.1053 | bcd e | 9 | 0.0269 |
| 120 | 1.0932 | cdef | 9 | 0.0265 |
| 150 | 1.0803 | def g | 9 | 0.0849 |
| 180 | 1.0629 | efg | 9 | 0.0555 |
| 210 | 1.0649 | efg | 9 | 0.0560 |
| 240 | 1.0573 | fg | 9 | 0.0632 |
| 300 | 1.0398 | gh | 9 | 0.1004 |
| 360 | 1.0017 | hi | 9 | 0.0980 |
| 420 | 0.9928 | i | 9 | 0.0499 |
| 480 | 0.9795 | i | 9 | 0.0660 |
| 540 | 0.9866 | i | 9 | 0.0541 |
| 600 | 0.9898 | i | 9 | 0.0595 |
| 900 | 0.9575 | i | 9 | 0.0253 |

Appendix Table 8 Mean comparison of apparent density values by DMRT of de-boned chicken meat during deep-fat frying at different levels of frying temperatures.

| Temperature (°C) | Apparent density Mean Value | | N | Std Deviation | |
|---------------------|-----------------------------------|---|----|---------------|--|
| 170 | 1.1612 | С | 63 | 0.0459 | |
| 180 | 1.1869 | а | 63 | 0.0571 | |
| 190 | 1.1728 | b | 63 | 0.0428 | |

Appendix Table 9 Mean comparison of apparent density values by DMRT of de-boned chicken meat during deep-fat frying at different levels of frying times.

| Time (s) | Apparent density Mean Value | | N | Std Deviation |
|----------|-----------------------------------|---------|---|---------------|
| 0 | 1.1530 | b | 9 | 0.0383 |
| 5 | 1.1265 | а | 9 | 0.0151 |
| 10 | 1.1253 | а | 9 | 0.0119 |
| 15 | 1.1321 | ab | 9 | 0.0105 |
| 20 | 1.1337 | ab c | 9 | 0.0181 |
| 30 | 1.1229 | а | 9 | 0.0105 |
| 45 | 1.1254 | а | 9 | 0.0152 |
| 60 | 1.1349 | ab c | 9 | 0.0175 |
| 90 | 1.1468 | bc d | 9 | 0.0174 |
| 120 | 1.1507 | bc d | 9 | 0.0146 |
| 150 | 1.1600 | cd e | 9 | 0.0172 |
| 180 | 1.1656 | def | 9 | 0.0209 |
| 210 | 1.1714 | de | 9 | 0.0252 |
| 240 | 1.1793 | f | 9 | 0.0225 |
| 300 | 1.2000 | g | 9 | 0.0227 |
| 360 | 1.2184 | h | 9 | 0.0251 |
| 420 | 1.2201 | h | 9 | 0.0288 |
| 480 | 1.2468 | i | 9 | 0.0272 |
| 540 | 1.2462 | i | 9 | 0.0435 |
| 600 | 1.2476 | i | 9 | 0.0338 |
| 900 | 1.2391 | i | 9 | 0.0270 |

Appendix Table 10 Analysis of variance of volumetric shrinkage for deboned chicken breast meat deep-fat at different FORs and time.

| Source of | | | | | |
|-------------|-----|---------------|-------------|--------------------|-----------|
| Variation | Df | Sum of Square | Mean Square | F _{Value} | $P_r > F$ |
| Time | 20 | 7.7979 | 0.3899 | 189.24 | 0.0001 |
| Temperature | 2 | 0.0190 | 0.0095 | 04.62 | 0.0116 |
| Time* Temp | 40 | 0.0574 | 0.0014 | 0.70 | 0.9031 |
| Error | 126 | 0.2596 | 0.0021 | | |
| Total | 188 | 8.1339 | | | |

^{**} Highly significant; * Significant; ns, not significant; R² = 0.97, CV = 6.7838

Appendix Table 11 Mean comparison of volumetric shrinkage by DMRT of de-boned chicken meat during deep-fat frying at different levels of frying temperatures.

| Temperature (°C) | Shrinkage volume Mean Value | | N | Std Deviation | |
|---------------------|-----------------------------------|---|----|---------------|--|
| 170 | 0.6829 | а | 63 | 0.2135 | |
| 180 | 0.6652 | b | 63 | 0.2077 | |
| 190 | 0.6592 | b | 63 | 0.2054 | |

Appendix Table 12 Mean comparison of volumetric shrinkage by DMRT of de-boned chicken meat during deep-fat frying at different levels of frying times.

| Time (s) | Shrinkage volume Mean Value | | N | Std Deviation |
|------------|-----------------------------------|--------|----|---------------|
| 0 | 1.0000 | а | 63 | 0.0000 |
| 5 | 0.9433 | b | 63 | 0.0577 |
| 10 | 0.9444 | b | 63 | 0.0479 |
| 15 | 0.9244 | bc | 63 | 0.0350 |
| 20 | 0.9067 | bc | 63 | 0.0450 |
| 30 | 0.8833 | С | 63 | 0.0262 |
| 4 5 | 0.8311 | d | 63 | 0.0318 |
| 60 | 0.7611 | е | 63 | 0.0401 |
| 90 | 0.7189 | ef | 63 | 0.0459 |
| 120 | 0.6879 | f | 63 | 0.0345 |
| 150 | 0.6233 | g | 63 | 0.0316 |
| 180 | 0.5933 | gh | 63 | 0.0474 |
| 210 | 0.5744 | hi | 63 | 0.0403 |
| 240 | 0.5433 | ij | 63 | 0.0424 |
| 300 | 0.5144 | j | 63 | 0.0611 |
| 360 | 0.4989 | jk | 63 | 0.0509 |
| 420 | 0.4256 | lm | 63 | 0.0482 |
| 480 | 0.4633 | kl | 63 | 0.0921 |
| 540 | 0.4511 | ı | 63 | 0.0389 |
| 600 | 0.3933 | m n | 63 | 0.0312 |
| 900 | 0.3689 | n | 63 | 0.0078 |

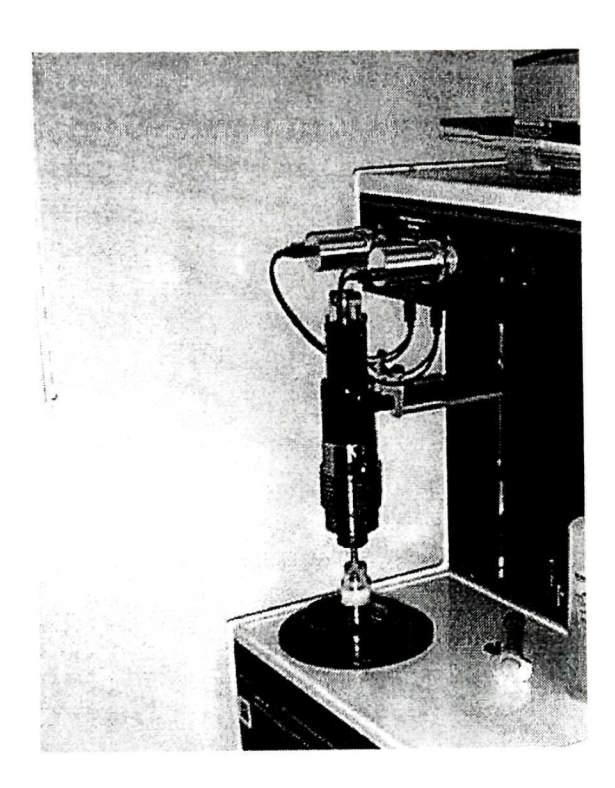
Appendix 1 Table 13 Effects of temperature (170, 180, and 190°C) and frying time (0, 5, 10 – 900 s) on porosity during deep-fat frying of de-boned chicken.

| Source of | | | | | |
|-------------|-----|---------------|-------------|-------------|-----------|
| Variation | Df | Sum of Square | Mean Square | F_{Value} | $P_r > F$ |
| Time | 20 | 1.4334 | 0.0716 | 43.8 | <0.01 |
| Temperature | 2 | 0.1100 | 0.0550 | 33.6 | <0.01 |
| Time x | 40 | 0.4600 | 0.0040 | 2.50 | -0.01 |
| Temperature | 40 | 0.1692 | 0.0042 | 2.59 | <0.01 |
| Error | 126 | 0.2060 | 0.0016 | | |
| Total | 188 | 1.9186 | | | |
| | | | | | |

 $R^2 = 0.89$; CV = 48.7%

Appendix 2: Mercury Porosimetry Unit

The mercury porosimetry used in this study is shown in Appendix 2 Figure 1. The equipment generates a maximum pressure of 207 MPa and has the capacity to measure pore diameters ranging approximately from 360 to 0.005 μ m. The equipment has a dual stage built-in unit, two low-pressure port and one high-pressure chamber, which are sequentially used during the porosimetry test.

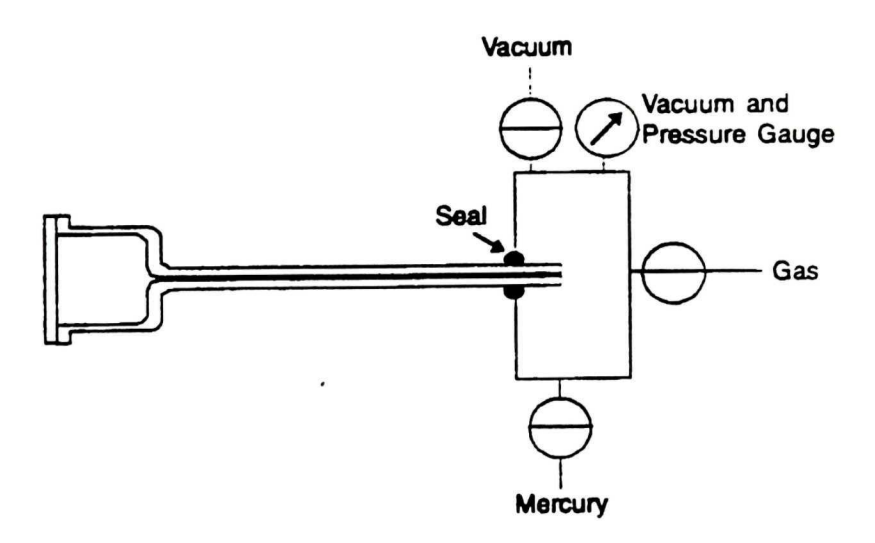


Appendix 2 Figure 1 The Mercury Intrusion Porosimeter used in this study.

2.1 Low Pressure System

The low pressure system consists of the following key components: evacuation valves, gas inlet valves, mercury fill and drain valves, mercury reservoir evacuation valves, mercury degasser and mercury trap. The low-pressure

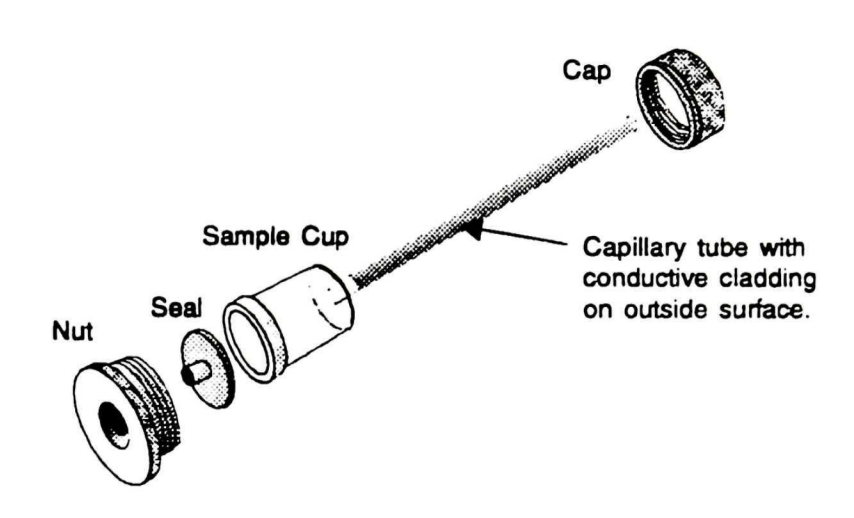
vessels are primarily used for evacuating and preparing samples. The samples in the penetrometer are evacuated to expel air and vapor in the pores, so as to prevent resistance to pressure build-up due to compression of air during intrusion of mercury. After sample evacuation, the penetrometer is filled with mercury under pressure (\leq 138 kPa). Contact is made between the seal and the cladding, thus the mercury in the capillary stem and capillary cladding creates a coaxial capacitor that senses the quantity of mercury. The schematic diagram is shown in Appendix 2 Figure 2. The penetrometer is mounted horizontally to minimize the effect of head pressure. The minimum practical pressure to which gas could be admitted is 3.4 kPa, which usually causes mercury to penetrate sample pores larger than 360 μ m in diameter.



Appendix 2 Figure 2 Schematic diagram of the low-pressure evacuation and filling system. (Source: Micromeritics operational manual).

2.1.1 Evacuation valves

These consist of three valves (slow, medium and fast) that, controls the rate of evacuation of samples and also prevent powders or smaller particles from fluidizing. During analysis, these valves are operated in sequence to avoid drawing samples inside the penetrometer (Appendix Figure 3) capillary stem and plumbing.



Appendix 2 Figure 3 Penetrometer assembly for sample holding. (Source:

Micromeritics operational manual).

2.1.2 Gas inlet valve

Pressures ranging from 0.0014 to 0.35 MPa can be generated by a programmed pulsing of the gas inlet solenoid valve in the low-pressure port. This permits gas to the admitted in discrete increments.

2.1.3 Mercury fill and drain valve

This valves controls the flow of mercury into the penetrometer and back into the reservoir.

2.1.4 Mercury reservoir evacuation valve

This valve connects the vacuum line to the mercury reservoir

2.1.5 Low pressure ports

Low pressure ports are located at the upper part of the equipment and they accommodate the penetrometer and connect them to the low pressure system. The penetrometer mounted into the low-pressure ports is vacuum-sealed against mercury leakage by compression of a gum rubber cylinder.

2.1.6 Mercury storage reservoir

The mercury storage reservoir has a capacity of about 2.6 to 3.7 kg of mercury.

The level of mercury is visible through a small inspection window in the front panel.

2.1.7 High Pressure System

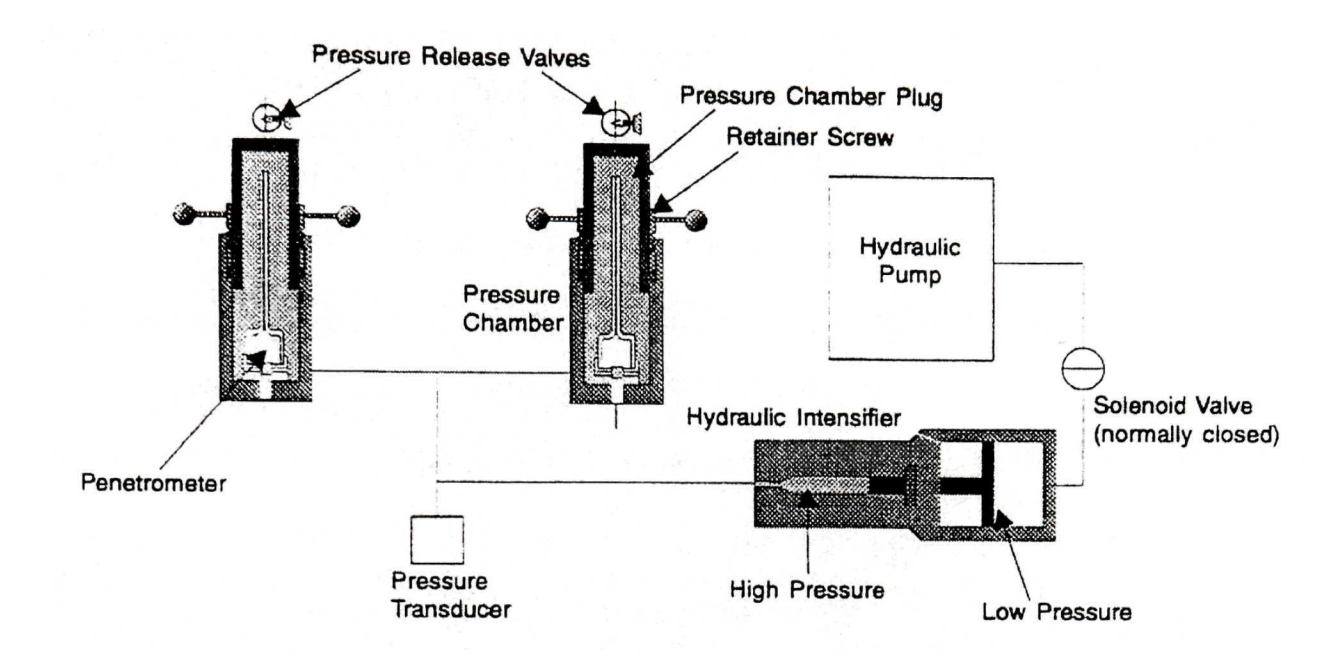
The high-pressure system consists of: hydraulic pump, intensifier, transducer, and the high-pressure chamber. The hydraulic pump serves as the basic high-pressure generator, and is an integral part of the hydraulic fluid reservoir. The pump is reversible and can generate positive and negative pressures, an attribute required for intrusion and extrusion of mercury during the test cycle. A

control module and motorized variable autotransformer maintain the targeted pressure and control the pump speed and direction of rotation.

The system generates high pressure through a dual-piston connected to the hydraulic pump. These are in the form of two limit switches located in the up and down stream of the hydraulic pump travel or stroke. One of the switches alerts the operating system while the other interrupts the system power. In this system, the penetrometer is installed vertically and surrounded by hydraulic fluid. An increase in fluid pressure is transmitted to the mercury in the penetrometer through the open capillary stem. As mercury penetrates the pores, its level in the capillary falls according to the volume of the pores entered. The mercury is then extruded, by reversing the hydraulic pump to lower the pressure.

The high-pressure transducer is responsible for the signal and is processed by electronic circuitry to yield two-pressure output signal.

The high-pressure chamber accommodates the penetrometer during the high-pressure test. Located on top of the closure is a manual valve for venting or purging air that may be trapped when the high-pressure chamber is closed. The porosimeter is harnessed to a microcomputer data acquisition system (Micromeritics: AutoPore III for Windows).



Appendix 2 Figure 4 Schematic diagram of the high-pressure system of the mercury porosimetry. (Source: Micromeritics operational manual).

APPENDIX 3: INDUSTRIAL FRYER

Industrial fryer was used for all the DFF experiments in this study. The fryer is a commercial programmable computerized pressure deep-fat fryer (Henny Penny Computron 7000 Pressure Fryer, Model 500C, Henny Penny Corporation, Eaton, OH.), with a fat holding capacity of about 30 L as shown in Appendix 3 Figure 1. The fryer is equipped with load compensation, load anticipation, and proportional control features. Its digital display features are the LED type, which shows the temperature of the oil and the timer countdown of the frying cycle. The fryer is programmable in many cycles within the temperatures ranges 77 to 200°C (170 to 390°F).



Appendix 3 Figure 1 Photo of an industrial fryer Computron 7000 Pressure Fryer.

FAT ANALYSIS

All fat analysis in this project was accomplished by using the electronic programmable solvent extractor (SER148, Velp Scientifica, Usmate, Italy) as shown in Appendix 3 Figure 2. The equipment consists of six extraction units, each unit consist of a magnetic connector for securing the extraction thimbles during processes. The heating elements are located at the base of the equipment and provide recesses to accommodate the extraction glass cups.



Appendix 3 Figure 2 Photo of the Velp Scientific Soxhlet fat extractor used for determination of oil/fat uptake.